

Refining radiative decay studies in singly heavy baryons

Yu-Xin Peng^{1,2,4,*}, Si-Qiang Luo^{1,2,3,4,†} and Xiang Liu^{1,2,3,4,‡}

¹School of Physical Science and Technology, Lanzhou University, Lanzhou 730000, China

²Lanzhou Center for Theoretical Physics, Key Laboratory of Quantum Theory and Applications of MoE,

Key Laboratory of Theoretical Physics of Gansu Province, Lanzhou University, Lanzhou 730000, China

³MoE Frontiers Science Center for Rare Isotopes, Lanzhou University, Lanzhou 730000, China

⁴Research Center for Hadron and CSR Physics, Lanzhou University & Institute of Modern Physics of CAS, Lanzhou 730000, China

In this work, we systematically study the radiative decays of singly heavy baryons, a crucial aspect of their spectroscopic behavior. To enhance the accuracy of our calculations, we utilize numerical spatial wave functions for the singly heavy baryons obtained through the Gaussian expansion method, which also yields their mass spectrum. As hadron spectroscopy enters an era of high precision, we believe our study of the radiative decays of singly heavy baryons will provide valuable insights for further exploration of these particles.

I. INTRODUCTION

Recent experimental efforts have led to the discovery of numerous new hadronic states, significantly advancing the field of hadron physics over the past two decades [1–15]. Among these discoveries, singly heavy baryons stand out as a particularly interesting group. These heavy-light hadronic systems are not only numerous but have also garnered significant attention from the hadron physics community [2, 3, 5, 9, 11].

A singly heavy baryon consists of one heavy quark and two light quarks, adhering well to heavy quark symmetry. This simplifies the study of certain properties by leveraging the fact that the heavy quark mass is significantly greater than the typical energy scale of strong interactions. The spectroscopy of singly heavy baryons involves analyzing their mass spectrum, decay behavior, and production processes. These studies are progressively deepening our understanding of the nonperturbative behavior of strong interactions.

Examining the over thirty single-charm baryons catalogued by the Particle Data Group (PDG) [16], we observe that their decay modes include not only common weak and strong decays but also radiative decays. For instance, the $\Xi_c^{'+}$ and Ξ_c^0 baryons, which lack Okubo-Zweig-Iizuka (OZI) allowed decay channels, predominantly decay via $\Xi_c^+\gamma$ and $\Xi_c^0\gamma$ channels, respectively, as observed by the CLEO Collaboration in 1998 [17]. Similarly, the Ω_c^0 was first detected in the $\Omega_c^0\gamma$ channel by the BaBar Collaboration in 2006 [18] and confirmed by the Belle Collaboration in 2008 [19]. In 2020, the Belle Collaboration [20] observed the radiative decays of the $\Xi_c^0(2790)$ and $\Xi_c^0(2815)$ via the $\Xi_c^0\gamma$ channel. Unlike $\Xi_c^{'+}$, Ξ_c^0 , and Ω_c^* , this marked the first observation of radiative decays of orbitally excited single-charm baryons. These findings demonstrate that radiative decays of single-charm baryons are experimentally accessible and warrant further study.

Several theoretical investigations have explored this topic. Previous works have studied radiative decays using various methods, such as light-cone QCD sum rules [21–26], heavy

quark effective theory [27–29], chiral perturbation theory [30–32], constituent quark models [33–42], lattice QCD [43], relativistic quark model [44, 45], chiral quark-soliton model [46, 47], and so on. Compared to strong decays, radiative decays exhibit different decay widths for hadrons with the same isospin but different charges. For example, theoretical calculations show that $\text{BR}(\Xi_c^0(2790) \rightarrow \Xi_c^0\gamma) > \text{BR}(\Xi_c^+(2790) \rightarrow \Xi_c^+\gamma)$ and $\text{BR}(\Xi_c^0(2815) \rightarrow \Xi_c^0\gamma) > \text{BR}(\Xi_c^+(2815) \rightarrow \Xi_c^+\gamma)$, aligning with experimental results [20]. These results indicate that radiative decays provide rich information about the internal structures of hadrons.

Hadron spectroscopy is entering an era of high precision. With the upgrade of the high-luminosity Large Hadron Collider and the operation of Belle II, more single-charm baryons will be discovered, and their properties revealed. This increase in experimental precision necessitates corresponding advancements in theoretical precision.

Given this context, our work focuses on the radiative decays of single-charm baryons, an area ripe for further exploration. Radiative decays are particularly sensitive to probing the internal structure of single-charm baryons. The calculated spatial wave function of these baryons is a crucial input for studying their radiative decays. Thus, this research provides a valuable platform for testing theoretical models.

On the other hand, over twenty single-bottom baryons have been observed in experiments. More than half of these discoveries were made from 2018, primarily due to the efforts of the LHCb and CMS Collaborations [48–56]. These observations underscore the capabilities of the LHCb and CMS Collaborations in identifying single-bottom baryons. However, to date, no single-bottom baryons have been observed through radiative decays. Similar to the study of single-charm baryons, radiative decay is an effective approach for studying singly heavy baryons. For instance, there is no OZI-allowed channel for Ω_b^{*-} , making $\Omega_b^-\gamma$ the dominant decay mode. Therefore, it is crucial to systematically study the radiative decays of single-bottom baryons, as this can provide different clues for their detection.

In Ref. [57], the Lanzhou group employed the Gaussian expansion method (GEM), a high-precision method for solving few-body problems [58], to systematically study the mass spectrum of singly heavy baryons using the potential model [57, 59]. This approach allowed for the decoding of

*Electronic address: pengyx21@lzu.edu.cn

†Electronic address: luosq15@lzu.edu.cn

‡Electronic address: xiangliu@lzu.edu.cn

observed singly heavy baryon properties and the prediction of spectroscopic behavior for missing states. The spatial wave functions obtained in this process form the basis of our current work.

We revisit the radiative decays of singly heavy baryons. Previous studies [34, 40–42] often used simple harmonic oscillator wave functions to represent spatial wave functions. In contrast, we use numerical spatial wave functions calculated by GEM as presented in Ref. [58]. The next section will compare these treatments and illustrate how they affect decay widths using a concrete example.

This timely work is in anticipation of data from Belle II [60, 61] and Run-3 and Run-4 at LHCb [62, 63]. Although detecting radiative decays of singly heavy baryons is more challenging than other decay modes, our study can provide theoretical guidance to experimentalists, aiding in the selection of suitable radiative decays as research topics. This will enrich observations of radiative decays of singly heavy baryons and highlight the value of our work.

This paper is organized as follows. After the Introduction, the deduction of the radiative decays of singly heavy baryons and the details of calculation are presented in Sec. II. Then the numerical results are given in Sec. III. The paper ends with a short summary in Sec. IV.

II. RADIATIVE DECAYS OF SINGLY HEAVY BARYONS

At the tree level, the Hamiltonian of the coupling of quarks and photon is

$$H_e = - \sum_j e_j \bar{\psi}_j \gamma_\mu^j A^\mu(\mathbf{k}, \mathbf{r}) \psi_j, \quad (1)$$

where e_j , γ_μ^j , and ψ_j are the charge, Dirac matrix, and spinor of the j th quark, respectively. A^μ in Eq. (1) is the photon field. In the nonrelativistic scheme, the Hamiltonian of the coupling of quarks and photons is given by [41, 64–68]

$$h_e \simeq \sum_j \left[e_j \mathbf{r}_j \cdot \boldsymbol{\epsilon} - \frac{e_j}{2m_j} \boldsymbol{\sigma}_j \cdot (\boldsymbol{\epsilon} \times \hat{\mathbf{k}}) \right] e^{-i\mathbf{k} \cdot \mathbf{r}_j}, \quad (2)$$

where \mathbf{r}_j , m_j , and $\boldsymbol{\sigma}_j$ are the coordinate, mass, and Pauli matrix of the j th quark, respectively. \mathbf{k} and $\boldsymbol{\epsilon}$ in Eq. (2) are the momentum and polarization vector of the photon, respectively. With the above Hamiltonian, the radiative decay amplitude is expressed as [68]

$$\mathcal{A} = -i \sqrt{\frac{\omega_\gamma}{2}} \langle f | h_e | i \rangle, \quad (3)$$

where $|i\rangle$ and $|f\rangle$ are the wave functions of the initial and final baryons, respectively. The photon energy ω_γ is defined by

$$\omega_\gamma = \frac{M_i^2 - M_f^2}{2M_i}, \quad (4)$$

where M_i and M_f are the masses of the initial and final baryons, respectively.

Finally, we can write out the general expression of the radiative decay width of a singly heavy baryon¹

$$\Gamma = \frac{|\mathbf{k}|^2}{\pi} \frac{2}{2J_i + 1} \frac{M_f}{M_i} \sum_{J_{fz}, J_{iz}} |\mathcal{A}_{J_{fz}, J_{iz}}|^2. \quad (5)$$

Here, J_{iz} and J_{fz} stand for the third components of the initial and final baryon angular momentum, respectively.

To obtain the radiative decay widths of singly heavy baryons, we require both their mass spectra and wave functions, which are derived from a nonrelativistic potential model [57, 59]:

$$\hat{H} = \sum_i \left(m_i + \frac{p_i^2}{2m_i} \right) + \sum_{i < j} V_{ij}, \quad (6)$$

where m_i and p_i are mass and momentum of the i th quark, respectively. The potential V_{ij} between two quarks includes the confinement potential V_{ij}^{conf} , hyperfine interaction V_{ij}^{hyp} , color-magnetic spin-orbit term $V_{ij}^{\text{so(cm)}}$, and Thomas-precession spin-orbit term $V_{ij}^{\text{so(tp)}}$: $V_{ij} = V_{ij}^{\text{conf}} + V_{ij}^{\text{hyp}} + V_{ij}^{\text{so(cm)}} + V_{ij}^{\text{so(tp)}}$. The explicit expressions for these terms are

$$\begin{aligned} V_{ij}^{\text{conf}} &= -\frac{2}{3} \frac{\alpha_s}{r_{ij}} + \frac{b}{2} r_{ij} + \frac{1}{2} C, \\ V_{ij}^{\text{hyp}} &= \frac{2\alpha_s}{3m_i m_j} \left[\frac{8\pi}{3} \tilde{\delta}(r_{ij}) \mathbf{s}_i \cdot \mathbf{s}_j + \frac{1}{r_{ij}^3} S(\mathbf{r}, \mathbf{s}_i, \mathbf{s}_j) \right], \\ V_{ij}^{\text{so(cm)}} &= \frac{2\alpha_s}{3r_{ij}^3} \left(\frac{\mathbf{r}_{ij} \times \mathbf{p}_i \cdot \mathbf{s}_i}{m_i^2} - \frac{\mathbf{r}_{ij} \times \mathbf{p}_j \cdot \mathbf{s}_j}{m_j^2} \right. \\ &\quad \left. - \frac{\mathbf{r}_{ij} \times \mathbf{p}_j \cdot \mathbf{s}_i - \mathbf{r}_{ij} \times \mathbf{p}_i \cdot \mathbf{s}_j}{m_i m_j} \right), \\ V_{ij}^{\text{so(tp)}} &= -\frac{1}{2r_{ij}} \frac{\partial H_{ij}^{\text{conf}}}{\partial r_{ij}} \left(\frac{\mathbf{r}_{ij} \times \mathbf{p}_i \cdot \mathbf{s}_i}{m_i^2} - \frac{\mathbf{r}_{ij} \times \mathbf{p}_j \cdot \mathbf{s}_j}{m_j^2} \right), \end{aligned} \quad (7)$$

where α_s is the coupling constant of the one-gluon exchange, b is the confinement strength, and C is a mass-anchoring constant. The smearing function $\tilde{\delta}(r) = \frac{\sigma^3}{\pi^{3/2}} e^{-\sigma^2 r^2}$ is introduced in the contact term related to $\mathbf{s}_i \cdot \mathbf{s}_j$, with σ as the smearing parameter. The tensor operator is defined as $S(\mathbf{r}, \mathbf{s}_i, \mathbf{s}_j) = \frac{3\mathbf{s}_i \cdot \mathbf{r}_{ij} \mathbf{s}_j \cdot \mathbf{r}_{ij}}{r_{ij}^2} - \mathbf{s}_i \cdot \mathbf{s}_j$.

We use the GEM [58, 69] to solve the potential model [57, 59] and obtain the numerical spatial wave functions of the singly heavy baryons. The Gaussian wave function is expressed as

$$\phi_{nlm}^{\text{Gau}}(\mathbf{r}) = R_{nl}^{\text{Gau}}(r) Y_{lm}(\hat{\mathbf{r}}), \quad (8)$$

¹ If we treat the quark charges as dimensionless, i.e., $e_u = \frac{2}{3}$, $e_d = -\frac{1}{3}$, $e_s = -\frac{1}{3}$, $e_c = \frac{2}{3}$, and $e_b = -\frac{1}{3}$, then Eq. (5) should be multiplied by a coefficient $4\pi\alpha_{\text{EM}}$, where $\alpha_{\text{EM}} \approx \frac{1}{137}$ is the fine structure constant.

where $R_{nl}^{\text{Gau}}(r)$ is the radial part given by

$$R_{nl}^{\text{Gau}}(r) = N_{nl} r^l e^{-\nu_n r^2}, \quad N_{nl} = \sqrt{\frac{2^{l+2}(2\nu_n)^{l+\frac{3}{2}}}{\sqrt{\pi}(2l+1)!!}}, \quad (9)$$

and ν_n is defined as

$$\nu_n = \frac{1}{r_n^2}, \quad r_n = r_1 a^{n-1} \quad (n = 1 - n_{\max}). \quad (10)$$

In a single-channel scheme, the base could be written as

$$|\psi_{JM}^{n_\rho n_\lambda}\rangle = \phi^{\text{color}} \phi^{\text{flavor}} |[[s_{q_1} s_{q_2}]_{s_\ell} [\phi_{n_\rho l_\rho}(\rho) \phi_{n_\lambda l_\lambda}(\lambda)]_L]_{j_\ell} s_{Q_3}]_{JM}\rangle, \quad (11)$$

where ϕ^{color} and ϕ^{flavor} are color and flavor wave functions, respectively. s_{q_1} , s_{q_2} , and s_{Q_3} are spins of the quarks, with $q = u, d, s$, and $Q = c, b$. s_ℓ and j_ℓ are spin and total angular momentum of the light flavor degree of freedom, respectively. A singly heavy baryon has two spatial degrees of freedom. We use the ρ mode to denote the relative coordinate of the two light quarks, and the λ mode to describe the relative position of the heavy quark and the center of mass of the two light quarks. In Eq. (11), the l_ρ , l_λ , and L are ρ -mode, λ mode, and total orbital angular momentum, respectively. Then the spatial part in the base is expanded by

$$[\phi_{n_\rho l_\rho}(\rho) \phi_{n_\lambda l_\lambda}(\lambda)]_{LM_L} = \sum_{m_\rho m_\lambda} \langle l_\rho m_\rho; l_\lambda m_\lambda | LM_L \rangle \times \phi_{n_\rho l_\rho m_\rho}(\rho) \phi_{n_\lambda l_\lambda m_\lambda}(\lambda). \quad (12)$$

The matrix elements could be calculated with

$$H_{n'_\rho n'_\lambda n_\rho n_\lambda} = \langle \psi_{JM}^{n'_\rho n'_\lambda} | \hat{H} | \psi_{JM}^{n_\rho n_\lambda} \rangle, \quad (13)$$

$$N_{n'_\rho n'_\lambda n_\rho n_\lambda} = \langle \psi_{JM}^{n'_\rho n'_\lambda} | \psi_{JM}^{n_\rho n_\lambda} \rangle. \quad (14)$$

Then eigenvalues E and eigenvectors $C_{n_\rho n_\lambda}$ could be obtained by the general eigenvalue equation

$$H_{n'_\rho n'_\lambda n_\rho n_\lambda} C_{n_\rho n_\lambda} = E N_{n'_\rho n'_\lambda n_\rho n_\lambda} C_{n_\rho n_\lambda}. \quad (15)$$

Finally the total wave function is

$$|\Psi_{JM}\rangle = \sum_{n_\rho n_\lambda} C_{n_\rho n_\lambda} |\psi_{JM}^{n_\rho n_\lambda}\rangle. \quad (16)$$

In calculation, we adjust the parameters $\{r_1, r_{\max}, n_{\max}\} = \{\rho_1, \rho_{\max}, n_{\max}^\rho\}$ and $\{r_1, r_{\max}, n_{\max}\} = \{\lambda_1, \lambda_{\max}, n_{\max}^\lambda\}$ in ρ and λ modes for optimal solutions. This is the simplest situation, i.e., the quantum numbers s_ℓ , l_ρ , l_λ , L , etc. are fixed. To be practical, we should consider the mixing effects. In this way, s_ℓ , l_ρ , l_λ , L , etc. are also the subscripts of the matrices. And each group of the bases has independent Gaussian parameters.

It is convenient to categorize the singly heavy baryons in SU(3) flavor symmetry. In each category, the singly heavy baryons have similar heavy quark spin symmetry. In SU(3)

flavor symmetry, the flavor wave functions of two light quarks can be decomposed as

$$3_f \otimes 3_f = \bar{3}_f \oplus 6_f. \quad (17)$$

For singly heavy baryons, Λ_c^+ , Ξ_c^0 , Ξ_c^+ , Λ_b^0 , Ξ_b^- , Ξ_b^0 belong to the $\bar{3}_f$ representation, where the flavor wave functions of the two light quarks are antisymmetric. The symmetric flavor wave functions in the 6_f representation include Σ_c^0 , Σ_c^+ , Σ_c^{++} , Ξ_c^0 , $\Xi_c^{'+}$, Ω_c^0 , Σ_b^- , Σ_b^0 , Σ_b^+ , $\Xi_b'^-$, Ξ_b^0 , and Ω_b^- .

TABLE I: The parameters involved in the adopted potential model.

System	α_s	b (GeV 2)	σ (GeV)	C (GeV)
Λ_c/Σ_c	0.560	0.122	1.600	-0.633
$\Xi_c^{(')}$	0.560	0.140	1.600	-0.693
Ω_c	0.578	0.144	1.732	-0.691
Λ_b/Σ_b	0.560	0.112	1.600	-0.411
$\Xi_b^{(')}$	0.560	0.123	1.600	-0.453
Ω_b	0.578	0.123	1.732	-0.435
$m_u = m_d = 0.370$ GeV $m_s = 0.600$ GeV				
$m_c = 1.880$ GeV $m_b = 4.977$ GeV				

We need consistent quark masses m , and potential parameters α_s , b , C , and σ . Using all $1S$ states, $1P$, $1D$, and $2S$ $\bar{3}_f$ candidates, we determine these parameters, which are presented in Table I. With these parameters, we also calculate the masses of not well-established states, such as $1F$ $\bar{3}_f$ states, $1P$, $1D$, $1F$, and $2S$ 6_f states. Their masses are presented in Table II. The results match the PDG [16] and previous studies [69–76].

In this work, the color, flavor, and spin wave functions are well known, and the remaining spatial wave functions are the key part, whether calculations of mass spectra or radiative decays. There are at least two approaches to obtain the spatial wave functions. The one is using the results from GEM, and the other is employing the approximations of simple harmonic oscillator (SHO) wave function [41, 57, 59, 77]. Here, we make a comparison between the two methods. For convenience, we ignore the orbital parts, and then the remaining spatial wave functions are only two dimensional. First, with the GEM, we obtain

$$R_{l_\rho l_\lambda}^{\text{GEM}}(\rho, \lambda) = \sum_{n_\rho n_\lambda} C_{n_\rho n_\lambda} R_{n_\rho l_\rho}^{\text{Gau}}(\rho) R_{n_\lambda l_\lambda}^{\text{Gau}}(\lambda). \quad (18)$$

On the other hand, with the simple harmonic oscillator wave functions, we have

$$R_{n_\rho l_\rho n_\lambda l_\lambda}^{\text{SHO}}(\rho, \lambda) = R_{n_\rho l_\rho}^{\text{SHO}}(\beta_\rho, \rho) R_{n_\lambda l_\lambda}^{\text{SHO}}(\beta_\lambda, \lambda), \quad (19)$$

where $R_{nl}^{\text{SHO}}(\beta, r)$ is the radial part, i.e.,

$$R_{nl}^{\text{SHO}}(\beta, r) = \beta^{l+\frac{3}{2}} \sqrt{\frac{2n!}{\Gamma(n+l+\frac{3}{2})}} e^{-\beta^2 r^2} L_n^{l+\frac{1}{2}}(\beta^2 r^2) r^l. \quad (20)$$

The β_ρ and β_λ are parameters to scale the SHO wave functions. In general, the β_ρ and β_λ values could not be obtained directly

TABLE II: Mass spectrum of singly heavy baryons [16, 48–57]. The masses of the well-established states in the PDG [16] or experimental results [48–56] are in bold, while the unbolted masses are theoretical results. The calculated masses of single-charm and single-bottom baryons are taken from Ref. [57] and the calculations of this work, respectively.

States	l_p	l_λ	L	s_ℓ	j_ℓ	J	M (MeV)		M (MeV)	
							Λ_c	Ξ_c	Λ_b	Ξ_b
$\bar{3}_f$	$\Lambda_Q/\Xi_Q(1S, \frac{1}{2}^+)$	0	0	0	0	$\frac{1}{2}$	2283	2472	5619	5796
							2286	2470	5619	5795
	$\Lambda_Q/\Xi_Q(1P, \frac{1}{2}^-)$	0	1	1	0	$\frac{1}{2}$	2595	2794	5915	6092
							2595	2790	5912	6087
	$\Lambda_Q/\Xi_Q(1P, \frac{3}{2}^-)$	0	1	1	0	$\frac{3}{2}$	2618	2817	5925	6102
							2625	2815	5920	6095
	$\Lambda_Q/\Xi_Q(1D, \frac{3}{2}^+)$	0	2	2	0	$\frac{3}{2}$	2856	3065	6147	6324
							2860	3055	6146	6327
	$\Lambda_Q/\Xi_Q(1D, \frac{5}{2}^+)$	0	2	2	0	$\frac{5}{2}$	2867	3075	6154	6330
							2880	3080	6152	6332
6_f	$\Lambda_Q/\Xi_Q(1F, \frac{5}{2}^-)$	0	3	3	0	$\frac{5}{2}$	3075	3292	6343	6520
	$\Lambda_Q/\Xi_Q(1F, \frac{7}{2}^-)$	0	3	3	0	$\frac{7}{2}$	3079	3295	6347	6524
	$\Lambda_Q/\Xi_Q(2S, \frac{1}{2}^+)$	0	0	0	0	$\frac{1}{2}$	2782	2985	6075	6249
							2765	2970	6072	
	$\Sigma_Q / \Xi'_Q / \Omega_Q (1S, \frac{1}{2}^+)$	0	0	0	1	$\frac{1}{2}$	Σ_c	Ξ'_c	Ω_c	Σ_b
							2469	2588	2695	5821
							2455	2580	2695	5815
	$\Sigma_Q^* / \Xi_Q^* / \Omega_Q^* (1S, \frac{3}{2}^+)$	0	0	0	1	$\frac{3}{2}$	2515	2640	2754	5839
							2520	2645	2765	5835
$\Sigma_Q / \Xi'_Q / \Omega_Q (1P, \frac{1}{2}^-)$	0	1	1	1	0	$\frac{1}{2}$	2785	2919	3030	6100
	$\Sigma_{Q1}/\Xi'_{Q1}/\Omega_{Q1}(1P, \frac{1}{2}^-)$	0	1	1	1	$\frac{1}{2}$	2771	2906	3020	6091
	$\Sigma_{Q1}/\Xi'_{Q1}/\Omega_{Q1}(1P, \frac{3}{2}^-)$	0	1	1	1	$\frac{3}{2}$	2798	2938	3056	6102
	$\Sigma_{Q2}/\Xi'_{Q2}/\Omega_{Q2}(1P, \frac{3}{2}^-)$	0	1	1	1	$\frac{3}{2}$	2780	2927	3053	6087
	$\Sigma_{Q2}/\Xi'_{Q2}/\Omega_{Q2}(1P, \frac{5}{2}^-)$	0	1	1	1	$\frac{5}{2}$	2797	2945	3073	6094
	$\Sigma_{Q1}/\Xi'_{Q1}/\Omega_{Q1}(1D, \frac{1}{2}^+)$	0	2	2	1	$\frac{1}{2}$	3043	3186	3298	6334
	$\Sigma_{Q1}/\Xi'_{Q1}/\Omega_{Q1}(1D, \frac{3}{2}^+)$	0	2	2	1	$\frac{3}{2}$	3058	3201	3315	6341
	$\Sigma_{Q2}/\Xi'_{Q2}/\Omega_{Q2}(1D, \frac{3}{2}^+)$	0	2	2	1	$\frac{3}{2}$	3031	3181	3303	6317
	$\Sigma_{Q2}/\Xi'_{Q2}/\Omega_{Q2}(1D, \frac{5}{2}^+)$	0	2	2	1	$\frac{5}{2}$	3043	3194	3317	6323
	$\Sigma_{Q3}/\Xi'_{Q3}/\Omega_{Q3}(1D, \frac{5}{2}^+)$	0	2	2	1	$\frac{5}{2}$	3010	3173	3307	6290
	$\Sigma_{Q3}/\Xi'_{Q3}/\Omega_{Q3}(1D, \frac{7}{2}^+)$	0	2	2	1	$\frac{7}{2}$	3017	3179	3314	6295
	$\Sigma_{Q2}/\Xi'_{Q2}/\Omega_{Q2}(1F, \frac{3}{2}^-)$	0	3	3	1	$\frac{3}{2}$	3277	3427	3540	6539
	$\Sigma_{Q2}/\Xi'_{Q2}/\Omega_{Q2}(1F, \frac{5}{2}^-)$	0	3	3	1	$\frac{5}{2}$	3283	3433	3546	6544
	$\Sigma_{Q3}/\Xi'_{Q3}/\Omega_{Q3}(1F, \frac{5}{2}^-)$	0	3	3	1	$\frac{5}{2}$	3247	3408	3532	6508
	$\Sigma_{Q3}/\Xi'_{Q3}/\Omega_{Q3}(1F, \frac{7}{2}^-)$	0	3	3	1	$\frac{7}{2}$	3252	3412	3536	6512
	$\Sigma_{Q4}/\Xi'_{Q4}/\Omega_{Q4}(1F, \frac{7}{2}^-)$	0	3	3	1	$\frac{7}{2}$	3208	3383	3521	6466
	$\Sigma_{Q4}/\Xi'_{Q4}/\Omega_{Q4}(1F, \frac{9}{2}^-)$	0	3	3	1	$\frac{9}{2}$	3209	3383	3521	6469
	$\Sigma_Q / \Xi'_Q / \Omega_Q (2S, \frac{1}{2}^+)$	0	0	0	1	$\frac{1}{2}$	2947	3090	3203	6248
	$\Sigma_Q^* / \Xi_Q^* / \Omega_Q^* (2S, \frac{3}{2}^+)$	0	0	0	1	$\frac{3}{2}$	2979	3124	3243	6260

from the concrete potential models. However, if we know the numerical spatial wave functions from solving the potential mode, the SHO parameter $\beta_{\rho,\lambda}$ could be estimated with several different approaches. With the method suggested in Refs. [57, 59, 74, 78], the $\beta_{\rho,\lambda}$ values are extracted with the spatial wave function of the GEM in Eq. (18), which is given by

$$\frac{1}{\beta_\rho^2} = \int_0^\infty |R_{l_\rho l_\lambda}^{\text{GEM}}(\rho, \lambda)|^2 \rho^4 \lambda^2 d\rho d\lambda, \quad (21)$$

$$\frac{1}{\beta_\lambda^2} = \int_0^\infty |R_{l_\rho l_\lambda}^{\text{GEM}}(\rho, \lambda)|^2 \rho^2 \lambda^4 d\rho d\lambda.$$

Here, we take the low-lying singly heavy baryon $\Lambda_c^+(1S, \frac{1}{2}^+)$ as an example. In the calculations, the parameters in the GEM are employed as

$$\begin{aligned} \{\rho_1, \rho_{\max}, n_{\max}^\rho\} &= \{0.1 \text{ fm}, 5.0 \text{ fm}, 10\}, \\ \{\lambda_1, \lambda_{\max}, n_{\max}^\lambda\} &= \{0.1 \text{ fm}, 5.0 \text{ fm}, 10\}. \end{aligned} \quad (22)$$

Then, using the Rayleigh-Ritz variational method, C_{n_ρ, n_λ} is obtained as

$$C_{n_\rho, n_\lambda} = 10^{-3} \times \begin{pmatrix} -0.093 & 0.689 & -0.687 & 2.178 & 4.442 & 4.688 & -0.876 & 0.391 & -0.155 & 0.039 \\ 2.085 & -4.407 & 9.332 & -2.680 & 33.777 & 21.436 & -2.020 & 0.612 & -0.159 & 0.024 \\ -0.973 & 9.959 & -15.248 & 27.579 & 22.564 & 36.328 & -8.591 & 4.093 & -1.698 & 0.438 \\ -1.737 & -0.326 & 32.856 & -32.591 & 89.858 & 37.447 & 0.736 & -1.416 & 0.858 & -0.268 \\ 3.663 & -12.114 & 7.243 & 94.438 & 46.207 & 87.520 & -22.094 & 10.581 & -4.360 & 1.111 \\ -3.269 & 12.907 & -24.201 & 3.425 & 367.804 & 201.317 & -20.484 & 6.643 & -2.013 & 0.398 \\ 2.771 & -11.889 & 28.970 & -50.831 & 62.840 & 203.767 & -36.996 & 16.537 & -6.458 & 1.579 \\ -1.385 & 5.842 & -13.721 & 22.097 & -19.483 & -37.457 & 9.740 & -4.572 & 1.870 & -0.474 \\ 0.609 & -2.541 & 5.867 & -9.182 & 7.537 & 12.288 & -3.246 & 1.554 & -0.647 & 0.167 \\ -0.164 & 0.680 & -1.548 & 2.381 & -1.922 & -2.743 & 0.729 & -0.353 & 0.149 & -0.039 \end{pmatrix}, \quad (23)$$

where n_ρ and n_λ are the row and column indices, respectively.² With the coefficients obtained above, one obtains $\beta_\rho = 0.290$ GeV and $\beta_\rho = 0.344$ GeV in the SHO wave function [see Eq. (19)] for the $\Lambda_c^+(1S, \frac{1}{2}^+)$.

We note that both $R_{n_\rho l_\rho n_\lambda l_\lambda}^{\text{SHO}}(\rho, \lambda)$ and $R_{l_\rho l_\lambda}^{\text{GEM}}(\rho, \lambda)$ are two-dimensional functions. To plot the curves conveniently, we set $\rho = 0$ or $\lambda = 0$ and obtain the functions depending on another variation. Here, we employ the $\Lambda_c^+(1S)$ as an example. The

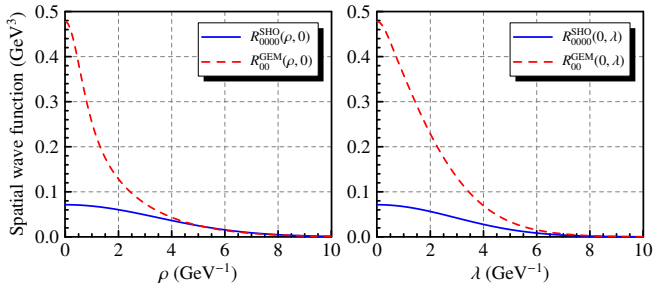


FIG. 1: The spatial wave functions $R_{n_\rho l_\rho n_\lambda l_\lambda}^{\text{SHO}}(\rho, \lambda)$ and $R_{l_\rho l_\lambda}^{\text{GEM}}(\rho, \lambda)$ dependent on ρ (left) and λ (right).

results are presented in Fig. 1. According to Fig. 1, there are obvious differences between the SHO and GEM wave functions. In the following discussions, we take the numerical spatial wave functions of singly heavy baryons from the potential model solved by the GEM [57], which are used as input to calculate their radiative decay behaviors.

III. NUMERICAL RESULTS

A. $\bar{3}_f \rightarrow 1S + \gamma$

Among these decay channels of $\bar{3}_f$ single-charm baryons, we first consider the simplest situation, i.e., $\bar{3}_f \rightarrow 1S + \gamma$, where the $1S$ stands for the $\Lambda_c(1S)$, $\Sigma_c(1S)$, and $\Xi_c^{(\prime)}(1S)$ states. The numerical results are presented in Table III.

For the $\Lambda_c^+(1P)$, the radiative decay widths of the $\Lambda_c^+(1S)/\Sigma_c(1S)\gamma$ modes are very small, where similar results are also obtained in Refs. [34, 41]. Thus, the experimental detection of these decay channels experimentally are a real challenge. But for the $\Lambda_c^+(1D)$, the $\Lambda_c^+(1D, \frac{3}{2}^+) \rightarrow \Lambda_c^+(1S, \frac{1}{2}^+)\gamma$ and $\Lambda_c^+(1D, \frac{3}{2}^+) \rightarrow \Lambda_c^+(1S, \frac{1}{2}^+)\gamma$ channels have considerable decay widths. We therefore suggest that the experimental colleague could concentrate on the radiative decays of the $\Lambda_c^+(1D, \frac{3}{2}^+)$ and $\Lambda_c^+(1D, \frac{5}{2}^+)$. However, the radiative decay widths of the $\Lambda_c^+(1F)/\Lambda_c(2S)$ transitions into $\Lambda_c^+(1S)/\Sigma_c^+(1S)\gamma$ are very small, which shows that finding them is also a difficult task for experiments.

² Since the singly heavy baryons discussed in this work are abundant, we do not have enough space to list all the values of C_{n_ρ, n_λ} . If readers are interested in these values, they can consult Ref. [57] for more details or ours.

TABLE III: The radiative decay widths (in units of keV) of single-charm baryons in the $\bar{3}_f$ representation decaying into the $\Lambda_c(1S)/\Sigma_c(1S)/\Xi_c^{(*)}(1S)\gamma$.

Process	Our	Ref. [41]	Ref. [34]	Process	Our	Ref. [41]	Ref. [34]	Experiment [20]
$\Lambda_c^+(1P, \frac{1}{2}^-) \rightarrow \Lambda_c^+(1S, \frac{1}{2}^+) \gamma$	0.1	0.26	0.1	$\Xi_c^0(1P, \frac{1}{2}^-) \rightarrow \Xi_c^0(1S, \frac{1}{2}^+) \gamma$	217.5	263	202.5	800 ± 320
$\Lambda_c^+(1P, \frac{1}{2}^-) \rightarrow \Sigma_c^+(1S, \frac{1}{2}^+) \gamma$	0.3	0.45	1.0	$\Xi_c^0(1P, \frac{1}{2}^-) \rightarrow \Xi_c^0(1S, \frac{1}{2}^+) \gamma$	0.0	0.0	0.0	...
$\Lambda_c^+(1P, \frac{1}{2}^-) \rightarrow \Sigma_c^{*+}(1S, \frac{3}{2}^+) \gamma$	0.0	0.05	0.0	$\Xi_c^0(1P, \frac{1}{2}^-) \rightarrow \Xi_c^{*0}(1S, \frac{3}{2}^+) \gamma$	0.0	0.0	0.0	...
$\Lambda_c^+(1P, \frac{3}{2}^-) \rightarrow \Lambda_c^+(1S, \frac{1}{2}^+) \gamma$	0.8	0.30	0.7	$\Xi_c^0(1P, \frac{3}{2}^-) \rightarrow \Xi_c^0(1S, \frac{1}{2}^+) \gamma$	243.1	292	292.6	$320 \pm 45^{+45}_{-80}$
$\Lambda_c^+(1P, \frac{3}{2}^-) \rightarrow \Sigma_c^+(1S, \frac{1}{2}^+) \gamma$	0.9	1.17	2.5	$\Xi_c^0(1P, \frac{3}{2}^-) \rightarrow \Xi_c^0(1S, \frac{1}{2}^+) \gamma$	0.0	0.0	0.1	...
$\Lambda_c^+(1P, \frac{3}{2}^-) \rightarrow \Sigma_c^{*+}(1S, \frac{3}{2}^+) \gamma$	0.2	0.26	0.2	$\Xi_c^0(1P, \frac{3}{2}^-) \rightarrow \Xi_c^{*0}(1S, \frac{3}{2}^+) \gamma$	0.0	0.0	0.0	...
				$\Xi_c^+(1P, \frac{1}{2}^-) \rightarrow \Xi_c^+(1S, \frac{1}{2}^+) \gamma$	1.7	4.65	7.4	< 350
				$\Xi_c^+(1P, \frac{1}{2}^-) \rightarrow \Xi_c^+(1S, \frac{1}{2}^+) \gamma$	1.2	1.43	1.3	...
				$\Xi_c^+(1P, \frac{1}{2}^-) \rightarrow \Xi_c^{*+}(1S, \frac{3}{2}^+) \gamma$	0.5	0.44	0.1	...
				$\Xi_c^+(1P, \frac{3}{2}^-) \rightarrow \Xi_c^+(1S, \frac{1}{2}^+) \gamma$	1.0	2.8	4.8	< 80
				$\Xi_c^+(1P, \frac{3}{2}^-) \rightarrow \Xi_c^+(1S, \frac{1}{2}^+) \gamma$	2.1	2.32	2.9	...
				$\Xi_c^+(1P, \frac{3}{2}^-) \rightarrow \Xi_c^{*+}(1S, \frac{3}{2}^+) \gamma$	1.2	0.99	0.3	...
Process	Our	Process	Our	Process	Our	Process	Our	Process
$\Lambda_c^+(1D, \frac{3}{2}^+) \rightarrow \Lambda_c^+(1S, \frac{1}{2}^+) \gamma$	41.3	$\Xi_c^0(1D, \frac{3}{2}^+) \rightarrow \Xi_c^0(1S, \frac{1}{2}^+) \gamma$	17.8	$\Xi_c^+(1D, \frac{3}{2}^+) \rightarrow \Xi_c^+(1S, \frac{1}{2}^+) \gamma$	28.2			
$\Lambda_c^+(1D, \frac{3}{2}^+) \rightarrow \Sigma_c^+(1S, \frac{1}{2}^+) \gamma$	1.4	$\Xi_c^0(1D, \frac{3}{2}^+) \rightarrow \Xi_c^0(1S, \frac{1}{2}^+) \gamma$	0.0	$\Xi_c^+(1D, \frac{3}{2}^+) \rightarrow \Xi_c^+(1S, \frac{1}{2}^+) \gamma$	1.3			
$\Lambda_c^+(1D, \frac{3}{2}^+) \rightarrow \Sigma_c^{*+}(1S, \frac{3}{2}^+) \gamma$	1.3	$\Xi_c^0(1D, \frac{3}{2}^+) \rightarrow \Xi_c^{*0}(1S, \frac{3}{2}^+) \gamma$	0.0	$\Xi_c^+(1D, \frac{3}{2}^+) \rightarrow \Xi_c^{*+}(1S, \frac{3}{2}^+) \gamma$	1.6			
$\Lambda_c^+(1D, \frac{5}{2}^+) \rightarrow \Lambda_c^+(1S, \frac{1}{2}^+) \gamma$	42.8	$\Xi_c^0(1D, \frac{5}{2}^+) \rightarrow \Xi_c^0(1S, \frac{1}{2}^+) \gamma$	21.4	$\Xi_c^+(1D, \frac{5}{2}^+) \rightarrow \Xi_c^+(1S, \frac{1}{2}^+) \gamma$	27.1			
$\Lambda_c^+(1D, \frac{5}{2}^+) \rightarrow \Sigma_c^+(1S, \frac{1}{2}^+) \gamma$	1.9	$\Xi_c^0(1D, \frac{5}{2}^+) \rightarrow \Xi_c^0(1S, \frac{1}{2}^+) \gamma$	0.0	$\Xi_c^+(1D, \frac{5}{2}^+) \rightarrow \Xi_c^+(1S, \frac{1}{2}^+) \gamma$	1.6			
$\Lambda_c^+(1D, \frac{5}{2}^+) \rightarrow \Sigma_c^{*+}(1S, \frac{3}{2}^+) \gamma$	2.0	$\Xi_c^0(1D, \frac{5}{2}^+) \rightarrow \Xi_c^{*0}(1S, \frac{3}{2}^+) \gamma$	0.0	$\Xi_c^+(1D, \frac{5}{2}^+) \rightarrow \Xi_c^{*+}(1S, \frac{3}{2}^+) \gamma$	2.0			
$\Lambda_c^+(1F, \frac{5}{2}^-) \rightarrow \Lambda_c^+(1S, \frac{1}{2}^+) \gamma$	4.6	$\Xi_c^0(1F, \frac{5}{2}^-) \rightarrow \Xi_c^0(1S, \frac{1}{2}^+) \gamma$	28.4	$\Xi_c^+(1F, \frac{5}{2}^-) \rightarrow \Xi_c^+(1S, \frac{1}{2}^+) \gamma$	0.1			
$\Lambda_c^+(1F, \frac{5}{2}^-) \rightarrow \Sigma_c^+(1S, \frac{1}{2}^+) \gamma$	0.9	$\Xi_c^0(1F, \frac{5}{2}^-) \rightarrow \Xi_c^0(1S, \frac{1}{2}^+) \gamma$	0.0	$\Xi_c^+(1F, \frac{5}{2}^-) \rightarrow \Xi_c^+(1S, \frac{1}{2}^+) \gamma$	0.6			
$\Lambda_c^+(1F, \frac{5}{2}^-) \rightarrow \Sigma_c^{*+}(1S, \frac{3}{2}^+) \gamma$	1.2	$\Xi_c^0(1F, \frac{5}{2}^-) \rightarrow \Xi_c^{*0}(1S, \frac{3}{2}^+) \gamma$	0.0	$\Xi_c^+(1F, \frac{5}{2}^-) \rightarrow \Xi_c^{*+}(1S, \frac{3}{2}^+) \gamma$	0.9			
$\Lambda_c^+(1F, \frac{7}{2}^-) \rightarrow \Lambda_c^+(1S, \frac{1}{2}^+) \gamma$	4.8	$\Xi_c^0(1F, \frac{7}{2}^-) \rightarrow \Xi_c^0(1S, \frac{1}{2}^+) \gamma$	26.9	$\Xi_c^+(1F, \frac{7}{2}^-) \rightarrow \Xi_c^+(1S, \frac{1}{2}^+) \gamma$	0.1			
$\Lambda_c^+(1F, \frac{7}{2}^-) \rightarrow \Sigma_c^+(1S, \frac{1}{2}^+) \gamma$	0.9	$\Xi_c^0(1F, \frac{7}{2}^-) \rightarrow \Xi_c^0(1S, \frac{1}{2}^+) \gamma$	0.0	$\Xi_c^+(1F, \frac{7}{2}^-) \rightarrow \Xi_c^+(1S, \frac{1}{2}^+) \gamma$	0.6			
$\Lambda_c^+(1F, \frac{7}{2}^-) \rightarrow \Sigma_c^{*+}(1S, \frac{3}{2}^+) \gamma$	1.2	$\Xi_c^0(1F, \frac{7}{2}^-) \rightarrow \Xi_c^{*0}(1S, \frac{3}{2}^+) \gamma$	0.0	$\Xi_c^+(1F, \frac{7}{2}^-) \rightarrow \Xi_c^{*+}(1S, \frac{3}{2}^+) \gamma$	0.9			
$\Lambda_c^+(2S, \frac{1}{2}^+) \rightarrow \Lambda_c^+(1S, \frac{1}{2}^+) \gamma$	0.0	$\Xi_c^0(2S, \frac{1}{2}^+) \rightarrow \Xi_c^0(1S, \frac{1}{2}^+) \gamma$	0.0	$\Xi_c^+(2S, \frac{1}{2}^+) \rightarrow \Xi_c^+(1S, \frac{1}{2}^+) \gamma$	0.0			
$\Lambda_c^+(2S, \frac{1}{2}^+) \rightarrow \Sigma_c^+(1S, \frac{1}{2}^+) \gamma$	0.0	$\Xi_c^0(2S, \frac{1}{2}^+) \rightarrow \Xi_c^0(1S, \frac{1}{2}^+) \gamma$	0.1	$\Xi_c^+(2S, \frac{1}{2}^+) \rightarrow \Xi_c^+(1S, \frac{1}{2}^+) \gamma$	0.9			
$\Lambda_c^+(2S, \frac{1}{2}^+) \rightarrow \Sigma_c^{*+}(1S, \frac{3}{2}^+) \gamma$	3.2	$\Xi_c^0(2S, \frac{1}{2}^+) \rightarrow \Xi_c^{*0}(1S, \frac{3}{2}^+) \gamma$	0.0	$\Xi_c^+(2S, \frac{1}{2}^+) \rightarrow \Xi_c^{*+}(1S, \frac{3}{2}^+) \gamma$	1.4			

The Ξ_c states contain two charge status, i.e., Ξ_c^0 and Ξ_c^+ . In radiative decays, the Ξ_c^0 and Ξ_c^+ have significantly different properties. A typical example is the different decay widths of $\Xi_c^0(1P, \frac{1}{2}^-)/\Xi_c^0(1P, \frac{3}{2}^-) \rightarrow \Xi_c^0(1S, \frac{1}{2}^+) \gamma$ and $\Xi_c^+(1P, \frac{1}{2}^-)/\Xi_c^+(1P, \frac{3}{2}^-) \rightarrow \Xi_c^+(1S, \frac{1}{2}^+) \gamma$. For the $\Xi_c^0(1P, \frac{1}{2}^-)/\Xi_c^0(1P, \frac{3}{2}^-) \rightarrow \Xi_c^0(1S, \frac{1}{2}^+) \gamma$ transitions, the theoretical widths are about 200 keV, while the widths of $\Xi_c^+(1P, \frac{1}{2}^-)/\Xi_c^+(1P, \frac{3}{2}^-) \rightarrow \Xi_c^+(1S, \frac{1}{2}^+) \gamma$ are only of the order of a few keV. Similar results are also obtained in Refs. [34, 41]. This could explain why the Belle Collaboration [20] successfully measured the relative branching ratios of $\Xi_c^0(1P, \frac{1}{2}^-)/\Xi_c^0(1P, \frac{3}{2}^-) \rightarrow \Xi_c^0(1S, \frac{1}{2}^+) \gamma$ with $\Xi_c^0(1P, \frac{1}{2}^-)/\Xi_c^0(1P, \frac{3}{2}^-) \rightarrow \Xi_c^+(1S, \frac{1}{2}^+) \pi^-/\Xi_c^0(1S, \frac{3}{2}^+) \pi^- \rightarrow \Xi_c^+(1S, \frac{1}{2}^+) \gamma \pi^-/\Xi_c^0(1S, \frac{1}{2}^+) \pi^+ \pi^-$, but only gave upper branch ratio limits of $\Xi_c^+(1P, \frac{1}{2}^-)/\Xi_c^+(1P, \frac{3}{2}^-) \rightarrow \Xi_c^+(1S, \frac{1}{2}^+) \gamma$ with $\Xi_c^+(1P, \frac{1}{2}^-)/\Xi_c^+(1P, \frac{3}{2}^-) \rightarrow \Xi_c^0(1S, \frac{1}{2}^+) \pi^+/\Xi_c^0(1S, \frac{3}{2}^+) \pi^+ \rightarrow \Xi_c^+(1S, \frac{1}{2}^+) \gamma \pi^+/\Xi_c^0(1S, \frac{1}{2}^+) \pi^-$.

$\Xi_c^0(1S, \frac{1}{2}^+) \gamma \pi^+/\Xi_c^+(1S, \frac{1}{2}^+) \pi^- \pi^+$. On the other hand, if we treat the light flavor-spatial wave functions of Ξ_c as antisymmetrical and Ξ_c' as symmetric, the couplings between the Ξ_c^0 and $\Xi_c' \gamma$ are forbidden, since the the charge expectations satisfy $\langle e_1 \rangle = \langle e_2 \rangle = \langle e_3 \rangle = 0$. If we consider the small constituent quark mass gap of $m_d - m_s$, the decays are allowed. But, in general, the decay widths are suppressed, i.e., most of the calculated results are less than 0.1 keV as shown in Table III. According to Table III we also find that some decay channels can have significant radiative decay widths, including $\Xi_c^{0,+}(1D) \rightarrow \Xi_c^{0,+}(1S) \gamma$ and $\Xi_c^0(1F) \rightarrow \Xi_c^0(1S) \gamma$. However, for other radiative decay processes in Table III, the calculated widths are about or less than 1 keV.

In Table III, we observe that some decay channels have similar widths, such as $\Gamma_{\Xi_c^0(1P, \frac{1}{2}^-) \rightarrow \Xi_c^0(1S, \frac{1}{2}^+) \gamma} \approx \Gamma_{\Xi_c^0(1P, \frac{3}{2}^-) \rightarrow \Xi_c^0(1S, \frac{1}{2}^+) \gamma}$ and $\Gamma_{\Lambda_c^+(1D, \frac{3}{2}^+) \rightarrow \Lambda_c^+(1S, \frac{1}{2}^+) \gamma} \approx \Gamma_{\Lambda_c^+(1D, \frac{5}{2}^+) \rightarrow \Lambda_c^+(1S, \frac{1}{2}^+) \gamma}$. Further analysis suggests that these states can be categorized within the same NL doublet. According to heavy quark spin symmetry,

TABLE IV: The radiative decay widths (in units of keV) of single-bottom baryons in the $\bar{3}_f$ representation decaying into the $\Lambda_b(1S)/\Sigma_b(1S)/\Xi_b^{(*)}(1S)\gamma$.

Process	Our	Ref. [41]	Ref. [34]	Process	Our	Ref. [41]	Ref. [34]
$\Lambda_b^0(1P, \frac{1}{2}^-) \rightarrow \Lambda_b^0(1S, \frac{1}{2}^+) \gamma$	47.0	50.2	40.7	$\Xi_b^-(1P, \frac{1}{2}^-) \rightarrow \Xi_b^-(1S, \frac{1}{2}^+) \gamma$	79.1	135	91.5
$\Lambda_b^0(1P, \frac{1}{2}^-) \rightarrow \Sigma_b^0(1S, \frac{1}{2}^+) \gamma$	0.1	0.14	0.2	$\Xi_b^-(1P, \frac{1}{2}^-) \rightarrow \Xi_b^-(1S, \frac{1}{2}^+) \gamma$	0.0	0.0	0.0
$\Lambda_b^0(1P, \frac{1}{2}^-) \rightarrow \Sigma_b^{*0}(1S, \frac{3}{2}^+) \gamma$	0.1	0.09	0.0	$\Xi_b^-(1P, \frac{1}{2}^-) \rightarrow \Xi_b^{*-}(1S, \frac{3}{2}^+) \gamma$	0.0	0.0	0.0
$\Lambda_b^0(1P, \frac{3}{2}^-) \rightarrow \Lambda_b^0(1S, \frac{1}{2}^+) \gamma$	49.1	52.8	43.4	$\Xi_b^-(1P, \frac{3}{2}^-) \rightarrow \Xi_b^-(1S, \frac{1}{2}^+) \gamma$	84.5	147	96.1
$\Lambda_b^0(1P, \frac{3}{2}^-) \rightarrow \Sigma_b^0(1S, \frac{1}{2}^+) \gamma$	0.1	0.21	0.3	$\Xi_b^-(1P, \frac{3}{2}^-) \rightarrow \Xi_b^-(1S, \frac{1}{2}^+) \gamma$	0.0	0.0	0.0
$\Lambda_b^0(1P, \frac{3}{2}^-) \rightarrow \Sigma_b^{*0}(1S, \frac{3}{2}^+) \gamma$	0.1	0.15	0.0	$\Xi_b^-(1P, \frac{3}{2}^-) \rightarrow \Xi_b^{*-}(1S, \frac{3}{2}^+) \gamma$	0.0	0.0	0.0
				$\Xi_b^0(1P, \frac{1}{2}^-) \rightarrow \Xi_b^0(1S, \frac{1}{2}^+) \gamma$	33.9	63.6	83.1
				$\Xi_b^0(1P, \frac{1}{2}^-) \rightarrow \Xi_b^{*0}(1S, \frac{1}{2}^+) \gamma$	0.4	1.32	0.6
				$\Xi_b^0(1P, \frac{1}{2}^-) \rightarrow \Xi_b^{*0}(1S, \frac{3}{2}^+) \gamma$	0.5	2.04	0.1
				$\Xi_b^0(1P, \frac{3}{2}^-) \rightarrow \Xi_b^0(1S, \frac{1}{2}^+) \gamma$	35.2	68.3	88.9
				$\Xi_b^0(1P, \frac{3}{2}^-) \rightarrow \Xi_b^0(1S, \frac{1}{2}^+) \gamma$	0.6	1.68	0.7
				$\Xi_b^0(1P, \frac{3}{2}^-) \rightarrow \Xi_b^{*0}(1S, \frac{3}{2}^+) \gamma$	0.6	2.64	0.2
Process	Our	Process	Our	Process	Our	Process	Our
$\Lambda_b^0(1D, \frac{3}{2}^+) \rightarrow \Lambda_b^0(1S, \frac{1}{2}^+) \gamma$	26.7	$\Xi_b^-(1D, \frac{3}{2}^+) \rightarrow \Xi_b^-(1S, \frac{1}{2}^+) \gamma$	78.9	$\Xi_b^0(1D, \frac{3}{2}^+) \rightarrow \Xi_b^0(1S, \frac{1}{2}^+) \gamma$	10.2		
$\Lambda_b^0(1D, \frac{3}{2}^+) \rightarrow \Sigma_b^0(1S, \frac{1}{2}^+) \gamma$	1.1	$\Xi_b^-(1D, \frac{3}{2}^+) \rightarrow \Xi_b^{*-}(1S, \frac{1}{2}^+) \gamma$	0.0	$\Xi_b^0(1D, \frac{3}{2}^+) \rightarrow \Xi_b^{*0}(1S, \frac{1}{2}^+) \gamma$	1.3		
$\Lambda_b^0(1D, \frac{3}{2}^+) \rightarrow \Sigma_b^{*0}(1S, \frac{3}{2}^+) \gamma$	1.7	$\Xi_b^-(1D, \frac{3}{2}^+) \rightarrow \Xi_b^{*-}(1S, \frac{3}{2}^+) \gamma$	0.0	$\Xi_b^0(1D, \frac{3}{2}^+) \rightarrow \Xi_b^{*0}(1S, \frac{3}{2}^+) \gamma$	2.1		
$\Lambda_b^0(1D, \frac{5}{2}^+) \rightarrow \Lambda_b^0(1S, \frac{1}{2}^+) \gamma$	27.2	$\Xi_b^-(1D, \frac{5}{2}^+) \rightarrow \Xi_b^-(1S, \frac{1}{2}^+) \gamma$	80.0	$\Xi_b^0(1D, \frac{5}{2}^+) \rightarrow \Xi_b^0(1S, \frac{1}{2}^+) \gamma$	10.3		
$\Lambda_b^0(1D, \frac{5}{2}^+) \rightarrow \Sigma_b^0(1S, \frac{1}{2}^+) \gamma$	1.3	$\Xi_b^-(1D, \frac{5}{2}^+) \rightarrow \Xi_b^{*-}(1S, \frac{1}{2}^+) \gamma$	0.0	$\Xi_b^0(1D, \frac{5}{2}^+) \rightarrow \Xi_b^{*0}(1S, \frac{1}{2}^+) \gamma$	1.4		
$\Lambda_b^0(1D, \frac{5}{2}^+) \rightarrow \Sigma_b^{*0}(1S, \frac{3}{2}^+) \gamma$	1.9	$\Xi_b^-(1D, \frac{5}{2}^+) \rightarrow \Xi_b^{*-}(1S, \frac{3}{2}^+) \gamma$	0.0	$\Xi_b^0(1D, \frac{5}{2}^+) \rightarrow \Xi_b^{*0}(1S, \frac{3}{2}^+) \gamma$	2.3		
$\Lambda_b^0(1F, \frac{5}{2}^-) \rightarrow \Lambda_b^0(1S, \frac{1}{2}^+) \gamma$	15.5	$\Xi_b^-(1F, \frac{5}{2}^-) \rightarrow \Xi_b^-(1S, \frac{1}{2}^+) \gamma$	33.1	$\Xi_b^0(1F, \frac{5}{2}^-) \rightarrow \Xi_b^0(1S, \frac{1}{2}^+) \gamma$	3.6		
$\Lambda_b^0(1F, \frac{5}{2}^-) \rightarrow \Sigma_b^0(1S, \frac{1}{2}^+) \gamma$	1.1	$\Xi_b^-(1F, \frac{5}{2}^-) \rightarrow \Xi_b^{*-}(1S, \frac{1}{2}^+) \gamma$	0.0	$\Xi_b^0(1F, \frac{5}{2}^-) \rightarrow \Xi_b^{*0}(1S, \frac{1}{2}^+) \gamma$	0.7		
$\Lambda_b^0(1F, \frac{5}{2}^-) \rightarrow \Sigma_b^{*0}(1S, \frac{3}{2}^+) \gamma$	2.0	$\Xi_b^-(1F, \frac{5}{2}^-) \rightarrow \Xi_b^{*-}(1S, \frac{3}{2}^+) \gamma$	0.0	$\Xi_b^0(1F, \frac{5}{2}^-) \rightarrow \Xi_b^{*0}(1S, \frac{3}{2}^+) \gamma$	1.3		
$\Lambda_b^0(1F, \frac{7}{2}^-) \rightarrow \Lambda_b^0(1S, \frac{1}{2}^+) \gamma$	15.4	$\Xi_b^-(1F, \frac{7}{2}^-) \rightarrow \Xi_b^-(1S, \frac{1}{2}^+) \gamma$	33.3	$\Xi_b^0(1F, \frac{7}{2}^-) \rightarrow \Xi_b^0(1S, \frac{1}{2}^+) \gamma$	3.5		
$\Lambda_b^0(1F, \frac{7}{2}^-) \rightarrow \Sigma_b^0(1S, \frac{1}{2}^+) \gamma$	1.1	$\Xi_b^-(1F, \frac{7}{2}^-) \rightarrow \Xi_b^{*-}(1S, \frac{1}{2}^+) \gamma$	0.0	$\Xi_b^0(1F, \frac{7}{2}^-) \rightarrow \Xi_b^{*0}(1S, \frac{1}{2}^+) \gamma$	0.7		
$\Lambda_b^0(1F, \frac{7}{2}^-) \rightarrow \Sigma_b^{*0}(1S, \frac{3}{2}^+) \gamma$	2.0	$\Xi_b^-(1F, \frac{7}{2}^-) \rightarrow \Xi_b^{*-}(1S, \frac{3}{2}^+) \gamma$	0.0	$\Xi_b^0(1F, \frac{7}{2}^-) \rightarrow \Xi_b^{*0}(1S, \frac{3}{2}^+) \gamma$	1.4		
$\Lambda_b^0(2S, \frac{1}{2}^+) \rightarrow \Lambda_b^0(1S, \frac{1}{2}^+) \gamma$	0.0	$\Xi_b^-(2S, \frac{1}{2}^+) \rightarrow \Xi_b^-(1S, \frac{1}{2}^+) \gamma$	0.0	$\Xi_b^0(2S, \frac{1}{2}^+) \rightarrow \Xi_b^0(1S, \frac{1}{2}^+) \gamma$	0.0		
$\Lambda_b^0(2S, \frac{1}{2}^+) \rightarrow \Sigma_b^0(1S, \frac{1}{2}^+) \gamma$	0.3	$\Xi_b^-(2S, \frac{1}{2}^+) \rightarrow \Xi_b^{*-}(1S, \frac{1}{2}^+) \gamma$	0.0	$\Xi_b^0(2S, \frac{1}{2}^+) \rightarrow \Xi_b^{*0}(1S, \frac{1}{2}^+) \gamma$	0.0		
$\Lambda_b^0(2S, \frac{1}{2}^+) \rightarrow \Sigma_b^{*0}(1S, \frac{3}{2}^+) \gamma$	2.1	$\Xi_b^-(2S, \frac{1}{2}^+) \rightarrow \Xi_b^{*-}(1S, \frac{3}{2}^+) \gamma$	0.0	$\Xi_b^0(2S, \frac{1}{2}^+) \rightarrow \Xi_b^{*0}(1S, \frac{3}{2}^+) \gamma$	0.5		

for the λ -mode orbital excited $\bar{3}_f$ states, they share the same j_ℓ with $j_\ell = L$. Each doublet thus includes states with $J = |L - \frac{1}{2}|$ and $J = |L + \frac{1}{2}|$. To clearly present how the splittings affect the

decay behavior, we expand the decay widths in terms of $\frac{1}{m_c}$. The numerical results are

$$\Gamma_{\Lambda_c^+(1P, \frac{1}{2}^-) \rightarrow \Lambda_c^+(1S, \frac{1}{2}^+)}(\text{keV}) \approx 0.41 - 0.82[\mathcal{O}(1/m_c)] + 0.41[\mathcal{O}(1/m_c^2)], \quad (24)$$

$$\Gamma_{\Lambda_c^+(1P, \frac{3}{2}^-) \rightarrow \Lambda_c^+(1S, \frac{1}{2}^+)}(\text{keV}) \approx 0.33 + 0.47[\mathcal{O}(1/m_c)] + 0.67[\mathcal{O}(1/m_c^2)],$$

$$\Gamma_{\Lambda_c^+(1D, \frac{3}{2}^+) \rightarrow \Lambda_c^+(1S, \frac{1}{2}^+)}(\text{keV}) \approx 39.55 + 3.15[\mathcal{O}(1/m_c)] + 0.08[\mathcal{O}(1/m_c^2)], \quad (25)$$

$$\Gamma_{\Lambda_c^+(1D, \frac{5}{2}^+) \rightarrow \Lambda_c^+(1S, \frac{1}{2}^+)}(\text{keV}) \approx 44.06 - 2.49[\mathcal{O}(1/m_c)] + 0.11[\mathcal{O}(1/m_c^2)],$$

$$\Gamma_{\Lambda_c^+(1F, \frac{5}{2}^-) \rightarrow \Lambda_c^+(1S, \frac{1}{2}^+)}(\text{keV}) \approx 4.76 - 0.35[\mathcal{O}(1/m_c)] + 0.01[\mathcal{O}(1/m_c^2)], \quad (26)$$

$$\Gamma_{\Lambda_c^+(1F, \frac{7}{2}^-) \rightarrow \Lambda_c^+(1S, \frac{1}{2}^+)}(\text{keV}) \approx 4.67 + 0.26[\mathcal{O}(1/m_c)] + 0.01[\mathcal{O}(1/m_c^2)],$$

$$\begin{aligned}\Gamma_{\Xi_c^0(1P,\frac{1}{2}^-) \rightarrow \Xi_c^0(1S,\frac{1}{2}^+)}(\text{keV}) &\approx 205.43 + 22.32[\mathcal{O}(1/m_c)] + 0.61[\mathcal{O}(1/m_c^2)], \\ \Gamma_{\Xi_c^0(1P,\frac{3}{2}^-) \rightarrow \Xi_c^0(1S,\frac{1}{2}^+)}(\text{keV}) &\approx 250.87 - 15.01[\mathcal{O}(1/m_c)] + 0.90[\mathcal{O}(1/m_c^2)],\end{aligned}\quad (27)$$

$$\begin{aligned}\Gamma_{\Xi_c^0(1D,\frac{3}{2}^+) \rightarrow \Xi_c^0(1S,\frac{1}{2}^+)}(\text{keV}) &\approx 19.29 - 2.83[\mathcal{O}(1/m_c)] + 0.14[\mathcal{O}(1/m_c^2)], \\ \Gamma_{\Xi_c^0(1D,\frac{5}{2}^+) \rightarrow \Xi_c^0(1S,\frac{1}{2}^+)}(\text{keV}) &\approx 20.23 + 2.11[\mathcal{O}(1/m_c)] + 0.17[\mathcal{O}(1/m_c^2)],\end{aligned}\quad (28)$$

$$\begin{aligned}\Gamma_{\Xi_c^0(1F,\frac{5}{2}^-) \rightarrow \Xi_c^0(1S,\frac{1}{2}^+)}(\text{keV}) &\approx 27.70 + 1.29[\mathcal{O}(1/m_c)] + 0.02[\mathcal{O}(1/m_c^2)], \\ \Gamma_{\Xi_c^0(1F,\frac{7}{2}^-) \rightarrow \Xi_c^0(1S,\frac{1}{2}^+)}(\text{keV}) &\approx 27.38 - 0.96[\mathcal{O}(1/m_c)] + 0.02[\mathcal{O}(1/m_c^2)],\end{aligned}\quad (29)$$

$$\begin{aligned}\Gamma_{\Xi_c^+(1P,\frac{1}{2}^-) \rightarrow \Xi_c^+(1S,\frac{1}{2}^+)}(\text{keV}) &\approx 0.77 + 1.37[\mathcal{O}(1/m_c)] + 0.61[\mathcal{O}(1/m_c^2)], \\ \Gamma_{\Xi_c^+(1P,\frac{3}{2}^-) \rightarrow \Xi_c^+(1S,\frac{1}{2}^+)}(\text{keV}) &\approx 1.30 - 1.08[\mathcal{O}(1/m_c)] + 0.90[\mathcal{O}(1/m_c^2)],\end{aligned}\quad (30)$$

$$\begin{aligned}\Gamma_{\Xi_c^+(1D,\frac{3}{2}^+) \rightarrow \Xi_c^+(1S,\frac{1}{2}^+)}(\text{keV}) &\approx 26.36 + 3.31[\mathcal{O}(1/m_c)] + 0.14[\mathcal{O}(1/m_c^2)], \\ \Gamma_{\Xi_c^+(1D,\frac{5}{2}^+) \rightarrow \Xi_c^+(1S,\frac{1}{2}^+)}(\text{keV}) &\approx 28.41 - 2.50[\mathcal{O}(1/m_c)] + 0.17[\mathcal{O}(1/m_c^2)],\end{aligned}\quad (31)$$

$$\begin{aligned}\Gamma_{\Xi_c^+(1F,\frac{5}{2}^-) \rightarrow \Xi_c^+(1S,\frac{1}{2}^+)}(\text{keV}) &\approx 0.08 - 0.07[\mathcal{O}(1/m_c)] + 0.02[\mathcal{O}(1/m_c^2)], \\ \Gamma_{\Xi_c^+(1F,\frac{7}{2}^-) \rightarrow \Xi_c^+(1S,\frac{1}{2}^+)}(\text{keV}) &\approx 0.07 + 0.05[\mathcal{O}(1/m_c)] + 0.02[\mathcal{O}(1/m_c^2)].\end{aligned}\quad (32)$$

Here, m_c is in unit of GeV. According to Eqs. (24)–(32), the leading-order widths within the same doublet have similar values. This suggests that heavy quark spin symmetry plays an important role in these processes. The next and next-next leading orders depend on $\frac{1}{m_c}$ and $\frac{1}{m_b}$. Notably, the coefficients of these terms exhibit significant differences between the $J = |L - \frac{1}{2}|$ and $J = |L + \frac{1}{2}|$ states. These differences primarily arise from the variations in the spatial wave functions and angular momentum structures.

For the $\bar{\Lambda}_f$ single-bottom baryons, we also calculate the radiative decay widths for the $\bar{\Lambda}_f \rightarrow 1S + \gamma$ processes. The numerical results are listed in Table IV.

In the Λ_b states, $\Lambda_b(5912)$ and $\Lambda_b(5920)$ are good candidates for $\Lambda_c(1P, \frac{1}{2}^-)$ and $\Lambda_b(1P, \frac{3}{2}^-)$, respectively. However, these states do not have two-body OZI-allowed decay channels and are observed through the three-body strong decay channel $\Lambda_b^0 \pi^+ \pi^-$. In this context, they are considered narrow states, and their radiative decays may constitute considerable fractions of their total decay widths. Our calculations show that the widths for the $\Lambda_b^0 \gamma$ decays of $\Lambda_c(1P, \frac{1}{2}^-)$ and $\Lambda_b(1P, \frac{3}{2}^-)$ are approximately 40 keV, which is significantly larger than those for the $\Sigma_b^{(*)0} \gamma$ channels.

The Ξ_b baryons have two charge states: negative and neutral, each with different electromagnetic properties. In the Ξ_b

family, the $\Xi_b^-(1P, \frac{3}{2}^-)$ candidate $\Xi_b^-(6100)$ was first observed by the CMS Collaboration and confirmed by the LHCb Collaboration. The $\Xi_b^0(1P, \frac{1}{2}^-)$ and $\Xi_b^0(1P, \frac{3}{2}^-)$ candidates were also established by the LHCb Collaboration. However, the $\Xi_b^-(1P, \frac{1}{2}^-)$ state has not been observed yet. As shown in Table IV, all $\Xi_b(1P) \rightarrow \Xi_b(1S)\gamma$ processes exhibit large widths. Therefore, besides searching for the $\Xi_b^-(1P, \frac{1}{2}^-)$ in the $\Xi_b^-\pi^+\pi^-$ channel, we also suggest searching for it in the $\Xi_b^-(1S, \frac{1}{2}^+)\gamma$ channel.

The $\Lambda_b(1D)$ candidates, $\Lambda_b(6146)$ and $\Lambda_b(6152)$, and the $\Xi_b(1D)$ candidates, $\Xi_b(6327)$ and $\Xi_b(6333)$, were observed by the LHCb Collaboration. According to the measured widths, these are all narrow states. As shown in Table IV, the decay processes $\Lambda_b(1D) \rightarrow \Lambda_b(1S)\gamma$ and $\Xi_b(1D) \rightarrow \Xi_b(1S)\gamma$ also have considerable decay widths.

Until now, the candidates for $\Lambda_b(1F)$, $\Xi_b(1F)$, and $\Xi_b(2S)$ have not been observed. In our calculations, the predicted widths for $\Lambda_b^0(1F) \rightarrow \Lambda_b^0(1S)\gamma$ and $\Xi_b^-(1F) \rightarrow \Xi_b^-(1S)\gamma$ are approximately 15 and 33 keV, respectively. However, we do not find any significant decay widths for the $\Xi_b^0(1F)$, $\Lambda_b(2S)$, and $\Xi_b(2S)$ in the $1S\gamma$ channels.

To analyze the dependence of the decay widths on $\frac{1}{m_b}$, we expand the decay widths in terms of $\frac{1}{m_b}$, i.e.,

$$\begin{aligned}\Gamma_{\Lambda_b^0(1P,\frac{1}{2}^-) \rightarrow \Lambda_b^0(1S,\frac{1}{2}^+)}(\text{keV}) &\approx 46.65 + 1.94[\mathcal{O}(1/m_b)] + 0.02[\mathcal{O}(1/m_b^2)], \\ \Gamma_{\Lambda_b^0(1P,\frac{3}{2}^-) \rightarrow \Lambda_b^0(1S,\frac{1}{2}^+)}(\text{keV}) &\approx 49.27 - 1.06[\mathcal{O}(1/m_b)] + 0.02[\mathcal{O}(1/m_b^2)],\end{aligned}\quad (33)$$

$$\begin{aligned}\Gamma_{\Lambda_b^0(1D, \frac{3}{2}^+) \rightarrow \Lambda_b^0(1S, \frac{1}{2}^+)}(\text{keV}) &\approx 26.77 - 0.25[\mathcal{O}(1/m_b)] + 0.001[\mathcal{O}(1/m_b^2)], \\ \Gamma_{\Lambda_b^0(1D, \frac{5}{2}^+) \rightarrow \Lambda_b^0(1S, \frac{1}{2}^+)}(\text{keV}) &\approx 27.19 + 0.17[\mathcal{O}(1/m_b)] + 0.001[\mathcal{O}(1/m_b^2)],\end{aligned}\quad (34)$$

$$\begin{aligned}\Gamma_{\Lambda_b^0(1F, \frac{5}{2}^-) \rightarrow \Lambda_b^0(1S, \frac{1}{2}^+)}(\text{keV}) &\approx 15.45 + 0.03[\mathcal{O}(1/m_b)] + 0.00002[\mathcal{O}(1/m_b^2)], \\ \Gamma_{\Lambda_b^0(1F, \frac{7}{2}^-) \rightarrow \Lambda_b^0(1S, \frac{1}{2}^+)}(\text{keV}) &\approx 15.44 - 0.02[\mathcal{O}(1/m_b)] + 0.00002[\mathcal{O}(1/m_b^2)],\end{aligned}\quad (35)$$

$$\begin{aligned}\Gamma_{\Xi_b^-(1P, \frac{1}{2}^-) \rightarrow \Xi_b^-(1S, \frac{1}{2}^+)}(\text{keV}) &\approx 79.63 - 2.72[\mathcal{O}(1/m_b)] + 0.02[\mathcal{O}(1/m_b^2)], \\ \Gamma_{\Xi_b^-(1P, \frac{3}{2}^-) \rightarrow \Xi_b^-(1S, \frac{1}{2}^+)}(\text{keV}) &\approx 84.20 + 1.49[\mathcal{O}(1/m_b)] + 0.03[\mathcal{O}(1/m_b^2)],\end{aligned}\quad (36)$$

$$\begin{aligned}\Gamma_{\Xi_b^-(1D, \frac{3}{2}^+) \rightarrow \Xi_b^-(1S, \frac{1}{2}^+)}(\text{keV}) &\approx 78.78 + 0.54[\mathcal{O}(1/m_b)] + 0.001[\mathcal{O}(1/m_b^2)], \\ \Gamma_{\Xi_b^-(1D, \frac{5}{2}^+) \rightarrow \Xi_b^-(1S, \frac{1}{2}^+)}(\text{keV}) &\approx 80.07 - 0.37[\mathcal{O}(1/m_b)] + 0.001[\mathcal{O}(1/m_b^2)],\end{aligned}\quad (37)$$

$$\begin{aligned}\Gamma_{\Xi_b^-(1F, \frac{5}{2}^-) \rightarrow \Xi_b^-(1S, \frac{1}{2}^+)}(\text{keV}) &\approx 33.11 - 0.06[\mathcal{O}(1/m_b)] + 0.00004[\mathcal{O}(1/m_b^2)], \\ \Gamma_{\Xi_b^-(1F, \frac{7}{2}^-) \rightarrow \Xi_b^-(1S, \frac{1}{2}^+)}(\text{keV}) &\approx 33.24 + 0.05[\mathcal{O}(1/m_b)] + 0.00004[\mathcal{O}(1/m_b^2)],\end{aligned}\quad (38)$$

$$\begin{aligned}\Gamma_{\Xi_b^0(1P, \frac{1}{2}^-) \rightarrow \Xi_b^0(1S, \frac{1}{2}^+)}(\text{keV}) &\approx 33.57 + 1.76[\mathcal{O}(1/m_b)] + 0.02[\mathcal{O}(1/m_b^2)], \\ \Gamma_{\Xi_b^0(1P, \frac{3}{2}^-) \rightarrow \Xi_b^0(1S, \frac{1}{2}^+)}(\text{keV}) &\approx 35.42 - 0.97[\mathcal{O}(1/m_b)] + 0.03[\mathcal{O}(1/m_b^2)],\end{aligned}\quad (39)$$

$$\begin{aligned}\Gamma_{\Xi_b^0(1D, \frac{3}{2}^+) \rightarrow \Xi_b^0(1S, \frac{1}{2}^+)}(\text{keV}) &\approx 10.28 - 0.20[\mathcal{O}(1/m_b)] + 0.001[\mathcal{O}(1/m_b^2)], \\ \Gamma_{\Xi_b^0(1D, \frac{5}{2}^+) \rightarrow \Xi_b^0(1S, \frac{1}{2}^+)}(\text{keV}) &\approx 10.30 + 0.13[\mathcal{O}(1/m_b)] + 0.001[\mathcal{O}(1/m_b^2)],\end{aligned}\quad (40)$$

$$\begin{aligned}\Gamma_{\Xi_b^0(1F, \frac{5}{2}^-) \rightarrow \Xi_b^0(1S, \frac{1}{2}^+)}(\text{keV}) &\approx 3.55 + 0.02[\mathcal{O}(1/m_b)] + 0.00004[\mathcal{O}(1/m_b^2)], \\ \Gamma_{\Xi_b^0(1F, \frac{7}{2}^-) \rightarrow \Xi_b^0(1S, \frac{1}{2}^+)}(\text{keV}) &\approx 3.52 - 0.01[\mathcal{O}(1/m_b)] + 0.00004[\mathcal{O}(1/m_b^2)].\end{aligned}\quad (41)$$

Here, m_b is in unit of GeV. By comparing our results with those for charmed baryons, we find that the decay widths within a doublet exhibit smaller differences in the bottom baryons. This can be attributed to the heavy quark spin symmetry, which is closely related to the mass of the heavy flavor quark. In the constituent quark model, we have $m_b > m_c$. Consequently, we expect that the radiative decay width gaps are smaller in bottom baryons.

B. $6_f \rightarrow 1S + \gamma$

In the radiative decay processes of 6_f single-charm baryons, we also calculate the widths of radiative decays with final states $\Lambda_c(1S)/\Sigma_c(1S)/\Xi_c^{(*)}(1S)/\Omega_c(1S)\gamma$ as the prior. The numerical results are given in Table V.

The transitions $\Sigma_c^{(*)}(1S) \rightarrow \Lambda_c(1S)\gamma$ and $\Sigma_c^{(*)}(1S) \rightarrow \Sigma_c(1S)\gamma$ involve changes only in the spin wave functions, making them typical M1 transitions. In the radiative decays of $\Sigma_c(1S)$, the decay widths for $\Sigma_c^+(1S, \frac{1}{2}^+) \rightarrow \Lambda_c^+(1S, \frac{1}{2}^+)\gamma$

and $\Sigma_c^{*+}(1S, \frac{3}{2}^+) \rightarrow \Lambda_c^+(1S, \frac{1}{2}^+)\gamma$ are calculated to be 59.2 and 132.8 keV, respectively, consistent with the quark model calculations in Refs. [34, 35, 41, 44, 45], and also match the calculations with light cone QCD sum rules [21, 23, 26], heavy quark effective theory [27, 29], chiral perturbation theory [31, 32], and chiral quark-soliton model [46, 47]. Given that the $\Lambda_c^+(1S, \frac{1}{2}^+)$ is well established, these processes are promising candidates for experimental observation, which would be crucial for understanding the internal structure of baryons. The $\Sigma_c^0(1S, \frac{1}{2}^+)$ and $\Sigma_c^{++}(1S, \frac{1}{2}^+)$ states do not undergo radiative decays, as they are the lowest states with the same quark content. But $\Sigma_c^*(1S, \frac{3}{2}^+)$ can decay into $\Sigma_c(1S, \frac{1}{2}^+)\gamma$. The calculated widths of $\Sigma_c^0(1S, \frac{3}{2}^+)$, $\Sigma_c^{*+}(1S, \frac{3}{2}^+)$, and $\Sigma_c^{*++}(1S, \frac{3}{2}^+)$ decaying into $\Sigma_c^0(1S, \frac{1}{2}^+)\gamma$, $\Sigma_c^+(1S, \frac{1}{2}^+)\gamma$, and $\Sigma_c^{++}(1S, \frac{1}{2}^+)\gamma$ are 1.3, < 0.1 , and 1.7 keV, respectively. Because of the small phase space, these widths are quite narrow. For the $\Sigma_c(1P)$ states, we note that some radiative decay widths are larger than 100 keV, such as $\Sigma_c^0(1P, \frac{1}{2}^-) \rightarrow \Sigma_c^0(1S, \frac{1}{2}^+)\gamma$, $\Sigma_c^0(1P, \frac{1}{2}^-) \rightarrow \Sigma_c^0(1S, \frac{1}{2}^+)\gamma$, and so on. But there are no large decay widths

TABLE V: The radiative decay widths (in units of keV) of single-charm baryons in the 6_f representation decaying into the $\Lambda_c(1S)/\Sigma_c(1S)/\Xi_c^{(\prime)}(1S)/\Omega_c(1S)\gamma$.

Process	Our	Ref. [41]	Ref. [34]	Ref. [35]	Process	Our	Ref. [41]	Ref. [34]	Ref. [35]
$\Sigma_c^{*0}(1S, \frac{3}{2}^+) \rightarrow \Sigma_c^0(1S, \frac{1}{2}^+) \gamma$	1.3	3.43	1.8	1.378	$\Xi_c^{*0}(1S, \frac{1}{2}^+) \rightarrow \Xi_c^0(1S, \frac{1}{2}^+) \gamma$	0.3	0.0	0.4	0.342
$\Sigma_c^+(1S, \frac{1}{2}^+) \rightarrow \Lambda_c^+(1S, \frac{1}{2}^+) \gamma$	59.2	80.6	87.2	93.5	$\Xi_c^{*0}(1S, \frac{3}{2}^+) \rightarrow \Xi_c^0(1S, \frac{1}{2}^+) \gamma$	1.1	0.0	1.6	1.322
$\Sigma_c^{*+}(1S, \frac{3}{2}^+) \rightarrow \Lambda_c^+(1S, \frac{1}{2}^+) \gamma$	132.8	373	199.4	231	$\Xi_c^{*0}(1S, \frac{3}{2}^+) \rightarrow \Xi_c^0(1S, \frac{1}{2}^+) \gamma$	1.0	3.03	1.4	1.262
$\Sigma_c^{*+}(1S, \frac{3}{2}^+) \rightarrow \Sigma_c^+(1S, \frac{1}{2}^+) \gamma$	0.0	0.004	0.0	0.00067	$\Xi_c^{*+}(1S, \frac{1}{2}^+) \rightarrow \Xi_c^+(1S, \frac{1}{2}^+) \gamma$	14.9	42.3	20.6	21.38
$\Sigma_c^{*++}(1S, \frac{3}{2}^+) \rightarrow \Sigma_c^{++}(1S, \frac{1}{2}^+) \gamma$	1.7	3.94	2.1	1.483	$\Xi_c^{*+}(1S, \frac{3}{2}^+) \rightarrow \Xi_c^+(1S, \frac{1}{2}^+) \gamma$	52.7	139	74.2	81.9
					$\Xi_c^{*+}(1S, \frac{3}{2}^+) \rightarrow \Xi_c^+(1S, \frac{1}{2}^+) \gamma$	0.1	0.004	0.1	0.029
					$\Omega_c^{*0}(1S, \frac{3}{2}^+) \rightarrow \Omega_c^0(1S, \frac{1}{2}^+) \gamma$	0.9	0.89	1.0	1.14
$\Sigma_c^0(1S, \frac{1}{2}^+) \gamma$	$\Sigma_c^{*0}(1S, \frac{3}{2}^+) \gamma$	$\Lambda_c^+(1S, \frac{1}{2}^+) \gamma$	$\Sigma_c^+(1S, \frac{1}{2}^+) \gamma$	$\Sigma_c^{*+}(1S, \frac{3}{2}^+) \gamma$	$\Sigma_c^{*+}(1S, \frac{1}{2}^+) \gamma$	$\Sigma_c^{*++}(1S, \frac{3}{2}^+) \gamma$			
$\Sigma_{c0}^{0,+,++}(1P, \frac{1}{2}^-)$	137.8	183.0	0.0	3.3	2.7	236.2			281.6
$\Sigma_{c1}^{0,+,++}(1P, \frac{1}{2}^-)$	202.7	68.4	84.5	1.5	0.9	279.0			93.4
$\Sigma_{c1}^{0,+,++}(1P, \frac{3}{2}^-)$	59.3	209.2	95.8	1.9	1.8	101.1			291.4
$\Sigma_{c2}^{0,+,++}(1P, \frac{3}{2}^-)$	158.8	25.5	49.9	1.9	0.7	133.6			26.8
$\Sigma_{c2}^{0,+,++}(1P, \frac{5}{2}^-)$	1.5	148.2	53.5	1.1	0.7	11.1			148.9
$\Sigma_{c1}^{0,+,++}(1D, \frac{1}{2}^+)$	0.8	76.6	11.0	0.1	56.0	2.5			562.5
$\Sigma_{c1}^{0,+,++}(1D, \frac{3}{2}^+)$	46.5	42.0	11.1	32.3	29.3	330.8			299.2
$\Sigma_{c2}^{0,+,++}(1D, \frac{3}{2}^+)$	26.0	24.6	29.8	22.9	20.6	214.6			195.7
$\Sigma_{c2}^{0,+,++}(1D, \frac{5}{2}^+)$	13.7	39.9	30.0	10.0	31.8	99.9			308.8
$\Sigma_{c3}^{0,+,++}(1D, \frac{5}{2}^+)$	13.6	4.9	14.6	19.7	5.3	156.6			45.7
$\Sigma_{c3}^{0,+,++}(1D, \frac{7}{2}^+)$	1.1	19.5	14.6	0.1	21.5	3.2			186.8
$\Sigma_{c2}^{0,+,++}(1F, \frac{3}{2}^-)$	0.2	63.5	3.7	0.1	7.3	1.2			178.3
$\Sigma_{c2}^{0,+,++}(1F, \frac{5}{2}^-)$	32.9	28.1	3.6	3.8	3.4	92.6			80.7
$\Sigma_{c3}^{0,+,++}(1F, \frac{5}{2}^-)$	17.3	22.8	8.2	1.7	2.4	45.7			62.1
$\Sigma_{c3}^{0,+,++}(1F, \frac{7}{2}^-)$	9.7	29.8	8.0	1.1	3.3	26.8			82.8
$\Sigma_{c4}^{0,+,++}(1F, \frac{7}{2}^-)$	14.1	5.3	3.8	1.0	0.5	32.7			13.4
$\Sigma_{c4}^{0,+,++}(1F, \frac{9}{2}^-)$	0.2	18.9	3.8	0.1	1.7	1.1			48.5
$\Sigma_c^{0,+,++}(2S, \frac{1}{2}^+)$	14.6	0.4	117.8	3.3	0.8	55.6			5.8
$\Sigma_c^{*0,+,++}(2S, \frac{3}{2}^+)$	10.8	11.5	151.2	0.7	3.5	24.3			50.9
$\Xi_c^0(1S, \frac{1}{2}^+) \gamma$	$\Xi_c^{*0}(1S, \frac{1}{2}^+) \gamma$	$\Xi_c^{*0}(1S, \frac{3}{2}^+) \gamma$	$\Xi_c^+(1S, \frac{1}{2}^+) \gamma$	$\Xi_c^+(1S, \frac{1}{2}^+) \gamma$	$\Xi_c^{*+}(1S, \frac{3}{2}^+) \gamma$	$\Xi_c^{*+}(1S, \frac{1}{2}^+) \gamma$	$\Omega_c^0(1S, \frac{1}{2}^+) \gamma$	$\Omega_c^{*0}(1S, \frac{3}{2}^+) \gamma$	
$\Xi_{c0}^{0,+}(1P, \frac{1}{2}^-)$	0.0	109.0	150.1	0.0	1.2	0.6	$\Omega_{c0}^0(1P, \frac{1}{2}^-)$	83.7	110.2
$\Xi_{c1}^{0,+}(1P, \frac{1}{2}^-)$	0.5	172.8	59.7	36.3	0.0	1.0	$\Omega_{c1}^0(1P, \frac{1}{2}^-)$	143.6	46.9
$\Xi_{c1}^{0,+}(1P, \frac{3}{2}^-)$	0.6	50.1	187.3	44.9	1.6	0.3	$\Omega_{c1}^0(1P, \frac{3}{2}^-)$	41.8	154.3
$\Xi_{c2}^{0,+}(1P, \frac{3}{2}^-)$	0.3	165.4	26.9	24.3	9.6	2.2	$\Omega_{c2}^0(1P, \frac{3}{2}^-)$	168.3	26.2
$\Xi_{c2}^{0,+}(1P, \frac{5}{2}^-)$	0.4	0.7	156.8	27.1	1.7	5.1	$\Omega_{c2}^0(1P, \frac{5}{2}^-)$	0.2	155.1
$\Xi_{c1}^{0,+}(1D, \frac{1}{2}^+)$	0.0	0.4	32.4	4.4	0.1	38.1	$\Omega_{c1}^0(1D, \frac{1}{2}^+)$	0.2	11.4
$\Xi_{c1}^{0,+}(1D, \frac{3}{2}^+)$	0.0	20.9	18.4	4.6	19.8	19.5	$\Omega_{c1}^0(1D, \frac{3}{2}^+)$	8.5	6.9
$\Xi_{c2}^{0,+}(1D, \frac{3}{2}^+)$	0.1	11.6	10.7	12.5	14.7	14.4	$\Omega_{c2}^0(1D, \frac{3}{2}^+)$	4.5	3.9
$\Xi_{c2}^{0,+}(1D, \frac{5}{2}^+)$	0.1	6.5	18.2	12.9	6.1	21.3	$\Omega_{c2}^0(1D, \frac{5}{2}^+)$	2.8	7.2
$\Xi_{c3}^{0,+}(1D, \frac{5}{2}^+)$	0.0	5.9	2.3	6.5	12.4	3.8	$\Omega_{c3}^0(1D, \frac{5}{2}^+)$	2.1	0.9
$\Xi_{c3}^{0,+}(1D, \frac{7}{2}^+)$	0.0	0.6	9.3	6.5	0.1	14.0	$\Omega_{c3}^0(1D, \frac{7}{2}^+)$	0.4	3.9
$\Xi_{c2}^{0,+}(1F, \frac{3}{2}^-)$	0.0	0.1	39.3	1.3	0.1	0.2	$\Omega_{c2}^0(1F, \frac{3}{2}^-)$	0.0	24.5
$\Xi_{c2}^{0,+}(1F, \frac{5}{2}^-)$	0.0	20.5	17.2	1.3	0.0	0.1	$\Omega_{c2}^0(1F, \frac{5}{2}^-)$	13.0	10.7
$\Xi_{c3}^{0,+}(1F, \frac{5}{2}^-)$	0.0	12.0	15.5	3.0	0.1	0.1	$\Omega_{c3}^0(1F, \frac{5}{2}^-)$	8.5	10.8
$\Xi_{c3}^{0,+}(1F, \frac{7}{2}^-)$	0.0	6.5	20.0	3.0	0.1	0.1	$\Omega_{c3}^0(1F, \frac{7}{2}^-)$	4.5	13.8
$\Xi_{c4}^{0,+}(1F, \frac{7}{2}^-)$	0.0	11.7	4.2	1.4	0.3	0.1	$\Omega_{c4}^0(1F, \frac{7}{2}^-)$	9.9	3.5
$\Xi_{c4}^{0,+}(1F, \frac{9}{2}^-)$	0.0	0.1	15.1	1.4	0.1	0.2	$\Omega_{c4}^0(1F, \frac{9}{2}^-)$	0.0	12.3
$\Xi_c^{0,+}(2S, \frac{1}{2}^+)$	1.2	7.4	0.0	46.9	6.2	1.1	$\Omega_c^0(2S, \frac{1}{2}^+)$	3.0	0.2
$\Xi_c^{0,+}(2S, \frac{3}{2}^+)$	1.3	7.6	5.4	74.9	1.4	6.0	$\Omega_c^0(2S, \frac{3}{2}^+)$	5.4	1.9

TABLE VI: The radiative decay widths (in units of keV) of single-bottom baryons in the 6_f representation decaying into the $\Lambda_b(1S)/\Sigma_b(1S)/\Xi_b^{(*)}(1S)/\Omega_b(1S)\gamma$.

Process	Our	Ref. [41]	Ref. [34]	Ref. [35]	Process	Our	Ref. [41]	Ref. [34]	Ref. [35]
$\Sigma_b^{*-}(1S, \frac{3}{2}^+) \rightarrow \Sigma_b^-(1S, \frac{1}{2}^+) \gamma$	0.0	0.06	0.0	0.0144	$\Xi_b^{*-}(1S, \frac{1}{2}^+) \rightarrow \Xi_b^-(1S, \frac{1}{2}^+) \gamma$	0.6	0.0	0.6	0.707
$\Sigma_b^0(1S, \frac{1}{2}^+) \rightarrow \Lambda_b^0(1S, \frac{1}{2}^+) \gamma$	94.7	130	128.1	151.9	$\Xi_b^{*-}(1S, \frac{3}{2}^+) \rightarrow \Xi_b^-(1S, \frac{1}{2}^+) \gamma$	0.8	0.0	1.0	1.044
$\Sigma_b^{*0}(1S, \frac{3}{2}^+) \rightarrow \Lambda_b^0(1S, \frac{1}{2}^+) \gamma$	120.2	335	168.8	198.8	$\Xi_b^{*-}(1S, \frac{3}{2}^+) \rightarrow \Xi_b^-(1S, \frac{1}{2}^+) \gamma$	0.0	15.0	0.0	0.0122
$\Sigma_b^{*0}(1S, \frac{3}{2}^+) \rightarrow \Sigma_b^0(1S, \frac{1}{2}^+) \gamma$	0.0	0.02	0.0	0.0059	$\Xi_b^0(1S, \frac{1}{2}^+) \rightarrow \Xi_b^0(1S, \frac{1}{2}^+) \gamma$	28.0	84.6	28.4	46.9
$\Sigma_b^{*+}(1S, \frac{3}{2}^+) \rightarrow \Sigma_b^+(1S, \frac{1}{2}^+) \gamma$	0.1	0.25	0.1	0.080	$\Xi_b^0(1S, \frac{3}{2}^+) \rightarrow \Xi_b^0(1S, \frac{1}{2}^+) \gamma$	40.8	104	45.2	65.0
					$\Xi_b^0(1S, \frac{3}{2}^+) \rightarrow \Xi_b^0(1S, \frac{1}{2}^+) \gamma$	0.0	5.19	0.0	0.0069
					$\Omega_b^{*-}(1S, \frac{3}{2}^+) \rightarrow \Omega_b^-(1S, \frac{1}{2}^+) \gamma$	0.0	0.1	0.0	0.056
$\Sigma_b^-(1S, \frac{1}{2}^+) \gamma$	$\Sigma_b^{*-}(1S, \frac{3}{2}^+) \gamma$	$\Lambda_b^0(1S, \frac{1}{2}^+) \gamma$	$\Sigma_b^0(1S, \frac{1}{2}^+) \gamma$	$\Sigma_b^{*0}(1S, \frac{3}{2}^+) \gamma$	$\Sigma_b^+(1S, \frac{1}{2}^+) \gamma$	$\Sigma_b^{*+}(1S, \frac{3}{2}^+) \gamma$			
$\Sigma_{b0}^{-,0,+}(1P, \frac{1}{2}^-)$	75.0	128.2	0.0	26.9	46.7	362.5			624.6
$\Sigma_{b1}^{-,0,+}(1P, \frac{1}{2}^-)$	100.1	46.4	116.8	38.4	17.6	501.9			230.7
$\Sigma_{b1}^{-,0,+}(1P, \frac{3}{2}^-)$	30.0	122.2	122.5	11.0	46.7	146.7			610.7
$\Sigma_{b2}^{-,0,+}(1P, \frac{3}{2}^-)$	56.2	12.3	63.7	25.3	5.1	308.0			64.3
$\Sigma_{b2}^{-,0,+}(1P, \frac{5}{2}^-)$	1.7	66.2	66.0	0.4	29.0	6.7			357.4
$\Sigma_{b1}^{-,0,+}(1D, \frac{1}{2}^+)$	0.9	193.7	16.9	0.2	44.3	3.6			741.1
$\Sigma_{b1}^{-,0,+}(1D, \frac{3}{2}^+)$	102.2	100.4	16.9	23.4	23.0	391.0			384.6
$\Sigma_{b2}^{-,0,+}(1D, \frac{3}{2}^+)$	63.9	64.3	45.3	14.4	14.6	243.0			244.8
$\Sigma_{b2}^{-,0,+}(1D, \frac{5}{2}^+)$	30.3	100.1	45.4	6.9	22.6	115.6			381.1
$\Sigma_{b3}^{-,0,+}(1D, \frac{5}{2}^+)$	44.1	14.0	21.8	9.6	3.1	165.1			52.7
$\Sigma_{b3}^{-,0,+}(1D, \frac{7}{2}^+)$	1.0	57.4	21.9	0.3	12.6	4.1			215.6
$\Sigma_{b2}^{-,0,+}(1F, \frac{3}{2}^-)$	0.5	88.7	6.2	0.1	22.7	1.9			359.2
$\Sigma_{b2}^{-,0,+}(1F, \frac{5}{2}^-)$	47.1	39.9	6.0	12.1	10.2	190.6			161.7
$\Sigma_{b3}^{-,0,+}(1F, \frac{5}{2}^-)$	23.6	31.4	13.8	6.1	8.0	95.7			127.2
$\Sigma_{b3}^{-,0,+}(1F, \frac{7}{2}^-)$	13.7	41.8	13.7	3.5	10.7	55.5			169.2
$\Sigma_{b4}^{-,0,+}(1F, \frac{7}{2}^-)$	18.1	6.9	6.5	4.7	1.8	73.6			28.2
$\Sigma_{b4}^{-,0,+}(1F, \frac{9}{2}^-)$	0.4	25.5	6.5	0.1	6.6	1.6			103.4
$\Sigma_b^{-,0,+}(2S, \frac{1}{2}^+)$	13.9	4.2	172.2	3.5	0.9	55.7			15.8
$\Sigma_b^{*-,0,+}(2S, \frac{3}{2}^+)$	4.8	15.9	187.9	1.3	3.9	20.2			63.3
$\Xi_b^-(1S, \frac{1}{2}^+) \gamma$	$\Xi_b^{*-}(1S, \frac{1}{2}^+) \gamma$	$\Xi_b^{*-}(1S, \frac{3}{2}^+) \gamma$	$\Xi_b^{*-}(1S, \frac{3}{2}^+) \gamma$	$\Xi_b^0(1S, \frac{1}{2}^+) \gamma$	$\Xi_b^0(1S, \frac{1}{2}^+) \gamma$	$\Xi_b^{*0}(1S, \frac{3}{2}^+) \gamma$	$\Omega_b^-(1S, \frac{1}{2}^+) \gamma$	$\Omega_b^{*-}(1S, \frac{3}{2}^+) \gamma$	
$\Xi_{b0}^{*-0}(1P, \frac{1}{2}^-)$	0.0	44.5	75.5	0.0	20.6	35.6	$\Omega_{b0}^-(1P, \frac{1}{2}^-)$	30.9	51.9
$\Xi_{b1}^{*-0}(1P, \frac{1}{2}^-)$	0.7	64.1	28.9	44.9	28.4	13.4	$\Omega_{b1}^-(1P, \frac{1}{2}^-)$	48.3	21.3
$\Xi_{b1}^{*-0}(1P, \frac{3}{2}^-)$	0.7	19.2	79.3	49.3	8.5	35.4	$\Omega_{b1}^-(1P, \frac{3}{2}^-)$	14.4	60.2
$\Xi_{b2}^{*-0}(1P, \frac{3}{2}^-)$	0.4	43.9	9.0	26.8	16.8	3.9	$\Omega_{b2}^-(1P, \frac{3}{2}^-)$	39.9	7.8
$\Xi_{b2}^{*-0}(1P, \frac{5}{2}^-)$	0.4	0.9	52.1	28.6	0.6	19.9	$\Omega_{b2}^-(1P, \frac{5}{2}^-)$	0.6	47.5
$\Xi_{b1}^{*-0}(1D, \frac{1}{2}^+)$	0.0	0.3	109.3	6.6	0.2	18.4	$\Omega_{b1}^-(1D, \frac{1}{2}^+)$	0.1	70.0
$\Xi_{b1}^{*-0}(1D, \frac{3}{2}^+)$	0.0	58.8	57.3	6.7	9.4	9.6	$\Omega_{b1}^-(1D, \frac{3}{2}^+)$	38.2	37.1
$\Xi_{b2}^{*-0}(1D, \frac{3}{2}^+)$	0.1	39.9	39.5	18.0	5.3	5.8	$\Omega_{b2}^-(1D, \frac{3}{2}^+)$	28.4	28.0
$\Xi_{b2}^{*-0}(1D, \frac{5}{2}^+)$	0.1	18.8	62.7	18.4	2.7	8.7	$\Omega_{b2}^-(1D, \frac{5}{2}^+)$	13.3	44.9
$\Xi_{b3}^{*-0}(1D, \frac{5}{2}^+)$	0.1	33.1	10.0	9.0	2.5	1.1	$\Omega_{b3}^-(1D, \frac{5}{2}^+)$	28.2	8.3
$\Xi_{b3}^{*-0}(1D, \frac{7}{2}^+)$	0.1	0.5	43.0	9.1	0.2	3.6	$\Omega_{b3}^-(1D, \frac{7}{2}^+)$	0.2	36.7
$\Xi_{b2}^{*-0}(1F, \frac{3}{2}^-)$	0.0	0.2	47.5	2.4	0.1	4.8	$\Omega_{b2}^-(1F, \frac{3}{2}^-)$	0.1	27.0
$\Xi_{b2}^{*-0}(1F, \frac{5}{2}^-)$	0.0	25.7	21.5	2.4	2.3	2.1	$\Omega_{b2}^-(1F, \frac{5}{2}^-)$	14.7	12.3
$\Xi_{b3}^{*-0}(1F, \frac{5}{2}^-)$	0.0	13.6	17.8	5.3	1.1	1.6	$\Omega_{b3}^-(1F, \frac{5}{2}^-)$	8.4	11.1
$\Xi_{b3}^{*-0}(1F, \frac{7}{2}^-)$	0.0	7.9	24.0	5.3	0.7	2.0	$\Omega_{b3}^-(1F, \frac{7}{2}^-)$	4.9	15.0
$\Xi_{b4}^{*-0}(1F, \frac{7}{2}^-)$	0.0	12.1	4.4	2.5	0.6	0.3	$\Omega_{b4}^-(1F, \frac{7}{2}^-)$	8.7	3.1
$\Xi_{b4}^{*-0}(1F, \frac{9}{2}^-)$	0.0	0.2	16.9	2.5	0.1	0.9	$\Omega_{b4}^-(1F, \frac{9}{2}^-)$	0.1	12.3
$\Xi_b^{*-0}(2S, \frac{1}{2}^+)$	1.2	5.5	1.4	64.4	4.6	1.1	$\Omega_b^-(2S, \frac{1}{2}^+)$	2.3	0.4
$\Xi_b^{*-0}(2S, \frac{3}{2}^+)$	1.3	2.2	6.4	77.8	1.8	5.1	$\Omega_b^-(2S, \frac{3}{2}^+)$	1.1	2.8

for the $\Sigma_c^+(1P) \rightarrow \Sigma_c^+(1S, \frac{1}{2}^+) \gamma$ and $\Sigma_c^+(1P) \rightarrow \Sigma_c^{*+}(1S, \frac{3}{2}^+) \gamma$ decays. According to Table V, we suggest looking for the $\Sigma_c^0(1S, \frac{1}{2}^+) \gamma$, $\Sigma_c^{*0}(1S, \frac{3}{2}^+) \gamma$, $\Lambda_c^+(1S, \frac{1}{2}^+) \gamma$, $\Sigma_c^{*+}(1S, \frac{1}{2}^+) \gamma$, and $\Sigma_c^{*++}(1S, \frac{3}{2}^+) \gamma$ modes of the $\Sigma_c(1P)$. For the the $\Sigma_c(1D)$ and $\Sigma_c(1F)$, we find large radiative decay widths from the $\Sigma_c^{*+}(1S, \frac{1}{2}^+) \gamma$ and $\Sigma_c^{*++}(1S, \frac{3}{2}^+) \gamma$ channels. Finally, for the two $\Sigma_c(2S)$ states, the partial widths of the $\Lambda_c^+(1S, \frac{1}{2}^+) \gamma$ mode are calculated to be larger than 100 keV. In addition, the $\Sigma_c^{*+}(1S, \frac{1}{2}^+) \gamma$ and $\Sigma_c^{*++}(1S, \frac{3}{2}^+) \gamma$ modes are also significant for the discussed $\Sigma_c(2S)$ state.

In the following, we will discuss the radiative decays of the Ξ'_c states. Two typical single-charm baryons are $\Xi_c^0(1S, \frac{1}{2}^+)$ and $\Xi_c^+(1S, \frac{1}{2}^+)$, where these two states have been observed in their radiative decays [17]. In Sec. III A, we point out that the coupling between the Ξ_c^0 state and $\Xi_c^0 \gamma$ is forbidden if we employ strict SU(3) flavor symmetry. The conclusion remains the same if we reverse the initial and final single-charm baryons in the above transition. But it is obviously in conflict with the experimental data [17]. In Sec. III A, we consider the mass differences of $m_d - m_s$ to obtain small decay widths. In this subsection, we use the same approach to obtain the decay width of $\Xi_c^0(1S, \frac{1}{2}^+) \rightarrow \Xi_c^0(1S, \frac{1}{2}^+) \gamma$ at 0.3 keV. We propose to measure the width of the $\Xi_c^0(1S, \frac{1}{2}^+)$ in high-precision experiments, which could test the SU(3) flavor symmetry and further unravel the structure of the single-charm baryon. In addition, the widths of the $\Xi_c^+(1S, \frac{1}{2}^+)$ and $\Xi_c^{*+}(1S, \frac{3}{2}^+)$ decays into $\Xi_c^+(1S, \frac{1}{2}^+) \gamma$ are 14.9 and 52.7 keV, respectively. For the $\Xi'_c(1P)$ states, we find some partial widths that are larger than 100 keV corresponding to the $\Xi_c^0(1S, \frac{1}{2}^+) \gamma$ and $\Xi_c^{*0}(1S, \frac{3}{2}^+) \gamma$ channels. So far, there are several good $\Xi'_c(1P)$ candidates that have been observed in experiment, i.e., the $\Xi_c(2880)$, $\Xi_c(2923)$, $\Xi_c(2939)$, and $\Xi_c(2965)$ [79, 80]. In previous experiments, these states have been studied by surveying their strong decays. In fact, the search for these states is also interesting using different approaches such as their radiative decays with $\Xi_c^0(1S, \frac{1}{2}^+) \gamma$ and $\Xi_c^{*0}(1S, \frac{3}{2}^+) \gamma$ channels. In this work, we do not find the radiative decay widths of the discussed $\Xi'_c(1D)$ and $\Xi'_c(1F)$ states that are larger than 50 keV as indicated in Table V. For the two $\Xi'_c(2S)$ states, the decay widths of their $\Xi_c^+(1S, \frac{1}{2}^+) \gamma$ modes are much larger than other radiative decay channels.

For the $\Omega_c^{*0}(1S, \frac{3}{2}^+)$ state, the dominant radiative decay channel is $\Omega_c^0(1S, \frac{1}{2}^+) \gamma$, which has been observed in experiments [18, 19]. In 2017, the LHCb Collaboration [81] observed the $\Omega_c(3000)$, $\Omega_c(3050)$, $\Omega_c(3065)$, $\Omega_c(3090)$, and $\Omega_c(3119)$ from the pp collisions. According to the theoretical mass spectra and decay widths [42, 82–94], they could be considered as $\Omega_c(1P)$ or $\Omega_c(2S)$ candidates. In 2023, these states were confirmed in the same productions [95]. In addition, except for $\Omega_c(3119)$, the remaining four states were observed in e^+e^- collisions by the Belle Collaboration [96] and in $\Omega_b^- \rightarrow \Omega_c^0(\text{?})\pi^- \rightarrow \Xi_c^+ K^- \pi^-$ by the LHCb Collaboration [97]. However, their J^P quantum numbers are still unknown. According to Table V, the radiative decay channels $\Omega_c^0(1S, \frac{1}{2}^+) \gamma$ and $\Omega_c^{*0}(1S, \frac{3}{2}^+) \gamma$ of the $\Omega_c(1P)$ have larger widths. This gives

us a new approach to study these states. We propose to study the $\Omega_c(1P)$ states in the $\Omega_c^0(1S, \frac{1}{2}^+) \gamma$ and $\Omega_c^{*0}(1S, \frac{3}{2}^+) \gamma$ channels. However, for the $\Omega_c(1D)$, $\Omega_c(1F)$, and $\Omega_c(2S)$, both partial widths of the $\Omega_c^0(1S, \frac{1}{2}^+) \gamma$ and $\Omega_c^{*0}(1S, \frac{3}{2}^+) \gamma$ channels are not obvious. Although observations of the higher excited states $\Omega_c(3188)$ and $\Omega_c(3327)$ help us to construct the $\Omega_c(2S)$ and $\Omega_c(1D)$ spectroscopy [59, 81, 95, 96, 98–101], the search for the $\Omega_c(1D)$, $\Omega_c(1F)$, and $\Omega_c(2S)$ in $\Omega_c^0(1S, \frac{1}{2}^+) \gamma$ and $\Omega_c^{*0}(1S, \frac{3}{2}^+) \gamma$ processes is really difficult in the expected future.

The radiative decays of 6_f single-bottom baryons into $\Lambda_b(1S) \gamma$, $\Sigma_b(1S) \gamma$, $\Xi_b^{(\prime)} \gamma$, and $\Omega_b(1S) \gamma$ are presented in Table VI. This table shows that there are no significant radiative decay widths for the Σ_b^\pm . For the $\Sigma_b^{(*)0}$, the decay widths involving the $\Lambda_b^0(1S, \frac{1}{2}^+) \gamma$ channel are approximately 100 keV. However, the neutral $\Sigma_c^{(*)0}$ states have not yet been observed. In addition to the $\Lambda_b^0 \pi^0$ channel, the $\Lambda_b^0 \gamma$ channel is also a viable method for searching for $\Sigma_c^{(*)0}$ states. Among the $\Xi_b'(1S)$ states, the $\Xi_b'^{-}(1S, \frac{1}{2}^+)$ and $\Xi_b^{*,0,-}(1S, \frac{3}{2}^+)$ have been established. However, the $\Xi_b'^{,0}(1S, \frac{1}{2}^+)$ remains undiscovered, possibly because the $\Xi_b^- \pi^+$ channel is kinematically forbidden. We note that the $\Xi_b^0 \pi^0$ channel might be open, so we suggest searching for the $\Xi_b'^{,0}(1S, \frac{1}{2}^+)$ in the $\Xi_b^0 \pi^0$ and $\Xi_b^0 \gamma$ channels simultaneously. Finally, for the $\Omega_b^-(1S, \frac{3}{2}^+)$, the calculated radiative decay widths are about or less than 0.1 keV. However, the $\Omega_b^-(1S, \frac{1}{2}^+) \gamma$ decay mode constitutes nearly 100% of the branching fraction, making the observation of the $\Omega_b^{*-}(1S, \frac{3}{2}^+)$ via the $\Omega_b^-(1S, \frac{1}{2}^+) \gamma$ process a promising possibility.

Besides the $1S$ 6_f states, the LHCb Collaboration has recently observed some $1P$ candidates, namely $\Sigma_b(6097)$ [49], $\Xi_b(6227)$ [48], $\Omega_b(6316)$, $\Omega_b(6330)$, $\Omega_b(6340)$, and $\Omega_b(6350)$ [53]. These states have been identified through their two-body strong decays in previous works. In this study, we also calculate their radiative decay widths. As shown in Table VI, some decay channels exhibit significantly large widths, such as $\Sigma_b^+(1P, \frac{1}{2}^-) \rightarrow \Sigma_b^{*+}(1S, \frac{3}{2}^+) \gamma$ and $\Sigma_b^+(1P, \frac{1}{2}^-) \rightarrow \Sigma_b^+(1S, \frac{1}{2}^+) \gamma$. These findings suggest that some missing $1P$ states may be discovered through their radiative decays.

Until now, there have been no strong candidates for the $1D$, $1F$, and $2S$ states in the 6_f bottom baryons. In this work, we calculate the mass spectra and radiative decay widths for these states. For the $\Sigma_b(1D)$ and $\Sigma_b(1F)$ states, we identify several radiative decay channels with widths in the hundreds of keV, which may provide valuable clues for searching for these states via radiative decays. However, for the $\Sigma_c(2S)$, $\Xi_c'(1D)$, $\Xi_c'(1F)$, $\Xi_c'(2S)$, $\Omega_c(1D)$, $\Omega_c(1F)$, and $\Omega_c(2S)$ states, the radiative decay widths listed in Table VI are significantly smaller than those of the $\Sigma_b(1D)$ and $\Sigma_b(1F)$ states.

The calculations above are based on the quenched quark model, where the baryon is treated as a simple three-quark system. However, in the unquenched quark model, quark-antiquark pairs can be created from the vacuum, leading to coupled channel effects [102–107]. Coupled channel effects can influence the properties of hadrons. Previous stud-

ies [108, 109] have suggested that if the mass of a hadron is near the thresholds of certain S -wave channels, significant coupled channel effects may arise. Notable examples include $D_{s0}^*(2317)$ [110–115], $D_s'(2460)$ [114, 115], $X(3872)$ [116–119], and $\Lambda(1405)$ [120]. The observed masses of these hadrons are approximately 100 MeV lower than the predictions of the quenched quark model, leading to what is known as the “low mass puzzle.” However, when the unquenched picture, including coupled channel effects, is considered [110–120], this puzzle can be alleviated. The low mass puzzle is also evident in single-charm baryons. While most observed single-charm baryons align well with theoretical predictions from the quenched quark model, the $\Lambda_c(2940)$ stands out as a peculiar case. It is considered a candidate for the $\Lambda_c(2P)$ state; however, quenched quark models predict the mass of the $\Lambda_c(2P)$ to be about 60 to 100 MeV higher than the observed mass of the $\Lambda_c(2940)$. On the other hand, the $\Lambda_c(2940)$ is very close to the threshold of the S -wave D^*N channel. In Refs. [121, 122], the authors introduced the D^*N channel in the $\Lambda_c(2P)$ calculation, and the mass was lowered to match the $\Lambda_c(2940)$. Given the significant coupled channel effect in $\Lambda_c(2940)$, its decay behaviors should also be studied within the unquenched quark model, considering the contributions of the D^*N channel. However, the $\Lambda_c(2940)$ is an exceptional case. Although the conditions required for significant coupled-channel effects are stringent, they do not entirely rule out the existence of states similar to $\Lambda_c(2940)$. Currently, most of the observed low-lying singly heavy baryons align well with quenched quark model calculations [69, 70, 72, 73, 75, 76, 123–125]. However, several predicted $1P$, $1D$, and $2S$ states remain unobserved. In our previous work [57], we also calculated the mass spectra of $1F$ single-charm baryons, which have yet to be experimentally confirmed. As experimental techniques advance, we anticipate the discovery of a more complete family of singly heavy baryons. This will deepen our understanding of the applicability of the quenched quark model.

C. Relativistic corrections in radiative decays

In Eq. (2), we consider only the two simplest terms of the Hamiltonian, representing the nonrelativistic approximation. However, in our calculations, the Hamiltonian involves more complex interactions [64, 66, 126–128], necessitating the inclusion of relativistic corrections. It is important to discuss the model’s applicability, but incorporating fully relativistic forms poses significant challenges. Therefore, we approximate by expanding the interactions in powers of $\frac{1}{m_q}$ or $\frac{1}{m_Q}$. Here, we take the relativistic correction [128] term

$$h_e^{\text{RC}} \sim \sum_j -e^{-ik \cdot r_j} \frac{\sigma_j \times p_j \cdot \epsilon}{4m_j^2}. \quad (42)$$

We now define the radiative decay width as follows:

$$\Gamma_{\text{RC}} = \Gamma_{\text{NR}} + \Delta\Gamma_{\text{RC}}, \quad (43)$$

where Γ_{NR} represents the decay width obtained from the non-relativistic model, where the Hamiltonian is given by Eq. (2).

The term $\Delta\Gamma_{\text{RC}}$ denotes the relativistic correction, which quantifies the impact of relativistic effects on the radiative decay width. Below, we present examples to illustrate these corrections:

Process	Γ_{NR} (keV)	$\Delta\Gamma_{\text{RC}}$ (keV)
$\Sigma_c^0(1S, \frac{3}{2}^+) \rightarrow \Sigma_c^0(1S, \frac{1}{2}^+) \gamma$	1.3	~ -0.07
$\Sigma_c^+(1S, \frac{1}{2}^+) \rightarrow \Lambda_c^+(1S, \frac{1}{2}^+) \gamma$	59.2	~ -9.5
$\Sigma_c^{*+}(1S, \frac{3}{2}^+) \rightarrow \Lambda_c^+(1S, \frac{1}{2}^+) \gamma$	132.8	~ -27.5
$\Sigma_c^{*+}(1S, \frac{3}{2}^+) \rightarrow \Sigma_c^+(1S, \frac{1}{2}^+) \gamma$	0.007	~ -0.002
$\Sigma_c^{*+}(1S, \frac{3}{2}^+) \rightarrow \Sigma_c^{++}(1S, \frac{1}{2}^+) \gamma$	1.7	~ -0.15

Process	Γ_{NR} (keV)	$\Delta\Gamma_{\text{RC}}$ (keV)
$\Xi_c^0(1S, \frac{1}{2}^+) \rightarrow \Xi_c^0(1S, \frac{1}{2}^+) \gamma$	0.3	~ -0.06
$\Xi_c^0(1S, \frac{3}{2}^+) \rightarrow \Xi_c^0(1S, \frac{1}{2}^+) \gamma$	1.1	~ -0.3
$\Xi_c^{*0}(1S, \frac{3}{2}^+) \rightarrow \Xi_c^{*0}(1S, \frac{1}{2}^+) \gamma$	1.0	~ -0.04
$\Xi_c^+(1S, \frac{1}{2}^+) \rightarrow \Xi_c^+(1S, \frac{1}{2}^+) \gamma$	14.9	~ -1.5
$\Xi_c^{*+}(1S, \frac{3}{2}^+) \rightarrow \Xi_c^+(1S, \frac{1}{2}^+) \gamma$	52.7	~ -7.9
$\Xi_c^{*+}(1S, \frac{3}{2}^+) \rightarrow \Xi_c^{*+}(1S, \frac{1}{2}^+) \gamma$	0.1	~ -0.01

Process	Γ_{NR} (keV)	$\Delta\Gamma_{\text{RC}}$ (keV)
$\Omega_c^0(1S, \frac{3}{2}^+) \rightarrow \Omega_c^0(1S, \frac{1}{2}^+) \gamma$	0.9	~ -0.03

Process	Γ_{NR} (keV)	$\Delta\Gamma_{\text{RC}}$ (keV)
$\Lambda_c^+(2S, \frac{1}{2}^+) \rightarrow \Lambda_c^+(1S, \frac{1}{2}^+) \gamma$	0.02	~ -0.02
$\Lambda_c^+(1P, \frac{1}{2}^-) \rightarrow \Lambda_c^+(1S, \frac{1}{2}^+) \gamma$	0.1	~ 0.4
$\Lambda_c^+(1D, \frac{3}{2}^+) \rightarrow \Lambda_c^+(1S, \frac{1}{2}^+) \gamma$	41.3	~ -1.5
$\Lambda_c^+(1F, \frac{5}{2}^-) \rightarrow \Lambda_c^+(1S, \frac{1}{2}^+) \gamma$	4.6	~ 0.15

Process	Γ_{NR} (keV)	$\Delta\Gamma_{\text{RC}}$ (keV)
$\Xi_c^0(2S, \frac{1}{2}^+) \rightarrow \Xi_c^0(1S, \frac{1}{2}^+) \gamma$	0.04	~ -0.04
$\Xi_c^0(1P, \frac{1}{2}^-) \rightarrow \Xi_c^0(1S, \frac{1}{2}^+) \gamma$	217.5	~ -13.7
$\Xi_c^0(1D, \frac{3}{2}^+) \rightarrow \Xi_c^0(1S, \frac{1}{2}^+) \gamma$	17.8	~ 1.3
$\Xi_c^0(1F, \frac{5}{2}^-) \rightarrow \Xi_c^0(1S, \frac{1}{2}^+) \gamma$	28.4	~ -0.6

Based on the above calculations, we observe that some corrections are significant, such as in the cases of $\Sigma_c^{*+}(1S, \frac{3}{2}^+) \rightarrow \Lambda_c^+(1S, \frac{1}{2}^+) \gamma$ and $\Xi_c^0(1P, \frac{1}{2}^-) \rightarrow \Xi_c^0(1S, \frac{1}{2}^+) \gamma$. However, most corrections in the calculations are relatively small. We find no clear correlation between the magnitude of the corrections and the orbital or radial quantum numbers.

It is worth noting that σ and p are one-order irreducible tensors related to spin and spatial wave functions. One possible scenario is that when the spin or orbital quantum numbers change by one unit ($\Delta S = 1$ or $\Delta L = 1$) during the decay process, relativistic corrections might become significant. However, the calculations in this work are not fully relativistic. More serious discussions on this issue could be obtained using relativistic approaches such as the Bethe-Salpeter (BS) equations [129–131], the light-front quark model [132], among others.

IV. SUMMARY

At the beginning of the 21st century, the situation of observing singly heavy baryons has changed, as more and more singly heavy baryons have been reported in various experiments such as Belle and LHCb. It can be reflected by checking the presently collected singly heavy baryons in the PDG [16]. Although the radiative decays of single-charm baryons have not been extensively reported compared to these observed strong and weak decay modes, the radiative decay of single-charm baryons is one aspect of the whole decay behavior of them that should be paid more attention. In particular, in the face of the high-precision era of hadron spectroscopy, we have reason to believe that more radiative decays of singly heavy baryons will become experimentally accessible. With the promotion of experimental precision, we need to increase theoretical precision.

In this work, we revisit the radiative decays of singly heavy baryons. In contrast to the treatment in the previous work [57], we adopt the numerical spatial wave function for the singly heavy baryon, which can be obtained by the concrete potential model and with that approach the GEM [58]. This treatment can meet the requirements of high-precision hadron spectroscopy. We also make a comparison with the current experimental data [20] and the theoretical results from other groups [34, 35, 41], as summarized in the last section.

With the running of Belle II [60, 61] and Run-3 and Run-4 of LHCb [62, 63], we can expect more observations of

singly heavy baryons. This information on the radiative decay of singly heavy baryons will stimulate our experimental colleagues to focus on exploring the spectroscopy of singly heavy baryons.

Acknowledgments

This work is supported by the National Natural Science Foundation of China under Grants No. 12335001, No. 12247101, and No. 1240050206, National Key Research and Development Program of China under Contract No. 2020YFA0406400, the 111 Project under Grant No. B20063, the fundamental Research Funds for the Central Universities, and the project for top-notch innovative talents of Gansu province.

Appendix A: Some additional radiative decay widths

In Tables VII–XIV, we also list the calculated results of other radiative decay widths of singly heavy baryons. The final states of these discussed radiative decays are involved in radial or orbital excited states of singly heavy baryons. This information is left to the readers who are interested in exploring these allowed radiative decays.

-
- [1] X. Liu, An overview of *XYZ* new particles, *Chin. Sci. Bull.* **59**, 3815–3830 (2014).
- [2] H. Y. Cheng, Charmed baryons circa 2015, *Front. Phys. (Beijing)* **10**, 101406 (2015).
- [3] H. X. Chen, W. Chen, X. Liu, Y. R. Liu, and S. L. Zhu, A review of the open charm and open bottom systems, *Rept. Prog. Phys.* **80**, 076201 (2017).
- [4] H. X. Chen, W. Chen, X. Liu, and S. L. Zhu, The hidden-charm pentaquark and tetraquark states, *Phys. Rept.* **639**, 1–121 (2016).
- [5] E. Klemt and J. M. Richard, Baryon spectroscopy, *Rev. Mod. Phys.* **82**, 1095–1153 (2010).
- [6] F. K. Guo, C. Hanhart, U. G. Meißner, Q. Wang, Q. Zhao, and B. S. Zou, Hadronic molecules, *Rev. Mod. Phys.* **90**, 015004 (2018), [Erratum: Rev.Mod.Phys. 94, 029901 (2022)].
- [7] N. Brambilla, S. Eidelman, C. Hanhart, A. Nefediev, C. P. Shen, C. E. Thomas, A. Vairo, and C. Z. Yuan, The *XYZ* states: Experimental and theoretical status and perspectives, *Phys. Rept.* **873**, 1–154 (2020).
- [8] Y. R. Liu, H. X. Chen, W. Chen, X. Liu, and S. L. Zhu, Pentaquark and tetraquark states, *Prog. Part. Nucl. Phys.* **107**, 237–320 (2019).
- [9] H. Y. Cheng, Charmed baryon physics circa 2021, *Chin. J. Phys.* **78**, 324–362 (2022).
- [10] L. Meng, B. Wang, G. J. Wang, and S. L. Zhu, Chiral perturbation theory for heavy hadrons and chiral effective field theory for heavy hadronic molecules, *Phys. Rept.* **1019**, 1–149 (2023).
- [11] H. X. Chen, W. Chen, X. Liu, Y. R. Liu, and S. L. Zhu, An updated review of the new hadron states, *Rept. Prog. Phys.* **86**, 026201 (2023).
- [12] X. Chu (BES III Collaboration), Hadron spectroscopy at BES III, *PoS HQL2016*, 028 (2017).
- [13] J. Wang (LHCb Collaboration), Heavy flavour and exotic production at LHCb, *PoS ICHEP2022*, 487 (2022).
- [14] J. Xu (LHCb Collaboration), LHCb results in charm baryons, *Nucl. Part. Phys. Proc.* **318-323**, 56–60 (2022).
- [15] Y. Onuki (Belle-II Collaboration), Belle II status and prospect, *Nucl. Part. Phys. Proc.* **318-323**, 78–84 (2022).
- [16] R. L. Workman *et al.* (Particle Data Group), Review of particle physics, *PTEP* **2022**, 083C01 (2022).
- [17] C. P. Jessop *et al.* (CLEO Collaboration), Observation of two narrow states decaying into $\Xi_c^+\gamma$ and $\Xi_c^0\gamma$, *Phys. Rev. Lett.* **82**, 492–496 (1999).
- [18] B. Aubert *et al.* (BaBar Collaboration), Observation of an excited charm baryon Ω_c^* decaying to $\Omega_c^0\gamma$, *Phys. Rev. Lett.* **97**, 232001 (2006).
- [19] E. Solovieva *et al.*, Study of Ω_c^0 and Ω_c^{*0} baryons at Belle, *Phys. Lett. B* **672**, 1–5 (2009).
- [20] J. Yelton *et al.* (Belle Collaboration), Study of electromagnetic decays of orbitally excited Ξ_c baryons, *Phys. Rev. D* **102**, 071103 (2020).
- [21] T. M. Aliev, K. Azizi, and A. Ozpineci, Radiative decays of the heavy flavored baryons in light cone QCD sum rules, *Phys. Rev. D* **79**, 056005 (2009).
- [22] T. M. Aliev, K. Azizi, and H. Sundu, Radiative $\Omega_Q^* \rightarrow \Omega_Q\gamma$ and $\Xi_Q^* \rightarrow \Xi_Q'\gamma$ transitions in light cone QCD, *Eur. Phys. J. C* **75**, 14 (2015).

TABLE VII: Radiative decay widths (in units of keV) of 3_f single-charm baryon decaying into radial or orbital excited states.

	$\Lambda_c^+/\Xi_c^{0,+}(1P, \frac{1}{2}^-)\gamma$			$\Lambda_c^+/\Xi_c^{0,+}(1P, \frac{3}{2}^-)\gamma$			$\Lambda_c^+/\Xi_c^{0,+}(2S, \frac{1}{2}^+)\gamma$		
	Λ_c^+	Ξ_c^0	Ξ_c^+	Λ_c^+	Ξ_c^0	Ξ_c^+	Λ_c^+	Ξ_c^0	Ξ_c^+
$\Lambda_c^+/\Xi_c^{0,+}(2S, \frac{1}{2}^+)$	0.3	45.9	0.0	0.2	68.1	0.1
$\Lambda_c^+/\Xi_c^{0,+}(1D, \frac{3}{2}^+)$	0.3	270.4	1.2	0.1	46.0	0.4	0.1	0.0	0.0
$\Lambda_c^+/\Xi_c^{0,+}(1D, \frac{5}{2}^+)$	0.3	0.6	0.1	1.1	298.8	0.6	0.3	0.1	0.1
$\Lambda_c^+/\Xi_c^{0,+}(1F, \frac{5}{2}^-)$	74.3	35.7	55.2	19.8	10.0	15.6	1.1	3.7	0.2
$\Lambda_c^+/\Xi_c^{0,+}(1F, \frac{7}{2}^-)$	0.7	0.7	0.2	81.5	48.4	61.7	1.2	3.9	0.3
	$\Lambda_c^+/\Xi_c^{0,+}(1D, \frac{3}{2}^+)\gamma$			$\Lambda_c^+/\Xi_c^{0,+}(1D, \frac{5}{2}^+)\gamma$			$\Sigma_c^+/\Xi_c^{0,+}(1P, \frac{1}{2}^-)\gamma$		
	Λ_c^+	Ξ_c^0	Ξ_c^+	Λ_c^+	Ξ_c^0	Ξ_c^+	Σ_c^+	Ξ_c^0	Ξ_c^+
$\Lambda_c^+/\Xi_c^{0,+}(2S, \frac{1}{2}^+)$	0.0	0.0
$\Lambda_c^+/\Xi_c^{0,+}(1D, \frac{3}{2}^+)$	0.0	0.0	0.1
$\Lambda_c^+/\Xi_c^{0,+}(1D, \frac{5}{2}^+)$	0.0	0.0	0.0	0.0	0.0	0.2	0.0
$\Lambda_c^+/\Xi_c^{0,+}(1F, \frac{5}{2}^-)$	0.5	398.6	1.7	0.0	26.6	0.3	0.3	0.0	0.5
$\Lambda_c^+/\Xi_c^{0,+}(1F, \frac{7}{2}^-)$	0.1	0.3	0.1	1.1	354.3	0.6	0.3	0.0	0.5
	$\Sigma_c^+/\Xi_c^{0,+}(1P, \frac{3}{2}^-)\gamma$			$\Sigma_c^+/\Xi_c^{0,+}(1P, \frac{3}{2}^-)\gamma$			$\Sigma_c^+/\Xi_c^{0,+}(1P, \frac{5}{2}^-)\gamma$		
	Σ_c^+	Ξ_c^0	Ξ_c^+	Σ_c^+	Ξ_c^0	Ξ_c^+	Σ_c^+	Ξ_c^0	Ξ_c^+
$\Lambda_c^+/\Xi_c^{0,+}(2S, \frac{1}{2}^+)$...	0.0	0.0	...	0.0	0.0	...	0.0	0.0
$\Lambda_c^+/\Xi_c^{0,+}(1D, \frac{3}{2}^+)$	0.0	0.0	0.1	0.1	0.0	0.5	0.0	0.0	0.0
$\Lambda_c^+/\Xi_c^{0,+}(1D, \frac{5}{2}^+)$	0.1	0.0	0.4	0.0	0.0	0.1	0.1	0.0	0.5
$\Lambda_c^+/\Xi_c^{0,+}(1F, \frac{5}{2}^-)$	0.3	0.0	0.5	1.5	0.0	2.1	0.3	0.0	0.5
$\Lambda_c^+/\Xi_c^{0,+}(1F, \frac{7}{2}^-)$	0.8	0.0	1.2	0.2	0.0	0.3	1.4	0.0	2.0
	$\Sigma_c^{*+}/\Xi_c^{*0,+}(2S, \frac{3}{2}^+)\gamma$			$\Sigma_c^{*+}/\Xi_c^{*0,+}(1D, \frac{1}{2}^+)\gamma$			$\Sigma_c^{*+}/\Xi_c^{*0,+}(1D, \frac{3}{2}^+)\gamma$		
	Σ_c^+	Ξ_c^0	Ξ_c^+	Σ_c^+	Ξ_c^0	Ξ_c^+	Σ_c^+	Ξ_c^0	Ξ_c^+
$\Lambda_c^+/\Xi_c^{0,+}(1F, \frac{5}{2}^-)$	0.0	0.0	0.0	0.0	0.0	0.1	0.0	0.0	0.0
$\Lambda_c^+/\Xi_c^{0,+}(1F, \frac{7}{2}^-)$	0.0	0.0	0.0	0.0	0.0	0.0	0.0	0.0	0.0
	$\Sigma_c^{*+}/\Xi_c^{*0,+}(1D, \frac{5}{2}^+)\gamma$			$\Sigma_c^{*+}/\Xi_c^{*0,+}(1D, \frac{5}{2}^+)\gamma$			$\Sigma_c^{*+}/\Xi_c^{*0,+}(1D, \frac{7}{2}^+)\gamma$		
	Σ_c^+	Ξ_c^0	Ξ_c^+	Σ_c^+	Ξ_c^0	Ξ_c^+	Σ_c^+	Ξ_c^0	Ξ_c^+
$\Lambda_c^+/\Xi_c^{0,+}(1F, \frac{5}{2}^-)$	0.0	0.0	0.0	0.0	0.0	0.5	0.0	0.0	0.0
$\Lambda_c^+/\Xi_c^{0,+}(1F, \frac{7}{2}^-)$	0.0	0.0	0.2	0.0	0.0	0.0	0.0	0.0	0.5
	$\Sigma_c^{*+}/\Xi_c^{*0,+}(1D, \frac{5}{2}^+)\gamma$			$\Sigma_c^{*+}/\Xi_c^{*0,+}(1D, \frac{5}{2}^+)\gamma$			$\Sigma_c^{*+}/\Xi_c^{*0,+}(1D, \frac{7}{2}^+)\gamma$		
	Σ_c^+	Ξ_c^0	Ξ_c^+	Σ_c^+	Ξ_c^0	Ξ_c^+	Σ_c^+	Ξ_c^0	Ξ_c^+
$\Lambda_c^+/\Xi_c^{0,+}(1F, \frac{5}{2}^-)$	0.0	0.0	0.0	0.0	0.0	0.5	0.0	0.0	0.0
$\Lambda_c^+/\Xi_c^{0,+}(1F, \frac{7}{2}^-)$	0.0	0.0	0.2	0.0	0.0	0.0	0.0	0.0	0.5

- [23] T. M. Aliev, T. Barakat, and M. Savci, Analysis of the radiative decays $\Sigma_Q \rightarrow \Lambda_Q\gamma$ and $\Xi'_Q \rightarrow \Xi_Q\gamma$ in light cone sum rules, [Phys. Rev. D **93**, 056007 \(2016\)](#).
- [24] Z. G. Wang, Analysis of the vertexes $\Omega_Q^*\Omega_Q\phi$ and radiative decays $\Omega_Q^* \rightarrow \Omega_Q\gamma$, [Phys. Rev. D **81**, 036002 \(2010\)](#).
- [25] Z. G. Wang, Analysis of the vertexes $\Xi_Q^*\Xi'_Q V$, $\Sigma_Q^*\Sigma_Q V$ and radiative decays $\Xi_Q^* \rightarrow \Xi'_Q\gamma$, $\Sigma_Q^* \rightarrow \Sigma_Q\gamma$, [Eur. Phys. J. A **44**, 105–117 \(2010\)](#).
- [26] S. L. Zhu and Y. B. Dai, Radiative decays of heavy hadrons from light cone QCD sum rules in the leading order of HQET, [Phys. Rev. D **59**, 114015 \(1999\)](#).
- [27] H. Y. Cheng, C. Y. Cheung, G. L. Lin, Y. C. Lin, T. M. Yan, and H. L. Yu, Chiral Lagrangians for radiative decays of heavy hadrons, [Phys. Rev. D **47**, 1030–1042 \(1993\)](#).
- [28] S. L. Zhu, Strong and electromagnetic decays of p -wave heavy baryons Λ_{c1} , Λ_{c1}^* , [Phys. Rev. D **61**, 114019 \(2000\)](#).
- [29] S. Tawfiq, J. G. Korner, and P. J. O'Donnell, Electromagnetic transitions of heavy baryons in the $SU(2N_f) \otimes O(3)$ symmetry, [Phys. Rev. D **63**, 034005 \(2001\)](#).
- [30] H. S. Li, L. Meng, Z. W. Liu, and S. L. Zhu, Radiative decays of the doubly charmed baryons in chiral perturbation theory, [Phys. Lett. B **777**, 169–176 \(2018\)](#).
- [31] N. Jiang, X. L. Chen, and S. L. Zhu, Electromagnetic decays of the charmed and bottom baryons in chiral perturbation theory, [Phys. Rev. D **92**, 054017 \(2015\)](#).
- [32] G. J. Wang, L. Meng, and S. L. Zhu, Radiative decays of the singly heavy baryons in chiral perturbation theory, [Phys. Rev. D **99**, 034021 \(2019\)](#).
- [33] K. Gandhi, Z. Shah, and A. K. Rai, Spectrum of nonstrange singly charmed baryons in the constituent quark model, [Int. J. Theor. Phys. **59**, 1129–1156 \(2020\)](#).
- [34] E. Ortiz-Pacheco and R. Bijker, Masses and radiative decay widths of S - and P -wave singly, doubly, and triply heavy charm and bottom baryons, [Phys. Rev. D **108**, 054014 \(2023\)](#).
- [35] A. Hazra, S. Rakshit, and R. Dhir, Radiative $M1$ transitions of heavy baryons: Effective quark mass scheme, [Phys. Rev. D **104**, 053002 \(2021\)](#).
- [36] F. L. Wang, S. Q. Luo, and X. Liu, Radiative decays and mag-

TABLE VIII: Radiative decay widths (in units of keV) of $\Sigma_c(1P)/\Xi'_c(1P)\Sigma_c(2S)/\Xi'_c(2S)/\Omega_c(2S)$ decaying into radial or orbital excited states of the single-charm baryon.

	$\Lambda_c^+/\Xi_c^{0,+}(1P, \frac{1}{2}^-)\gamma$			$\Lambda_c^+/\Xi_c^{0,+}(1P, \frac{3}{2}^-)\gamma$			$\Lambda_c^+/\Xi_c^{0,+}(2S, \frac{1}{2}^+)\gamma$					
	Λ_c^+	Ξ_c^0	Ξ_c^+	Λ_c^+	Ξ_c^0	Ξ_c^+	Λ_c^+	Ξ_c^0	Ξ_c^+			
$\Sigma_{c0}^+/\Xi_{c0}^{0,+}(1P, \frac{1}{2}^-)$	28.4	0.2	7.8	33.0	0.2	7.3	0.0			
$\Sigma_{c1}^+/\Xi_{c1}^{0,+}(1P, \frac{1}{2}^-)$	43.7	0.2	11.5	12.2	0.1	2.5	0.0			
$\Sigma_{c1}^+/\Xi_{c1}^{0,+}(1P, \frac{3}{2}^-)$	15.3	0.1	5.5	47.7	0.3	14.8	0.0			
$\Sigma_{c2}^+/\Xi_{c2}^{0,+}(1P, \frac{3}{2}^-)$	61.3	0.5	22.2	7.2	0.0	2.3	0.0			
$\Sigma_{c2}^+/\Xi_{c2}^{0,+}(1P, \frac{5}{2}^-)$	0.1	0.0	0.0	55.9	0.4	21.0	0.0			
$\Sigma_c^+/\Xi_c^{0,+}(2S, \frac{1}{2}^+)$	11.7	0.1	4.4	19.5	0.1	6.9	63.0	0.4	18.4			
$\Sigma_c^{*+}/\Xi_c^{*0,+}(2S, \frac{3}{2}^+)$	13.3	0.1	5.9	23.9	0.2	9.9	88.1	0.7	35.3			
<hr/>												
	$\Lambda_c^+/\Xi_c^{0,+}(1D, \frac{3}{2}^+)\gamma$			$\Lambda_c^+/\Xi_c^{0,+}(1D, \frac{5}{2}^+)\gamma$			$\Sigma_{c0}^{0,+,++}/\Xi_{c0}^{0,+}/\Omega_c^+(1P, \frac{1}{2}^-)\gamma$					
	Λ_c^+	Ξ_c^0	Ξ_c^+	Λ_c^+	Ξ_c^0	Ξ_c^+	Σ_c^0	Σ_c^+	Σ_c^{++}			
$\Sigma_c^{0,+,++}/\Xi_c^{0,+}/\Omega_c^+(2S, \frac{1}{2}^+)$	0.0	0.0	0.0	0.0	0.0	0.0	10.0	0.0	8.4	10.5	0.3	10.0
$\Sigma_c^{*0,+,++}/\Xi_c^{*0,+}/\Omega_c^{*0}(2S, \frac{3}{2}^+)$	0.0	0.0	0.0	0.0	0.0	0.0	12.3	0.0	10.1	13.4	0.5	13.7
<hr/>												
	$\Sigma_{c1}^{0,+,++}/\Xi_{c1}^{0,+}/\Omega_{c1}^+(1P, \frac{1}{2}^-)\gamma$					$\Sigma_{c1}^{0,+,++}/\Xi_{c1}^{0,+}/\Omega_{c1}^+(1P, \frac{3}{2}^-)\gamma$						
	Σ_c^0	Σ_c^+	Σ_c^{++}	$\Xi_c'^0$	$\Xi_c'^+$	Ω_c^0	Σ_c^0	Σ_c^+	Σ_c^{++}	$\Xi_c'^0$	$\Xi_c'^+$	Ω_c^0
$\Sigma_c^{0,+,++}/\Xi_c^{0,+}/\Omega_c^0(2S, \frac{1}{2}^+)$	28.5	0.0	29.6	27.5	0.3	24.0	11.5	0.1	12.4	10.6	0.2	8.6
$\Sigma_c^{*0,+,++}/\Xi_c^{*0,+}/\Omega_c^{*0}(2S, \frac{3}{2}^+)$	8.9	0.1	10.6	8.7	0.2	8.0	39.3	0.0	40.7	38.1	0.5	34.8
<hr/>												
	$\Sigma_{c2}^{0,+,++}/\Xi_{c2}^{0,+}/\Omega_{c2}^+(1P, \frac{3}{2}^-)\gamma$					$\Sigma_{c2}^{0,+,++}/\Xi_{c2}^{0,+}/\Omega_{c2}^+(1P, \frac{5}{2}^-)\gamma$						
	Σ_c^0	Σ_c^+	Σ_c^{++}	$\Xi_c'^0$	$\Xi_c'^+$	Ω_c^0	Σ_c^0	Σ_c^+	Σ_c^{++}	$\Xi_c'^0$	$\Xi_c'^+$	Ω_c^0
$\Sigma_c^{0,+,++}/\Xi_c^{0,+}/\Omega_c^0(2S, \frac{1}{2}^+)$	103.0	1.0	145.4	77.8	0.2	51.5	0.2	0.1	1.2	0.1	0.1	0.0
$\Sigma_c^{*0,+,++}/\Xi_c^{*0,+}/\Omega_c^{*0}(2S, \frac{3}{2}^+)$	14.4	0.3	23.0	11.3	0.2	8.5	121.1	0.8	162.0	95.2	0.2	70.2
<hr/>												
	$\Sigma_c^{0,+,++}/\Xi_c^{0,+}/\Omega_c^+(2S, \frac{1}{2}^+)\gamma$											
	Σ_c^0	Σ_c^+	Σ_c^{++}	$\Xi_c'^0$	$\Xi_c'^+$	Ω_c^0						
$\Sigma_c^{0,+,++}/\Xi_c^{0,+}/\Omega_c^0(2S, \frac{1}{2}^+)$						
$\Sigma_c^{*0,+,++}/\Xi_c^{*0,+}/\Omega_c^{*0}(2S, \frac{3}{2}^+)$	0.2	0.0	0.2	0.1	0.0	0.2						

- netic moments of the predicted B_c -like molecules, [Phys. Rev. D **107**, 114017 \(2023\)](#).
- [37] M. S. Liu, Q. F. Lü, and X. H. Zhong, Triply charmed and bottom baryons in a constituent quark model, [Phys. Rev. D **101**, 074031 \(2020\)](#).
- [38] Q. F. Lü, K. L. Wang, L. Y. Xiao, and X. H. Zhong, Mass spectra and radiative transitions of doubly heavy baryons in a relativized quark model, [Phys. Rev. D **96**, 114006 \(2017\)](#).
- [39] L. Y. Xiao, K. L. Wang, Q. F. Lü, X. H. Zhong, and S. L. Zhu, Strong and radiative decays of the doubly charmed baryons, [Phys. Rev. D **96**, 094005 \(2017\)](#).
- [40] Y. X. Yao, K. L. Wang, and X. H. Zhong, Strong and radiative decays of the low-lying D -wave singly heavy baryons, [Phys. Rev. D **98**, 076015 \(2018\)](#).
- [41] K. L. Wang, Y. X. Yao, X. H. Zhong, and Q. Zhao, Strong and radiative decays of the low-lying S - and P -wave singly heavy baryons, [Phys. Rev. D **96**, 116016 \(2017\)](#).
- [42] K. L. Wang, L. Y. Xiao, X. H. Zhong, and Q. Zhao, Understanding the newly observed Ω_c states through their decays, [Phys. Rev. D **95**, 116010 \(2017\)](#).
- [43] H. Bahtiyar, K. U. Can, G. Erkol, M. Oka, and T. T. Takahashi, $\Xi_c\gamma \rightarrow \Xi'_c$ transition in lattice QCD, [Phys. Lett. B **772**, 121–126 \(2017\)](#).
- [44] M. A. Ivanov, J. G. Korner, and V. E. Lyubovitskij, One photon transitions between heavy baryons in a relativistic three quark model, [Phys. Lett. B **448**, 143–151 \(1999\)](#).
- [45] M. A. Ivanov, J. G. Korner, V. E. Lyubovitskij, and A. G. Rusetsky, Strong and radiative decays of heavy flavored baryons, [Phys. Rev. D **60**, 094002 \(1999\)](#).
- [46] G. S. Yang and H. C. Kim, Magnetic transitions and radiative decays of singly heavy baryons, [Phys. Lett. B **801**, 135142 \(2020\)](#).
- [47] J. Y. Kim, H. C. Kim, G. S. Yang, and M. Oka, Electromagnetic transitions of the singly charmed baryons with spin 3/2, [Phys. Rev. D **103**, 074025 \(2021\)](#).
- [48] R. Aaij *et al.* (LHCb Collaboration), Observation of a new Ξ_b^- resonance, [Phys. Rev. Lett. **121**, 072002 \(2018\)](#).
- [49] R. Aaij *et al.* (LHCb Collaboration), Observation of two resonances in the $\Lambda_b^0\pi^\pm$ systems and precise measurement of Σ_b^\pm and $\Sigma_b^{*\pm}$ properties, [Phys. Rev. Lett. **122**, 012001 \(2019\)](#).
- [50] R. Aaij *et al.* (LHCb Collaboration), Observation of new resonances in the $\Lambda_b^0\pi^+\pi^-$ system, [Phys. Rev. Lett. **123**, 152001 \(2019\)](#).
- [51] A. M. Sirunyan *et al.* (CMS Collaboration), Study of excited Λ_b^0 states decaying to $\Lambda_b^0\pi^+\pi^-$ in proton-proton collisions at $\sqrt{s} = 13$ TeV, [Phys. Lett. B **803**, 135345 \(2020\)](#).

TABLE IX: Radiative decay widths (in units of keV) of $\Sigma_c(1D)/\Xi'_c(1D)/\Omega_c(1D)$ decaying into radial or orbital excited states of the single-charm baryon.

	$\Lambda_c^+/\Xi_c^{0,+}(1P, \frac{1}{2}^-)\gamma$			$\Lambda_c^+/\Xi_c^{0,+}(1P, \frac{3}{2}^-)\gamma$			$\Lambda_c^+/\Xi_c^{0,+}(2S, \frac{1}{2}^+)\gamma$					
	Λ_c^+	Ξ_c^0	Ξ_c^+	Λ_c^+	Ξ_c^0	Ξ_c^+	Λ_c^+	Ξ_c^0	Ξ_c^+			
$\Sigma_{c1}^+/\Xi_{c1}^{0,+}(1D, \frac{1}{2}^+)$	38.7	0.2	16.1	19.7	0.1	7.6	0.4	0.0	0.0			
$\Sigma_{c1}^+/\Xi_{c1}^{0,+}(1D, \frac{3}{2}^+)$	13.1	0.1	5.4	45.6	0.3	19.2	0.6	0.0	0.1			
$\Sigma_{c2}^+/\Xi_{c2}^{0,+}(1D, \frac{3}{2}^+)$	86.4	0.6	38.1	20.4	0.1	8.7	1.0	0.0	0.1			
$\Sigma_{c2}^+/\Xi_{c2}^{0,+}(1D, \frac{5}{2}^+)$	4.6	0.0	2.0	94.8	0.7	42.4	1.4	0.0	0.2			
$\Sigma_{c3}^+/\Xi_{c3}^{0,+}(1D, \frac{5}{2}^+)$	48.8	0.3	23.0	11.4	0.1	5.3	0.4	0.0	0.0			
$\Sigma_{c3}^+/\Xi_{c3}^{0,+}(1D, \frac{7}{2}^+)$	0.3	0.0	0.0	53.0	0.4	25.2	0.4	0.0	0.1			
<hr/>												
	$\Lambda_c^+/\Xi_c^{0,+}(1D, \frac{3}{2}^+)\gamma$			$\Lambda_c^+/\Xi_c^{0,+}(1D, \frac{5}{2}^+)\gamma$			$\Sigma_{c0}^{0,+,++}/\Xi_{c0}^{0,+}/\Omega_{c0}^0(1P, \frac{1}{2}^-)\gamma$					
	Λ_c^+	Ξ_c^0	Ξ_c^+	Λ_c^+	Ξ_c^0	Ξ_c^+	Σ_c^0	Σ_c^+	Σ_c^{++}	Ξ_c^0	Ξ_c^+	Ω_c^0
$\Sigma_{c1}^{0,+,++}/\Xi_{c1}^{0,+}/\Omega_{c1}^0(1D, \frac{1}{2}^+)$	71.0	0.5	23.5	0.0	0.0	0.0	242.8	0.9	306.3	217.3	0.1	187.7
$\Sigma_{c1}^{0,+,++}/\Xi_{c1}^{0,+}/\Omega_{c1}^0(1D, \frac{3}{2}^+)$	8.5	0.1	3.2	55.4	0.4	19.3	260.8	2.1	361.3	231.6	0.1	203.1
$\Sigma_{c2}^{0,+,++}/\Xi_{c2}^{0,+}/\Omega_{c2}^0(1D, \frac{3}{2}^+)$	50.2	0.4	18.7	3.9	0.0	1.3	2.1	0.5	8.4	1.3	0.9	0.7
$\Sigma_{c2}^{0,+,++}/\Xi_{c2}^{0,+}/\Omega_{c2}^0(1D, \frac{5}{2}^+)$	4.3	0.0	1.8	43.4	0.3	16.8	2.5	0.6	10.1	1.6	1.1	0.9
$\Sigma_{c3}^{0,+,++}/\Xi_{c3}^{0,+}/\Omega_{c3}^0(1D, \frac{5}{2}^+)$	38.7	0.3	16.0	1.8	0.0	0.7	0.1	0.0	0.3	0.1	0.0	0.1
$\Sigma_{c3}^{0,+,++}/\Xi_{c3}^{0,+}/\Omega_{c3}^0(1D, \frac{7}{2}^+)$	0.0	0.0	0.0	30.3	0.3	12.6	0.1	0.0	0.4	0.1	0.0	0.1
<hr/>												
	$\Sigma_{c1}^{0,+,++}/\Xi_{c1}^{0,+}/\Omega_{c1}^0(1P, \frac{1}{2}^-)\gamma$						$\Sigma_{c1}^{0,+,++}/\Xi_{c1}^{0,+}/\Omega_{c1}^0(1P, \frac{3}{2}^-)\gamma$					
	Σ_c^0	Σ_c^+	Σ_c^{++}	$\Xi_c'^0$	$\Xi_c'^+$	Ω_c^0	Σ_c^0	Σ_c^+	Σ_c^{++}	Ξ_c^0	Ξ_c^+	Ω_c^0
$\Sigma_{c1}^{0,+,++}/\Xi_{c1}^{0,+}/\Omega_{c1}^0(1D, \frac{1}{2}^+)$	165.4	2.4	254.1	137.3	0.6	109.7	71.0	0.8	101.8	57.6	0.3	44.4
$\Sigma_{c1}^{0,+,++}/\Xi_{c1}^{0,+}/\Omega_{c1}^0(1D, \frac{3}{2}^+)$	45.3	1.1	77.7	37.1	0.5	29.9	193.7	3.0	298.8	157.2	1.1	124.9
$\Sigma_{c2}^{0,+,++}/\Xi_{c2}^{0,+}/\Omega_{c2}^0(1D, \frac{3}{2}^+)$	220.7	0.5	244.4	216.1	2.2	206.0	39.1	0.4	43.5	37.5	0.9	34.9
$\Sigma_{c2}^{0,+,++}/\Xi_{c2}^{0,+}/\Omega_{c2}^0(1D, \frac{5}{2}^+)$	0.7	0.5	4.9	0.3	0.7	0.1	236.5	0.8	285.2	225.1	1.1	210.4
$\Sigma_{c3}^{0,+,++}/\Xi_{c3}^{0,+}/\Omega_{c3}^0(1D, \frac{5}{2}^+)$	1.7	0.4	6.5	1.2	0.8	0.8	0.4	0.1	1.4	0.3	0.1	0.2
$\Sigma_{c3}^{0,+,++}/\Xi_{c3}^{0,+}/\Omega_{c3}^0(1D, \frac{7}{2}^+)$	0.1	0.0	0.3	0.1	0.0	0.1	1.6	0.4	6.2	1.1	0.7	0.7
<hr/>												
	$\Sigma_{c2}^{0,+,++}/\Xi_{c2}^{0,+}/\Omega_{c2}^0(1P, \frac{3}{2}^-)\gamma$						$\Sigma_{c2}^{0,+,++}/\Xi_{c2}^{0,+}/\Omega_{c2}^0(1P, \frac{5}{2}^-)\gamma$					
	Σ_c^0	Σ_c^+	Σ_c^{++}	$\Xi_c'^0$	$\Xi_c'^+$	Ω_c^0	Σ_c^0	Σ_c^+	Σ_c^{++}	Ξ_c^0	Ξ_c^+	Ω_c^0
$\Sigma_{c1}^{0,+,++}/\Xi_{c1}^{0,+}/\Omega_{c1}^0(1D, \frac{1}{2}^+)$	23.6	1.0	46.0	16.2	0.7	10.4	1.7	0.3	5.6	0.6	0.1	0.2
$\Sigma_{c1}^{0,+,++}/\Xi_{c1}^{0,+}/\Omega_{c1}^0(1D, \frac{3}{2}^+)$	4.5	0.5	12.0	2.5	0.2	1.5	23.2	1.0	44.9	15.6	0.6	10.2
$\Sigma_{c2}^{0,+,++}/\Xi_{c2}^{0,+}/\Omega_{c2}^0(1D, \frac{3}{2}^+)$	116.7	1.7	179.3	94.6	0.4	74.0	12.6	0.1	17.5	10.1	0.0	7.8
$\Sigma_{c2}^{0,+,++}/\Xi_{c2}^{0,+}/\Omega_{c2}^0(1D, \frac{5}{2}^+)$	9.4	0.3	17.4	7.3	0.1	5.7	121.4	1.8	186.3	97.6	0.4	76.5
$\Sigma_{c3}^{0,+,++}/\Xi_{c3}^{0,+}/\Omega_{c3}^0(1D, \frac{5}{2}^+)$	216.0	1.0	206.0	227.0	6.7	231.2	15.3	0.3	14.3	16.1	0.9	16.4
$\Sigma_{c3}^{0,+,++}/\Xi_{c3}^{0,+}/\Omega_{c3}^0(1D, \frac{7}{2}^+)$	0.2	0.3	2.4	0.1	0.5	0.0	213.3	0.5	221.1	219.6	4.2	220.5
<hr/>												
	$\Sigma_c^{0,+,++}/\Xi_c^{0,+}/\Omega_c^0(2S, \frac{1}{2}^+)\gamma$						$\Sigma_c^{0,+,++}/\Xi_c^{0,+}/\Omega_c^0(2S, \frac{3}{2}^+)\gamma$					
	Σ_c^0	Σ_c^+	Σ_c^{++}	$\Xi_c'^0$	$\Xi_c'^+$	Ω_c^0	Σ_c^0	Σ_c^+	Σ_c^{++}	Ξ_c^0	Ξ_c^+	Ω_c^0
$\Sigma_{c1}^{0,+,++}/\Xi_{c1}^{0,+}/\Omega_{c1}^0(1D, \frac{1}{2}^+)$	0.0	0.0	0.0	0.0	0.0	0.0	0.0	0.0	0.2	0.0	0.0	0.0
$\Sigma_{c1}^{0,+,++}/\Xi_{c1}^{0,+}/\Omega_{c1}^0(1D, \frac{3}{2}^+)$	0.2	0.1	1.3	0.1	0.1	0.0	0.0	0.0	0.3	0.0	0.0	0.0
$\Sigma_{c2}^{0,+,++}/\Xi_{c2}^{0,+}/\Omega_{c2}^0(1D, \frac{3}{2}^+)$	0.0	0.0	0.3	0.0	0.0	0.0	0.0	0.0	0.0	0.0	0.0	0.0
$\Sigma_{c2}^{0,+,++}/\Xi_{c2}^{0,+}/\Omega_{c2}^0(1D, \frac{5}{2}^+)$	0.0	0.0	0.3	0.0	0.0	0.0	0.0	0.0	0.1	0.0	0.0	0.0
$\Sigma_{c3}^{0,+,++}/\Xi_{c3}^{0,+}/\Omega_{c3}^0(1D, \frac{5}{2}^+)$	0.0	0.0	0.1	0.0	0.0	0.0	0.0	0.0	0.0	0.0	0.0	0.0
$\Sigma_{c3}^{0,+,++}/\Xi_{c3}^{0,+}/\Omega_{c3}^0(1D, \frac{7}{2}^+)$	0.0	0.0	0.0	0.0	0.0	0.0	0.0	0.0	0.0	0.0	0.0	0.0

[52] R. Aaij *et al.* (LHCb Collaboration), Observation of a new

baryon state in the $\Lambda_b^0\pi^+\pi^-$ mass spectrum, [JHEP 06, 136 \(2020\)](#).

[53] R. Aaij *et al.* (LHCb Collaboration), First observation of ex-

cited Ω_b^- states, [Phys. Rev. Lett. 124, 082002 \(2020\)](#).

[54] A. M. Sirunyan *et al.* (CMS Collaboration), Observation of a new excited beauty strange baryon decaying to $\Xi_b^-\pi^+\pi^-$, [Phys. Rev. Lett. 126, 252003 \(2021\)](#).

TABLE X: Radiative decay widths (in units of keV) of $\Sigma_c(1F)/\Xi'_c(1F)/\Omega_c(1F)$ decaying into radial or orbital excited states of the single-charm baryon.

	$\Lambda_c^+/\Xi_c^{0,+}(1P, \frac{1}{2}^-)\gamma$			$\Lambda_c^+/\Xi_c^{0,+}(1P, \frac{3}{2}^-)\gamma$			$\Lambda_c^+/\Xi_c^{0,+}(2S, \frac{1}{2}^+)\gamma$					
	Λ_c^+	Ξ_c^0	Ξ_c^+	Λ_c^+	Ξ_c^0	Ξ_c^+	Λ_c^+	Ξ_c^0	Ξ_c^+			
$\Sigma_{c2}^+/\Xi_{c2}^{0,+}(1F, \frac{3}{2}^-)$	23.3	0.1	9.5	10.3	0.0	3.9	2.0	0.0	0.3			
$\Sigma_{c2}^+/\Xi_{c2}^{0,+}(1F, \frac{5}{2}^-)$	3.6	0.0	1.3	29.4	0.1	11.8	2.3	0.0	0.3			
$\Sigma_{c3}^+/\Xi_{c3}^{0,+}(1F, \frac{5}{2}^-)$	45.9	0.1	19.1	14.6	0.0	5.8	3.6	0.0	0.6			
$\Sigma_{c3}^+/\Xi_{c3}^{0,+}(1F, \frac{7}{2}^-)$	1.6	0.0	0.5	56.5	0.2	23.3	3.9	0.0	0.6			
$\Sigma_{c4}^+/\Xi_{c4}^{0,+}(1F, \frac{7}{2}^-)$	22.0	0.1	9.4	7.0	0.0	2.9	1.1	0.0	0.2			
$\Sigma_{c4}^+/\Xi_{c4}^{0,+}(1F, \frac{9}{2}^-)$	0.3	0.0	0.0	26.8	0.1	11.4	1.2	0.0	0.2			
<hr/>												
	$\Lambda_c^+/\Xi_c^{0,+}(1D, \frac{3}{2}^+)\gamma$			$\Lambda_c^+/\Xi_c^{0,+}(1D, \frac{5}{2}^+)\gamma$			$\Lambda_c^+/\Xi_c^{0,+}(1F, \frac{5}{2}^-)\gamma$		$\Lambda_c^+/\Xi_c^{0,+}(1F, \frac{7}{2}^-)\gamma$			
	Λ_c^+	Ξ_c^0	Ξ_c^+	Λ_c^+	Ξ_c^0	Ξ_c^+	Λ_c^+	Ξ_c^0	Ξ_c^+			
$\Sigma_{c2}^{0,+,++}/\Xi_{c2}^{0,+}/\Omega_{c2}^0(1F, \frac{3}{2}^-)$	75.4	0.5	34.1	9.5	0.1	4.0	80.4	0.5	25.6	0.1	0.0	0.0
$\Sigma_{c2}^{0,+,++}/\Xi_{c2}^{0,+}/\Omega_{c2}^0(1F, \frac{5}{2}^-)$	7.6	0.0	3.3	71.4	0.5	32.3	4.2	0.0	1.4	78.5	0.5	25.9
$\Sigma_{c3}^{0,+,++}/\Xi_{c3}^{0,+}/\Omega_{c3}^0(1F, \frac{5}{2}^-)$	99.4	0.7	47.4	9.1	0.1	4.3	48.7	0.3	15.7	2.3	0.0	0.7
$\Sigma_{c3}^{0,+,++}/\Xi_{c3}^{0,+}/\Omega_{c3}^0(1F, \frac{7}{2}^-)$	2.6	0.0	1.2	94.6	0.7	45.3	1.9	0.0	0.6	49.7	0.3	16.4
$\Sigma_{c4}^{0,+,++}/\Xi_{c4}^{0,+}/\Omega_{c4}^0(1F, \frac{7}{2}^-)$	50.1	0.4	25.1	4.6	0.0	2.3	27.1	0.2	8.1	0.9	0.0	0.3
$\Sigma_{c4}^{0,+,++}/\Xi_{c4}^{0,+}/\Omega_{c4}^0(1F, \frac{9}{2}^-)$	0.1	0.0	0.0	45.9	0.4	23.1	0.0	0.0	0.0	26.9	0.2	7.8
<hr/>												
	$\Sigma_{c0}^{0,+,++}/\Xi_{c0}^{0,+}/\Omega_{c0}^0(1P, \frac{1}{2}^-)\gamma$					$\Sigma_{c1}^{0,+,++}/\Xi_{c1}^{0,+}/\Omega_{c1}^0(1P, \frac{1}{2}^-)\gamma$						
	Σ_c^0	Σ_c^+	Σ_c^{++}	Ξ_c^0	$\Xi_c^{'+}$	Ω_c^0	Σ_c^0	Σ_c^+	Σ_c^{++}	Ξ_c^0	$\Xi_c^{'+}$	Ω_c^0
$\Sigma_{c2}^{0,+,++}/\Xi_{c2}^{0,+}/\Omega_{c2}^0(1F, \frac{3}{2}^-)$	66.2	56.6	537.5	29.5	40.5	11.2	46.3	34.6	344.1	20.8	24.2	8.1
$\Sigma_{c2}^{0,+,++}/\Xi_{c2}^{0,+}/\Omega_{c2}^0(1F, \frac{5}{2}^-)$	70.6	54.9	539.0	33.0	37.6	13.7	21.3	14.8	151.8	10.0	10.0	4.2
$\Sigma_{c3}^{0,+,++}/\Xi_{c3}^{0,+}/\Omega_{c3}^0(1F, \frac{5}{2}^-)$	1.7	0.4	7.0	0.9	0.5	0.4	43.9	43.8	393.8	20.2	31.3	7.9
$\Sigma_{c3}^{0,+,++}/\Xi_{c3}^{0,+}/\Omega_{c3}^0(1F, \frac{7}{2}^-)$	1.8	0.4	7.2	0.9	0.5	0.4	1.6	0.3	5.5	0.7	0.1	0.4
$\Sigma_{c4}^{0,+,++}/\Xi_{c4}^{0,+}/\Omega_{c4}^0(1F, \frac{7}{2}^-)$	0.2	0.1	1.1	0.1	0.0	0.0	1.5	0.4	6.2	0.8	0.4	0.4
$\Sigma_{c4}^{0,+,++}/\Xi_{c4}^{0,+}/\Omega_{c4}^0(1F, \frac{9}{2}^-)$	0.2	0.1	1.1	0.1	0.0	0.0	0.2	0.1	0.8	0.1	0.0	0.0
<hr/>												
	$\Sigma_{c1}^{0,+,++}/\Xi_{c1}^{0,+}/\Omega_{c1}^0(1P, \frac{3}{2}^-)\gamma$					$\Sigma_{c2}^{0,+,++}/\Xi_{c2}^{0,+}/\Omega_{c2}^0(1P, \frac{3}{2}^-)\gamma$						
	Σ_c^0	Σ_c^+	Σ_c^{++}	Ξ_c^0	$\Xi_c^{'+}$	Ω_c^0	Σ_c^0	Σ_c^+	Σ_c^{++}	Ξ_c^0	$\Xi_c^{'+}$	Ω_c^0
$\Sigma_{c2}^{0,+,++}/\Xi_{c2}^{0,+}/\Omega_{c2}^0(1F, \frac{3}{2}^-)$	42.8	33.5	327.9	18.4	23.9	6.7	15.0	9.4	99.9	6.4	6.4	2.3
$\Sigma_{c2}^{0,+,++}/\Xi_{c2}^{0,+}/\Omega_{c2}^0(1F, \frac{5}{2}^-)$	72.0	51.1	518.4	32.3	35.3	12.7	9.0	4.0	48.6	3.1	2.1	1.0
$\Sigma_{c3}^{0,+,++}/\Xi_{c3}^{0,+}/\Omega_{c3}^0(1F, \frac{5}{2}^-)$	13.9	12.6	116.0	6.1	9.2	2.3	42.2	31.7	314.3	18.8	22.4	7.3
$\Sigma_{c3}^{0,+,++}/\Xi_{c3}^{0,+}/\Omega_{c3}^0(1F, \frac{7}{2}^-)$	59.3	51.8	487.6	28.2	36.1	11.8	6.4	4.0	42.3	2.9	2.5	1.2
$\Sigma_{c4}^{0,+,++}/\Xi_{c4}^{0,+}/\Omega_{c4}^0(1F, \frac{7}{2}^-)$	0.6	0.2	2.6	0.3	0.1	0.1	41.1	47.7	407.2	19.3	34.3	7.6
$\Sigma_{c4}^{0,+,++}/\Xi_{c4}^{0,+}/\Omega_{c4}^0(1F, \frac{9}{2}^-)$	1.8	0.5	7.2	0.9	0.5	0.4	0.6	0.1	1.6	0.4	0.0	0.2
<hr/>												
	$\Sigma_{c2}^{0,+,++}/\Xi_{c2}^{0,+}/\Omega_{c2}^0(1P, \frac{5}{2}^-)\gamma$					$\Sigma_{c2}^{0,+,++}/\Xi_{c2}^{0,+}/\Omega_{c2}^0(1P, \frac{3}{2}^-)\gamma$						
	Σ_c^0	Σ_c^+	Σ_c^{++}	Ξ_c^0	$\Xi_c^{'+}$	Ω_c^0	Σ_c^0	Σ_c^+	Σ_c^{++}	Ξ_c^0	$\Xi_c^{'+}$	Ω_c^0
$\Sigma_{c2}^{0,+,++}/\Xi_{c2}^{0,+}/\Omega_{c2}^0(1F, \frac{3}{2}^-)$	11.6	5.8	66.8	3.8	3.3	1.1						
$\Sigma_{c2}^{0,+,++}/\Xi_{c2}^{0,+}/\Omega_{c2}^0(1F, \frac{5}{2}^-)$	19.4	11.5	124.5	7.8	7.6	2.8						
$\Sigma_{c3}^{0,+,++}/\Xi_{c3}^{0,+}/\Omega_{c3}^0(1F, \frac{5}{2}^-)$	10.7	8.4	81.6	4.4	5.9	1.5						
$\Sigma_{c3}^{0,+,++}/\Xi_{c3}^{0,+}/\Omega_{c3}^0(1F, \frac{7}{2}^-)$	48.6	35.1	353.4	21.7	24.5	8.5						
$\Sigma_{c4}^{0,+,++}/\Xi_{c4}^{0,+}/\Omega_{c4}^0(1F, \frac{7}{2}^-)$	4.9	5.6	47.5	2.2	4.2	0.8						
$\Sigma_{c4}^{0,+,++}/\Xi_{c4}^{0,+}/\Omega_{c4}^0(1F, \frac{9}{2}^-)$	48.3	49.4	440.0	23.7	34.7	10.2						

-Continue.-

-Continue.-

$\Sigma_c^{0,+} / \Xi_c^{0,+} / \Omega_c^0 (2S, \frac{1}{2}^+) \gamma$						$\Sigma_c^{*0,+} / \Xi_c^{*0,+} / \Omega_c^0 (2S, \frac{3}{2}^+) \gamma$					
Σ_c^0	Σ_c^+	Σ_c^{++}	Ξ_c^0	Ξ_c'	Ω_c^0	Σ_c^0	Σ_c^+	Σ_c^{++}	Ξ_c^0	Ξ_c'	Ω_c^0
$\Sigma_{c2}^{0,+} / \Xi_{c2}'^{0,+} / \Omega_{c2}^0 (1F, \frac{3}{2}^-)$	0.0	0.0	0.1	0.0	0.0	7.6	1.2	24.8	3.2	0.3	1.5
$\Sigma_{c2}^{0,+} / \Xi_{c2}'^{0,+} / \Omega_{c2}^0 (1F, \frac{5}{2}^-)$	7.6	1.2	24.8	3.4	0.3	1.7	4.0	0.7	13.0	1.7	0.1
$\Sigma_{c3}^{0,+} / \Xi_{c3}'^{0,+} / \Omega_{c3}^0 (1F, \frac{5}{2}^-)$	2.6	0.4	8.5	1.5	0.1	1.0	2.0	0.3	6.4	1.1	0.1
$\Sigma_{c3}^{0,+} / \Xi_{c3}'^{0,+} / \Omega_{c3}^0 (1F, \frac{7}{2}^-)$	1.7	0.3	5.4	0.9	0.1	0.6	3.0	0.5	9.8	1.6	0.1
$\Sigma_{c4}^{0,+} / \Xi_{c4}'^{0,+} / \Omega_{c4}^0 (1F, \frac{7}{2}^-)$	1.6	0.2	4.9	1.3	0.1	1.2	0.3	0.0	0.9	0.2	0.0
$\Sigma_{c4}^{0,+} / \Xi_{c4}'^{0,+} / \Omega_{c4}^0 (1F, \frac{9}{2}^-)$	0.0	0.0	0.0	0.0	0.0	1.2	0.2	3.8	1.0	0.1	0.9
$\Sigma_{c2}^{0,+} / \Xi_{c2}'^{0,+} / \Omega_{c2}^0 (1D, \frac{1}{2}^+) \gamma$						$\Sigma_{c2}^{0,+} / \Xi_{c2}'^{0,+} / \Omega_{c2}^0 (1D, \frac{3}{2}^+) \gamma$					
Σ_c^0	Σ_c^+	Σ_c^{++}	Ξ_c^0	Ξ_c'	Ω_c^0	Σ_c^0	Σ_c^+	Σ_c^{++}	Ξ_c^0	Ξ_c'	Ω_c^0
$\Sigma_{c2}^{0,+} / \Xi_{c2}'^{0,+} / \Omega_{c2}^0 (1F, \frac{3}{2}^-)$	391.7	1.7	501.0	352.2	0.1	306.6	73.2	0.2	87.5	66.3	0.2
$\Sigma_{c2}^{0,+} / \Xi_{c2}'^{0,+} / \Omega_{c2}^0 (1F, \frac{5}{2}^-)$	0.7	0.0	1.2	0.5	0.0	0.3	432.9	3.4	592.2	382.1	0.5
$\Sigma_{c3}^{0,+} / \Xi_{c3}'^{0,+} / \Omega_{c3}^0 (1F, \frac{5}{2}^-)$	2.2	0.5	8.6	1.5	1.0	0.9	0.5	0.1	2.1	0.4	0.2
$\Sigma_{c3}^{0,+} / \Xi_{c3}'^{0,+} / \Omega_{c3}^0 (1F, \frac{7}{2}^-)$	0.1	0.0	0.2	0.0	0.0	0.0	2.4	0.6	9.4	1.6	0.9
$\Sigma_{c4}^{0,+} / \Xi_{c4}'^{0,+} / \Omega_{c4}^0 (1F, \frac{7}{2}^-)$	0.0	0.0	0.0	0.0	0.0	0.0	0.0	0.0	0.0	0.0	0.0
$\Sigma_{c4}^{0,+} / \Xi_{c4}'^{0,+} / \Omega_{c4}^0 (1F, \frac{9}{2}^-)$	0.0	0.0	0.0	0.0	0.0	0.0	0.0	0.0	0.0	0.0	0.0
$\Sigma_{c3}^{0,+} / \Xi_{c3}'^{0,+} / \Omega_{c3}^0 (1D, \frac{3}{2}^+) \gamma$						$\Sigma_{c3}^{0,+} / \Xi_{c3}'^{0,+} / \Omega_{c3}^0 (1D, \frac{5}{2}^+) \gamma$					
Σ_c^0	Σ_c^+	Σ_c^{++}	Ξ_c^0	Ξ_c'	Ω_c^0	Σ_c^0	Σ_c^+	Σ_c^{++}	Ξ_c^0	Ξ_c'	Ω_c^0
$\Sigma_{c2}^{0,+} / \Xi_{c2}'^{0,+} / \Omega_{c2}^0 (1F, \frac{3}{2}^-)$	132.0	3.0	221.3	100.7	1.5	73.5	15.4	0.3	24.5	11.5	0.2
$\Sigma_{c2}^{0,+} / \Xi_{c2}'^{0,+} / \Omega_{c2}^0 (1F, \frac{5}{2}^-)$	10.8	0.5	22.0	7.7	0.3	5.5	132.9	3.3	224.4	100.1	1.8
$\Sigma_{c3}^{0,+} / \Xi_{c3}'^{0,+} / \Omega_{c3}^0 (1F, \frac{5}{2}^-)$	328.1	0.5	367.1	317.5	2.1	295.4	22.9	0.1	23.0	22.5	0.4
$\Sigma_{c3}^{0,+} / \Xi_{c3}'^{0,+} / \Omega_{c3}^0 (1F, \frac{7}{2}^-)$	0.1	0.2	1.0	0.0	0.2	0.0	324.1	0.8	388.3	308.1	0.9
$\Sigma_{c4}^{0,+} / \Xi_{c4}'^{0,+} / \Omega_{c4}^0 (1F, \frac{7}{2}^-)$	1.2	0.3	4.7	1.0	0.6	0.7	0.1	0.0	0.4	0.1	0.1
$\Sigma_{c4}^{0,+} / \Xi_{c4}'^{0,+} / \Omega_{c4}^0 (1F, \frac{9}{2}^-)$	0.0	0.0	0.0	0.0	0.0	0.0	1.0	0.3	4.1	0.9	0.6
$\Sigma_{c4}^{0,+} / \Xi_{c4}'^{0,+} / \Omega_{c4}^0 (1D, \frac{5}{2}^-) \gamma$						$\Sigma_{c4}^{0,+} / \Xi_{c4}'^{0,+} / \Omega_{c4}^0 (1D, \frac{7}{2}^+) \gamma$					
Σ_c^0	Σ_c^+	Σ_c^{++}	Ξ_c^0	Ξ_c'	Ω_c^0	Σ_c^0	Σ_c^+	Σ_c^{++}	Ξ_c^0	Ξ_c'	Ω_c^0
$\Sigma_{c2}^{0,+} / \Xi_{c2}'^{0,+} / \Omega_{c2}^0 (1F, \frac{3}{2}^-)$	9.6	0.7	22.0	5.6	0.5	3.1	0.4	0.1	1.3	0.1	0.0
$\Sigma_{c2}^{0,+} / \Xi_{c2}'^{0,+} / \Omega_{c2}^0 (1F, \frac{5}{2}^-)$	0.8	0.1	2.4	0.4	0.1	0.2	9.7	0.7	21.7	5.7	0.5
$\Sigma_{c3}^{0,+} / \Xi_{c3}'^{0,+} / \Omega_{c3}^0 (1F, \frac{5}{2}^-)$	93.1	2.0	154.7	70.2	0.8	50.4	5.2	0.1	7.6	3.9	0.0
$\Sigma_{c3}^{0,+} / \Xi_{c3}'^{0,+} / \Omega_{c3}^0 (1F, \frac{7}{2}^-)$	3.6	0.2	7.5	2.5	0.1	1.8	94.6	2.1	157.4	70.8	0.9
$\Sigma_{c4}^{0,+} / \Xi_{c4}'^{0,+} / \Omega_{c4}^0 (1F, \frac{7}{2}^-)$	264.0	0.8	259.9	274.8	6.0	273.1	10.5	0.2	9.3	11.2	0.6
$\Sigma_{c4}^{0,+} / \Xi_{c4}'^{0,+} / \Omega_{c4}^0 (1F, \frac{9}{2}^-)$	0.1	0.2	1.2	0.0	0.3	0.0	256.4	0.4	270.3	262.6	3.8

TABLE XI: Radiative decay widths (in units of keV) of 3_f single-bottom baryon decaying into radial or orbital excited states.

	$\Lambda_b^0/\Xi_b^{-,0}(1P, \frac{1}{2}^-)\gamma$			$\Lambda_b^0/\Xi_b^{-,0}(1P, \frac{3}{2}^-)\gamma$			$\Lambda_b^0/\Xi_b^{-,0}(2S, \frac{1}{2}^+)\gamma$		
	Λ_b^0	Ξ_b^-	Ξ_b^0	Λ_b^0	Ξ_b^-	Ξ_b^0	Λ_b^0	Ξ_b^-	Ξ_b^0
$\Lambda_b^0/\Xi_b^{-,0}(2S, \frac{1}{2}^+)$	10.6	19.9	8.6	19.8	36.9	16.1
$\Lambda_b^0/\Xi_b^{-,0}(1D, \frac{3}{2}^+)$	54.2	103.0	44.9	10.7	20.1	8.8	0.0	0.1	0.0
$\Lambda_b^0/\Xi_b^{-,0}(1D, \frac{5}{2}^+)$	0.3	0.5	0.1	65.2	124.4	53.3	0.0	0.1	0.0
$\Lambda_b^0/\Xi_b^{-,0}(1F, \frac{5}{2}^-)$	43.4	129.3	19.3	14.0	39.1	6.0	2.0	3.3	0.7
$\Lambda_b^0/\Xi_b^{-,0}(1F, \frac{7}{2}^-)$	1.1	1.6	0.3	57.6	169.7	25.6	2.1	3.7	0.8
	$\Lambda_b^0/\Xi_b^{-,0}(1D, \frac{3}{2}^+)\gamma$			$\Lambda_b^0/\Xi_b^{-,0}(1D, \frac{5}{2}^+)\gamma$			$\Sigma_{b0}^0/\Xi_{b0}'^{-,0}(1P, \frac{1}{2}^-)\gamma$		
	Λ_b^0	Ξ_b^-	Ξ_b^0	Λ_b^0	Ξ_b^-	Ξ_b^0	Σ_{b0}^0	$\Xi_{b0}'^-$	Ξ_{b0}^0
$\Lambda_b^0/\Xi_b^{-,0}(2S, \frac{1}{2}^+)$	0.0	0.0
$\Lambda_b^0/\Xi_b^{-,0}(1D, \frac{3}{2}^+)$	0.0	0.0	0.1
$\Lambda_b^0/\Xi_b^{-,0}(1D, \frac{5}{2}^+)$	0.0	0.0	0.0	0.0	0.0	0.1	0.0
$\Lambda_b^0/\Xi_b^{-,0}(1F, \frac{5}{2}^-)$	67.2	114.7	50.6	4.7	7.9	3.6	0.2	0.0	0.4
$\Lambda_b^0/\Xi_b^{-,0}(1F, \frac{7}{2}^-)$	0.1	0.1	0.0	70.8	124.0	54.1	0.2	0.0	0.4
	$\Sigma_{b1}^0/\Xi_{b1}'^{-,0}(1P, \frac{3}{2}^-)\gamma$			$\Sigma_{b2}^0/\Xi_{b2}'^{-,0}(1P, \frac{3}{2}^-)\gamma$			$\Sigma_{b2}^0/\Xi_{b2}'^{-,0}(1P, \frac{5}{2}^-)\gamma$		
	Σ_{b1}^0	$\Xi_{b1}'^-$	Ξ_{b1}^0	Σ_{b2}^0	$\Xi_{b2}'^-$	Ξ_{b2}^0	Σ_{b2}^0	$\Xi_{b2}'^-$	Ξ_{b2}^0
$\Lambda_b^0/\Xi_b^{-,0}(2S, \frac{1}{2}^+)$...	0.0	0.0	...	0.0	0.0	...	0.0	0.0
$\Lambda_b^0/\Xi_b^{-,0}(1D, \frac{3}{2}^+)$	0.0	0.0	0.1	0.0	0.0	0.5	0.0	0.0	0.1
$\Lambda_b^0/\Xi_b^{-,0}(1D, \frac{5}{2}^+)$	0.0	0.0	0.2	0.0	0.0	0.1	0.0	0.0	0.4
$\Lambda_b^0/\Xi_b^{-,0}(1F, \frac{5}{2}^-)$	0.3	0.0	0.5	1.3	0.0	1.9	0.3	0.0	0.5
$\Lambda_b^0/\Xi_b^{-,0}(1F, \frac{7}{2}^-)$	0.7	0.0	1.2	0.2	0.0	0.3	1.4	0.0	2.1
	$\Sigma_{b1}^{*0}/\Xi_{b1}^{*-,0}(2S, \frac{3}{2}^+)\gamma$			$\Sigma_{b1}^0/\Xi_{b1}'^{-,0}(1D, \frac{1}{2}^+)\gamma$			$\Sigma_{b1}^0/\Xi_{b1}'^{-,0}(1D, \frac{3}{2}^+)\gamma$		
	Σ_{b1}^{*0}	$\Xi_{b1}'^-$	Ξ_{b1}^0	Σ_{b1}^0	$\Xi_{b1}'^-$	Ξ_{b1}^0	Σ_{b1}^0	$\Xi_{b1}'^-$	Ξ_{b1}^0
$\Lambda_b^0/\Xi_b^{-,0}(1F, \frac{5}{2}^-)$	0.0	0.0	0.0	0.0	0.0	0.0	0.0	0.0	0.0
$\Lambda_b^0/\Xi_b^{-,0}(1F, \frac{7}{2}^-)$	0.0	0.0	0.0	0.0	0.0	0.0	0.0	0.0	0.0
	$\Sigma_{b2}^0/\Xi_{b2}'^{-,0}(1D, \frac{5}{2}^+)\gamma$			$\Sigma_{b3}^0/\Xi_{b3}'^{-,0}(1D, \frac{5}{2}^+)\gamma$			$\Sigma_{b3}^0/\Xi_{b3}'^{-,0}(1D, \frac{7}{2}^+)\gamma$		
	Σ_{b2}^0	$\Xi_{b2}'^-$	Ξ_{b2}^0	Σ_{b3}^0	$\Xi_{b3}'^-$	Ξ_{b3}^0	Σ_{b3}^0	$\Xi_{b3}'^-$	Ξ_{b3}^0
$\Lambda_b^0/\Xi_b^{-,0}(1F, \frac{5}{2}^-)$	0.0	0.0	0.0	0.0	0.0	0.3	0.0	0.0	0.0
$\Lambda_b^0/\Xi_b^{-,0}(1F, \frac{7}{2}^-)$	0.0	0.0	0.1	0.0	0.0	0.0	0.0	0.0	0.3

- [55] R. Aaij *et al.* (LHCb Collaboration), Observation of two new excited Ξ_b^0 states decaying to $\Lambda_b^0 K^- \pi^+$, [Phys. Rev. Lett. **128**, 162001 \(2022\)](#).
- [56] R. Aaij *et al.* (LHCb Collaboration), Observation of new baryons in the $\Xi_b^- \pi^+ \pi^-$ and $\Xi_b^0 \pi^+ \pi^-$ systems, [Phys. Rev. Lett. **131**, 171901 \(2023\)](#).
- [57] S. Q. Luo and X. Liu, Investigating the spectroscopy behavior of undetected $1F$ -wave charmed baryons, [Phys. Rev. D **108**, 034002 \(2023\)](#).
- [58] E. Hiyama, Y. Kino, and M. Kamimura, Gaussian expansion method for few-body systems, [Prog. Part. Nucl. Phys. **51**, 223–307 \(2003\)](#).
- [59] S. Q. Luo and X. Liu, Newly observed $\Omega_c(3327)$: A good candidate for a D -wave charmed baryon, [Phys. Rev. D **107**, 074041 \(2023\)](#).
- [60] J. Kahn (Belle-II Collaboration), The Belle II experiment, 2017, [doi:10.23727/CERN-Proceedings-2017-001.45](#).
- [61] W. Altmannshofer *et al.* (Belle-II Collaboration), The Belle II physics book, [PTEP **2019**, 123C01 \(2019\)](#), [Erratum: PTEP 2020, 029201 (2020)].
- [62] P. Di Nezza (LHCb Collaboration), LHC Run 3 and Run 4 prospects for heavy-ion physics with LHCb, [Nucl. Phys. A **1005**, 121872 \(2021\)](#).
- [63] S. Belin, LHC Run 3 and Run 4 prospects for heavy-ion physics with LHCb, [PoS HardProbes2020, 176 \(2021\)](#).
- [64] S. J. Brodsky and J. R. Primack, The electromagnetic interactions of composite systems, [Annals Phys. **52**, 315–365 \(1969\)](#).
- [65] F. E. Close and L. A. Copley, Electromagnetic interactions of weakly bound composite systems, [Nucl. Phys. B **19**, 477–500 \(1970\)](#).
- [66] Z. P. Li, The threshold pion photoproduction of nucleons in the chiral quark model, [Phys. Rev. D **50**, 5639–5646 \(1994\)](#).
- [67] Z. P. Li, H. X. Ye, and M. H. Lu, An unified approach to pseudoscalar meson photoproductions off nucleons in the quark model, [Phys. Rev. C **56**, 1099–1113 \(1997\)](#).
- [68] W. J. Deng, H. Liu, L. C. Gui, and X. H. Zhong, Charmonium spectrum and their electromagnetic transitions with higher multipole contributions, [Phys. Rev. D **95**, 034026 \(2017\)](#).

TABLE XII: Radiative decay widths (in units of keV) of $\Sigma_b(1P)/\Xi'_b(1P)\Sigma_b(2S)/\Xi'_b(2S)/\Omega_b(2S)$ decaying into radial or orbital excited states of the single-bottom baryon.

	$\Lambda_b^0/\Xi_b^{-,0}(1P, \frac{1}{2}^-)\gamma$			$\Lambda_b^0/\Xi_b^{-,0}(1P, \frac{3}{2}^-)\gamma$			$\Lambda_b^0/\Xi_b^{-,0}(2S, \frac{1}{2}^+)\gamma$					
	Λ_b^0	Ξ_b^-	Ξ_b^0	Λ_b^0	Ξ_b^-	Ξ_b^0	Λ_b^0	Ξ_b^-	Ξ_b^0			
$\Sigma_{b0}^0/\Xi_{b0}^{-,0}(1P, \frac{1}{2}^-)$	28.3	0.2	7.4	50.5	0.3	12.2	0.0			
$\Sigma_{b1}^0/\Xi_{b1}^{-,0}(1P, \frac{1}{2}^-)$	45.6	0.3	12.5	20.5	0.1	5.1	0.0			
$\Sigma_{b1}^0/\Xi_{b1}^{-,0}(1P, \frac{3}{2}^-)$	13.2	0.1	4.1	59.0	0.4	17.3	0.0			
$\Sigma_{b2}^0/\Xi_{b2}^{-,0}(1P, \frac{3}{2}^-)$	53.6	0.4	17.3	9.6	0.1	2.9	0.0			
$\Sigma_{b2}^0/\Xi_{b2}^{-,0}(1P, \frac{5}{2}^-)$	0.1	0.0	0.0	64.2	0.4	21.1	0.0			
$\Sigma_b^0/\Xi_b^{-,0}(2S, \frac{1}{2}^+)$	13.9	0.1	5.1	27.9	0.2	9.7	59.6	0.3	15.9			
$\Sigma_b^{*,0}/\Xi_b^{*,0}(2S, \frac{3}{2}^+)$	14.4	0.1	5.7	29.2	0.2	11.0	67.9	0.4	21.0			
$\Lambda_b^0/\Xi_b^{-,0}(1D, \frac{3}{2}^+)\gamma$			$\Lambda_b^0/\Xi_b^{-,0}(1D, \frac{5}{2}^+)\gamma$			$\Sigma_{b0}^{-,0,+}/\Xi_{b0}^{-,0}/\Omega_{b0}^-(1P, \frac{1}{2}^-)\gamma$						
Λ_b^0	Ξ_b^-	Ξ_b^0	Λ_b^0	Ξ_b^-	Ξ_b^0	Σ_b^-	Σ_b^0	Σ_b^+	$\Xi_b'^-$	$\Xi_b'^0$	Ω_b^-	
$\Sigma_b^{-,0,+}/\Xi_b^{-,0}/\Omega_b^-(2S, \frac{1}{2}^+)$	0.0	0.0	0.0	0.0	0.0	0.0	3.9	1.7	21.2	3.3	1.2	2.8
$\Sigma_b^{*,0,+}/\Xi_b^{*,0}/\Omega_b^{*-}(2S, \frac{3}{2}^+)$	0.0	0.0	0.0	0.0	0.0	0.0	4.2	1.9	23.4	3.7	1.4	3.2
$\Sigma_{b1}^{-,0,+}/\Xi_{b1}^{-,0}/\Omega_{b1}^-(1P, \frac{1}{2}^-)\gamma$						$\Sigma_{b1}^{-,0,+}/\Xi_{b1}^{-,0}/\Omega_{b1}^-(1P, \frac{3}{2}^-)\gamma$						
Σ_b^-	Σ_b^0	Σ_b^+	$\Xi_b'^-$	$\Xi_b'^0$	Ω_b^-	Σ_b^-	Σ_b^0	Σ_b^+	$\Xi_b'^-$	$\Xi_b'^0$	Ω_b^-	
$\Sigma_b^{-,0,+}/\Xi_b^{-,0}/\Omega_b^-(2S, \frac{1}{2}^+)$	11.9	5.1	63.2	9.2	3.7	7.0	5.6	2.3	29.3	4.1	1.7	3.0
$\Sigma_b^{*,0,+}/\Xi_b^{*,0}/\Omega_b^{*-}(2S, \frac{3}{2}^+)$	3.5	1.5	18.3	2.7	1.1	2.1	15.3	6.5	81.2	11.7	4.8	9.1
$\Sigma_{b2}^{-,0,+}/\Xi_{b2}^{-,0}/\Omega_{b2}^-(1P, \frac{3}{2}^-)\gamma$						$\Sigma_{b2}^{-,0,+}/\Xi_{b2}^{-,0}/\Omega_{b2}^-(1P, \frac{5}{2}^-)\gamma$						
Σ_b^-	Σ_b^0	Σ_b^+	$\Xi_b'^-$	$\Xi_b'^0$	Ω_b^-	Σ_b^-	Σ_b^0	Σ_b^+	$\Xi_b'^-$	$\Xi_b'^0$	Ω_b^-	
$\Sigma_b^{-,0,+}/\Xi_b^{-,0}/\Omega_b^-(2S, \frac{1}{2}^+)$	59.2	22.6	296.0	36.0	16.2	21.1	0.4	0.1	1.5	0.2	0.1	0.0
$\Sigma_b^{*,0,+}/\Xi_b^{*,0}/\Omega_b^{*-}(2S, \frac{3}{2}^+)$	7.2	2.7	35.3	4.4	2.0	2.7	56.9	21.9	285.5	34.8	15.9	21.2
$\Sigma_b^{-,0,+}/\Xi_b^{-,0}/\Omega_b^-(2S, \frac{1}{2}^+)\gamma$												
Σ_b^-	Σ_b^0	Σ_b^+	$\Xi_b'^-$	$\Xi_b'^0$	Ω_b^-							
$\Sigma_b^{-,0,+}/\Xi_b^{-,0}/\Omega_b^-(2S, \frac{1}{2}^+)$							
$\Sigma_b^{*,0,+}/\Xi_b^{*,0}/\Omega_b^{*-}(2S, \frac{3}{2}^+)$	0.0	0.0	0.0	0.0	0.0							

- [69] T. Yoshida, E. Hiyama, A. Hosaka, M. Oka, and K. Sadato, Spectrum of heavy baryons in the quark model, [Phys. Rev. D **92**, 114029 \(2015\)](#).
- [70] W. Roberts and M. Pervin, Heavy baryons in a quark model, [Int. J. Mod. Phys. A **23**, 2817–2860 \(2008\)](#).
- [71] D. Ebert, K. G. Klimenko, and V. L. Yudichev, Mass spectrum of diquarks and mesons in the color-flavor locked phase of dense quark matter, [Eur. Phys. J. C **53**, 65–76 \(2008\)](#).
- [72] D. Ebert, R. N. Faustov, and V. O. Galkin, Spectroscopy and Regge trajectories of heavy baryons in the relativistic quark-diquark picture, [Phys. Rev. D **84**, 014025 \(2011\)](#).
- [73] Z. Shah, K. Thakkar, A. K. Rai, and P. C. Vinodkumar, Mass spectra and Regge trajectories of Λ_c^+ , Σ_c^0 , Ξ_c^0 and Ω_c^0 baryons, [Chin. Phys. C **40**, 123102 \(2016\)](#).
- [74] B. Chen, K. W. Wei, X. Liu, and T. Matsuki, Low-lying charmed and charmed-strange baryon states, [Eur. Phys. J. C **77**, 154 \(2017\)](#).
- [75] G. L. Yu, Z. Y. Li, Z. G. Wang, J. Lu, and M. Yan, Systematic analysis of single heavy baryons Λ_Q , Σ_Q and Ω_Q , [Nucl. Phys. B **990**, 116183 \(2023\)](#).
- [76] H. Garcia-Tecocoatzi, A. Giachino, J. Li, A. Ramirez-Morales, and E. Santopinto, Strong decay widths and mass spectra of charmed baryons, [Phys. Rev. D **107**, 034031 \(2023\)](#).
- [77] C. H. Wang, L. Tang, T. Y. Li, G. P. Zheng, J. F. Hu, and C. Q. Pang, The effective β value in a simple harmonic oscillator wave function, [Nucl. Phys. Rev. **39**, 160–171 \(2022\)](#).
- [78] B. Chen, K. W. Wei, X. Liu, and A. Zhang, Role of newly discovered $\Xi_b(6227)^-$ for constructing excited bottom baryon family, [Phys. Rev. D **98**, 031502 \(2018\)](#).
- [79] R. Aaij *et al.* (LHCb Collaboration), Observation of new Ξ_c^0 baryons decaying to $\Lambda_c^+ K^-$, [Phys. Rev. Lett. **124**, 222001 \(2020\)](#).
- [80] R. Aaij *et al.* (LHCb Collaboration), Study of the $B^- \rightarrow \Lambda_c^+ \bar{\Lambda}_c^- K^-$ decay, [Phys. Rev. D **108**, 012020 \(2023\)](#).
- [81] R. Aaij *et al.* (LHCb Collaboration), Observation of five new narrow Ω_c^0 states decaying to $\Xi_c^+ K^-$, [Phys. Rev. Lett. **118**, 182001 \(2017\)](#).
- [82] S. S. Agaev, K. Azizi, and H. Sundu, On the nature of the newly discovered Ω states, [EPL **118**, 61001 \(2017\)](#).
- [83] S. S. Agaev, K. Azizi, and H. Sundu, Interpretation of the new Ω_c^0 states via their mass and width, [Eur. Phys. J. C **77**, 395 \(2017\)](#).
- [84] A. Ali, L. Maiani, A. V. Borisov, I. Ahmed, M. Jamil Aslam, A. Y. Parkhomenko, A. D. Polosa, and A. Rehman, A new look at the Y tetraquarks and Ω_c baryons in the diquark model, [Eur. Phys. J. C **78**, 29 \(2018\)](#).

TABLE XIII: Radiative decay widths (in units of keV) of $\Sigma_b(1D)/\Xi'_b(1D)/\Omega_b(1D)$ decaying into radial or orbital excited states of the single-bottom baryon.

	$\Lambda_b^0/\Xi_b^{-,0}(1P, \frac{1}{2}^-)\gamma$			$\Lambda_b^0/\Xi_b^{-,0}(1P, \frac{3}{2}^-)\gamma$			$\Lambda_b^0/\Xi_b^{-,0}(2S, \frac{1}{2}^+)\gamma$					
	Λ_b^0	Ξ_b^-	Ξ_b^0	Λ_b^0	Ξ_b^-	Ξ_b^0	Λ_b^0	Ξ_b^-	Ξ_b^0			
$\Sigma_{b1}^{-,0,+}/\Xi_{b1}'^{-,0}/\Omega_{b1}^-(1D, \frac{1}{2}^-)$	43.8	0.3	17.3	27.8	0.2	9.9	0.7	0.0	0.0			
$\Sigma_{b1}^{-,0,+}/\Xi_{b1}'^{-,0}/\Omega_{b1}^-(1D, \frac{3}{2}^-)$	15.0	0.1	5.6	58.5	0.3	22.8	0.8	0.0	0.1			
$\Sigma_{b2}^{-,0,+}/\Xi_{b2}'^{-,0}/\Omega_{b2}^-(1D, \frac{3}{2}^-)$	94.4	0.6	38.7	26.8	0.2	10.5	1.3	0.0	0.1			
$\Sigma_{b2}^{-,0,+}/\Xi_{b2}'^{-,0}/\Omega_{b2}^-(1D, \frac{5}{2}^-)$	5.1	0.0	2.0	117.7	0.8	48.4	1.6	0.0	0.1			
$\Sigma_{b3}^{-,0,+}/\Xi_{b3}'^{-,0}/\Omega_{b3}^-(1D, \frac{3}{2}^-)$	50.7	0.3	21.7	14.5	0.1	5.9	0.4	0.0	0.0			
$\Sigma_{b3}^{-,0,+}/\Xi_{b3}'^{-,0}/\Omega_{b3}^-(1D, \frac{7}{2}^-)$	0.4	0.0	0.1	65.0	0.4	27.7	0.4	0.0	0.0			
$\Lambda_b^0/\Xi_b^{-,0}(1D, \frac{3}{2}^+)\gamma$			$\Lambda_b^0/\Xi_b^{-,0}(1D, \frac{5}{2}^+)\gamma$			$\Sigma_{b0}^{-,0,+}/\Xi_{b0}'^{-,0}/\Omega_{b0}^-(1P, \frac{1}{2}^-)\gamma$						
Λ_b^0	Ξ_b^-	Ξ_b^0	Λ_b^0	Ξ_b^-	Ξ_b^0	Σ_b^-	Σ_b^0	Σ_b^+	$\Xi_b'^-$	$\Xi_b'^0$	Ω_b^-	
$\Sigma_{b1}^{-,0,+}/\Xi_{b1}'^{-,0}/\Omega_{b1}^-(1D, \frac{1}{2}^-)$	75.3	0.4	18.4	0.1	0.0	0.0	115.5	45.2	585.4	81.1	37.0	57.1
$\Sigma_{b1}^{-,0,+}/\Xi_{b1}'^{-,0}/\Omega_{b1}^-(1D, \frac{3}{2}^-)$	8.2	0.0	2.2	68.2	0.4	17.5	124.0	48.0	624.7	88.1	39.4	63.2
$\Sigma_{b2}^{-,0,+}/\Xi_{b2}'^{-,0}/\Omega_{b2}^-(1D, \frac{3}{2}^-)$	48.9	0.3	12.8	5.0	0.0	1.2	1.8	0.5	7.3	1.1	0.7	0.6
$\Sigma_{b2}^{-,0,+}/\Xi_{b2}'^{-,0}/\Omega_{b2}^-(1D, \frac{5}{2}^-)$	3.9	0.0	1.1	50.6	0.3	13.8	2.0	0.5	8.2	1.2	0.8	0.6
$\Sigma_{b3}^{-,0,+}/\Xi_{b3}'^{-,0}/\Omega_{b3}^-(1D, \frac{3}{2}^-)$	34.6	0.2	8.8	2.2	0.0	0.5	0.1	0.0	0.4	0.1	0.0	0.1
$\Sigma_{b3}^{-,0,+}/\Xi_{b3}'^{-,0}/\Omega_{b3}^-(1D, \frac{7}{2}^-)$	0.0	0.0	0.0	36.0	0.2	9.4	0.1	0.0	0.4	0.1	0.0	0.1
$\Sigma_{b1}^{-,0,+}/\Xi_{b1}'^{-,0}/\Omega_{b1}^-(1P, \frac{1}{2}^-)\gamma$						$\Sigma_{b1}^{-,0,+}/\Xi_{b1}'^{-,0}/\Omega_{b1}^-(1P, \frac{3}{2}^-)\gamma$						
Σ_b^-	Σ_b^0	Σ_b^+	$\Xi_b'^-$	$\Xi_b'^0$	Ω_b^-	Σ_b^-	Σ_b^0	Σ_b^+	$\Xi_b'^-$	$\Xi_b'^0$	Ω_b^-	
$\Sigma_{b1}^{-,0,+}/\Xi_{b1}'^{-,0}/\Omega_{b1}^-(1D, \frac{1}{2}^-)$	85.6	31.6	420.1	55.9	26.5	36.1	39.7	14.7	195.3	25.2	12.2	15.7
$\Sigma_{b1}^{-,0,+}/\Xi_{b1}'^{-,0}/\Omega_{b1}^-(1D, \frac{3}{2}^-)$	23.7	8.6	115.1	15.6	7.3	10.2	105.2	38.8	515.8	68.0	32.2	43.8
$\Sigma_{b2}^{-,0,+}/\Xi_{b2}'^{-,0}/\Omega_{b2}^-(1D, \frac{3}{2}^-)$	90.1	37.1	469.9	69.1	29.6	53.7	17.6	7.1	90.8	13.0	5.7	9.7
$\Sigma_{b2}^{-,0,+}/\Xi_{b2}'^{-,0}/\Omega_{b2}^-(1D, \frac{5}{2}^-)$	0.9	0.2	3.6	0.5	0.2	0.2	106.4	43.3	551.2	81.1	34.3	62.7
$\Sigma_{b3}^{-,0,+}/\Xi_{b3}'^{-,0}/\Omega_{b3}^-(1D, \frac{3}{2}^-)$	1.1	0.3	4.6	0.8	0.5	0.5	0.3	0.1	1.4	0.2	0.1	0.1
$\Sigma_{b3}^{-,0,+}/\Xi_{b3}'^{-,0}/\Omega_{b3}^-(1D, \frac{7}{2}^-)$	0.1	0.0	0.3	0.1	0.0	0.0	1.3	0.3	5.4	0.9	0.6	0.6
$\Sigma_{b2}^{-,0,+}/\Xi_{b2}'^{-,0}/\Omega_{b2}^-(1P, \frac{3}{2}^-)\gamma$						$\Sigma_{b2}^{-,0,+}/\Xi_{b2}'^{-,0}/\Omega_{b2}^-(1P, \frac{5}{2}^-)\gamma$						
Σ_b^-	Σ_b^0	Σ_b^+	$\Xi_b'^-$	$\Xi_b'^0$	Ω_b^-	Σ_b^-	Σ_b^0	Σ_b^+	$\Xi_b'^-$	$\Xi_b'^0$	Ω_b^-	
$\Sigma_{b1}^{-,0,+}/\Xi_{b1}'^{-,0}/\Omega_{b1}^-(1D, \frac{1}{2}^-)$	16.0	5.4	74.9	8.7	4.5	4.6	3.2	0.8	12.8	0.9	0.3	0.3
$\Sigma_{b1}^{-,0,+}/\Xi_{b1}'^{-,0}/\Omega_{b1}^-(1D, \frac{3}{2}^-)$	4.4	1.3	18.7	1.8	0.8	0.8	16.0	5.3	74.2	8.3	4.2	4.3
$\Sigma_{b2}^{-,0,+}/\Xi_{b2}'^{-,0}/\Omega_{b2}^-(1D, \frac{3}{2}^-)$	63.9	23.6	313.3	40.9	19.3	25.8	7.2	2.6	34.9	4.3	2.0	2.6
$\Sigma_{b2}^{-,0,+}/\Xi_{b2}'^{-,0}/\Omega_{b2}^-(1D, \frac{5}{2}^-)$	5.7	2.0	27.0	3.5	1.6	2.2	66.6	24.5	326.5	42.4	20.0	26.8
$\Sigma_{b3}^{-,0,+}/\Xi_{b3}'^{-,0}/\Omega_{b3}^-(1D, \frac{3}{2}^-)$	82.8	36.0	445.3	68.4	27.4	57.4	6.0	2.6	31.8	4.8	2.0	3.9
$\Sigma_{b3}^{-,0,+}/\Xi_{b3}'^{-,0}/\Omega_{b3}^-(1D, \frac{7}{2}^-)$	0.4	0.1	1.6	0.2	0.1	0.1	88.1	37.9	470.4	72.5	28.8	60.8
$\Sigma_b^{-,0,+}/\Xi_b'^{-,0}/\Omega_c^-(2S, \frac{1}{2}^+)\gamma$						$\Sigma_b^{-,0,+}/\Xi_b'^{-,0}/\Omega_c^*(2S, \frac{3}{2}^+)\gamma$						
Σ_b^-	Σ_b^0	Σ_b^+	$\Xi_b'^-$	$\Xi_b'^0$	Ω_b^-	Σ_b^-	Σ_b^0	Σ_b^+	$\Xi_b'^-$	$\Xi_b'^0$	Ω_b^-	
$\Sigma_{b1}^{-,0,+}/\Xi_{b1}'^{-,0}/\Omega_{b1}^-(1D, \frac{1}{2}^-)$	0.0	0.0	0.0	0.0	0.0	0.0	0.2	0.0	0.6	0.1	0.0	0.0
$\Sigma_{b1}^{-,0,+}/\Xi_{b1}'^{-,0}/\Omega_{b1}^-(1D, \frac{3}{2}^-)$	0.2	0.1	1.0	0.1	0.0	0.1	0.1	0.0	0.5	0.1	0.0	0.0
$\Sigma_{b2}^{-,0,+}/\Xi_{b2}'^{-,0}/\Omega_{b2}^-(1D, \frac{3}{2}^-)$	0.1	0.0	0.2	0.0	0.0	0.0	0.0	0.0	0.1	0.0	0.0	0.0
$\Sigma_{b2}^{-,0,+}/\Xi_{b2}'^{-,0}/\Omega_{b2}^-(1D, \frac{5}{2}^-)$	0.0	0.0	0.1	0.0	0.0	0.0	0.1	0.0	0.2	0.0	0.0	0.0
$\Sigma_{b3}^{-,0,+}/\Xi_{b3}'^{-,0}/\Omega_{b3}^-(1D, \frac{3}{2}^-)$	0.0	0.0	0.0	0.0	0.0	0.0	0.0	0.0	0.0	0.0	0.0	0.0
$\Sigma_{b3}^{-,0,+}/\Xi_{b3}'^{-,0}/\Omega_{b3}^-(1D, \frac{7}{2}^-)$	0.0	0.0	0.0	0.0	0.0	0.0	0.0	0.0	0.0	0.0	0.0	0.0

[85] H. X. Chen, Q. Mao, W. Chen, A. Hosaka, X. Liu, and S. L. Zhu, Decay properties of P -wave charmed baryons from light-cone QCD sum rules, [Phys. Rev. D 95, 094008 \(2017\)](#).

[86] B. Chen and X. Liu, New Ω_c^0 baryons discovered by LHCb as

the members of $1P$ and $2S$ states, [Phys. Rev. D 96, 094015 \(2017\)](#).

[87] H. Y. Cheng and C. W. Chiang, Quantum numbers of Ω_c states and other charmed baryons, [Phys. Rev. D 95, 094018 \(2017\)](#).

TABLE XIV: Radiative decay widths (in units of keV) of $\Sigma_b(1F)/\Xi'_b(1F)/\Omega_b(1F)$ decaying into radial or orbital excited states of the single-bottom baryon.

	$\Lambda_b^0/\Xi_b^{-0}(1P, \frac{1}{2}^-)\gamma$			$\Lambda_b^0/\Xi_b^{-0}(1P, \frac{3}{2}^-)\gamma$			$\Lambda_b^0/\Xi_b^{-0}(2S, \frac{1}{2}^+)\gamma$					
	Λ_b^0	Ξ_b^-	Ξ_b^0	Λ_b^0	Ξ_b^-	Ξ_b^0	Λ_b^0	Ξ_b^-	Ξ_b^0			
$\Sigma_{b2}^{-0,+}/\Xi_{b2}^{\prime-0}/\Omega_{b2}^-(1F, \frac{3}{2}^-)$	29.6	0.1	12.2	15.3	0.0	5.5	3.3	0.0	0.4			
$\Sigma_{b2}^{-0,+}/\Xi_{b2}^{\prime-0}/\Omega_{b2}^-(1F, \frac{5}{2}^-)$	5.3	0.0	1.8	40.2	0.1	16.3	3.5	0.0	0.5			
$\Sigma_{b3}^{-0,+}/\Xi_{b3}^{\prime-0}/\Omega_{b3}^-(1F, \frac{5}{2}^-)$	58.1	0.2	23.9	21.1	0.1	7.9	5.3	0.0	0.8			
$\Sigma_{b3}^{-0,+}/\Xi_{b3}^{\prime-0}/\Omega_{b3}^-(1F, \frac{7}{2}^-)$	2.7	0.0	0.7	77.6	0.3	31.5	5.6	0.0	0.8			
$\Sigma_{b4}^{-0,+}/\Xi_{b4}^{\prime-0}/\Omega_{b4}^-(1F, \frac{7}{2}^-)$	27.5	0.1	11.3	10.0	0.0	3.9	1.5	0.0	0.2			
$\Sigma_{b4}^{-0,+}/\Xi_{b4}^{\prime-0}/\Omega_{b4}^-(1F, \frac{9}{2}^-)$	0.6	0.0	0.1	37.4	0.1	15.2	1.6	0.0	0.3			
<hr/>												
	$\Lambda_b^0/\Xi_b^{-0}(1D, \frac{3}{2}^+)\gamma$			$\Lambda_b^0/\Xi_b^{-0}(1D, \frac{5}{2}^+)\gamma$			$\Lambda_b^0/\Xi_b^{-0}(1F, \frac{5}{2}^-)\gamma$		$\Lambda_b^0/\Xi_b^{-0}(1F, \frac{7}{2}^-)\gamma$			
	Λ_b^0	Ξ_b^-	Ξ_b^0	Λ_b^0	Ξ_b^-	Ξ_b^0	Λ_b^0	Ξ_b^-	Ξ_b^0			
$\Sigma_{b2}^{-0,+}/\Xi_{b2}^{\prime-0}/\Omega_{b2}^-(1F, \frac{3}{2}^-)$	80.1	0.5	29.8	12.0	0.1	4.0	74.4	0.5	23.0			
$\Sigma_{b2}^{-0,+}/\Xi_{b2}^{\prime-0}/\Omega_{b2}^-(1F, \frac{5}{2}^-)$	8.5	0.0	2.9	83.9	0.5	31.5	3.8	0.0	1.2			
$\Sigma_{b3}^{-0,+}/\Xi_{b3}^{\prime-0}/\Omega_{b3}^-(1F, \frac{5}{2}^-)$	102.3	0.6	39.0	10.7	0.1	4.0	42.8	0.3	13.2			
$\Sigma_{b3}^{-0,+}/\Xi_{b3}^{\prime-0}/\Omega_{b3}^-(1F, \frac{7}{2}^-)$	2.7	0.0	1.0	109.8	0.7	42.4	1.7	0.0	0.5			
$\Sigma_{b4}^{-0,+}/\Xi_{b4}^{\prime-0}/\Omega_{b4}^-(1F, \frac{7}{2}^-)$	50.1	0.3	18.9	5.5	0.0	2.0	22.5	0.1	5.9			
$\Sigma_{b4}^{-0,+}/\Xi_{b4}^{\prime-0}/\Omega_{b4}^-(1F, \frac{9}{2}^-)$	0.1	0.0	0.0	54.5	0.4	20.7	0.0	0.0	22.8			
<hr/>												
	$\Sigma_{b0}^{-0,+}/\Xi_{b0}^{\prime-0}/\Omega_{b0}^-(1P, \frac{1}{2}^-)\gamma$					$\Sigma_{b1}^{-0,+}/\Xi_{b1}^{\prime-0}/\Omega_{b1}^-(1P, \frac{1}{2}^-)\gamma$						
	Σ_b^-	Σ_b^0	Σ_b^+	$\Xi_b'^-$	Ξ_b^0	Ω_b^-	Σ_b^-	Σ_b^0	Σ_b^+	$\Xi_b'^-$	Ξ_b^0	Ω_b^-
$\Sigma_{b2}^{-0,+}/\Xi_{b2}^{\prime-0}/\Omega_{b2}^-(1F, \frac{3}{2}^-)$	149.1	33.7	567.5	96.5	15.3	62.7	96.3	22.0	368.2	59.3	10.6	36.4
$\Sigma_{b2}^{-0,+}/\Xi_{b2}^{\prime-0}/\Omega_{b2}^-(1F, \frac{5}{2}^-)$	152.0	34.4	579.1	99.0	15.6	64.9	43.1	9.8	164.9	26.9	4.7	16.7
$\Sigma_{b3}^{-0,+}/\Xi_{b3}^{\prime-0}/\Omega_{b3}^-(1F, \frac{5}{2}^-)$	1.9	0.5	7.6	0.9	0.5	0.4	105.8	23.7	400.6	74.9	9.7	53.8
$\Sigma_{b3}^{-0,+}/\Xi_{b3}^{\prime-0}/\Omega_{b3}^-(1F, \frac{7}{2}^-)$	2.0	0.5	7.9	1.0	0.5	0.4	2.1	0.5	8.3	0.9	0.3	0.4
$\Sigma_{b4}^{-0,+}/\Xi_{b4}^{\prime-0}/\Omega_{b4}^-(1F, \frac{7}{2}^-)$	0.4	0.1	1.6	0.2	0.0	0.1	1.7	0.4	6.7	0.9	0.4	0.4
$\Sigma_{b4}^{-0,+}/\Xi_{b4}^{\prime-0}/\Omega_{b4}^-(1F, \frac{9}{2}^-)$	0.4	0.1	1.7	0.2	0.0	0.1	0.3	0.1	1.1	0.1	0.0	0.1
<hr/>												
	$\Sigma_{b1}^{-0,+}/\Xi_{b1}^{\prime-0}/\Omega_{b1}^-(1P, \frac{3}{2}^-)\gamma$					$\Sigma_{b2}^{-0,+}/\Xi_{b2}^{\prime-0}/\Omega_{b2}^-(1P, \frac{3}{2}^-)\gamma$						
	Σ_b^-	Σ_b^0	Σ_b^+	$\Xi_b'^-$	Ξ_b^0	Ω_b^-	Σ_b^-	Σ_b^0	Σ_b^+	$\Xi_b'^-$	Ξ_b^0	Ω_b^-
$\Sigma_{b2}^{-0,+}/\Xi_{b2}^{\prime-0}/\Omega_{b2}^-(1F, \frac{3}{2}^-)$	93.0	21.2	355.4	56.7	10.1	34.3	29.4	6.8	113.2	16.3	3.5	8.8
$\Sigma_{b2}^{-0,+}/\Xi_{b2}^{\prime-0}/\Omega_{b2}^-(1F, \frac{5}{2}^-)$	148.8	34.0	569.1	91.1	16.3	55.7	18.8	4.5	73.8	7.7	1.5	3.5
$\Sigma_{b3}^{-0,+}/\Xi_{b3}^{\prime-0}/\Omega_{b3}^-(1F, \frac{5}{2}^-)$	32.5	7.3	123.6	21.8	3.2	15.1	89.7	20.5	342.8	55.6	9.6	34.7
$\Sigma_{b3}^{-0,+}/\Xi_{b3}^{\prime-0}/\Omega_{b3}^-(1F, \frac{7}{2}^-)$	136.4	30.6	517.5	95.5	12.7	68.0	13.2	3.0	50.7	7.7	1.3	4.7
$\Sigma_{b4}^{-0,+}/\Xi_{b4}^{\prime-0}/\Omega_{b4}^-(1F, \frac{7}{2}^-)$	0.9	0.2	3.5	0.5	0.2	0.2	108.7	24.0	409.3	84.2	8.6	66.4
$\Sigma_{b4}^{-0,+}/\Xi_{b4}^{\prime-0}/\Omega_{b4}^-(1F, \frac{9}{2}^-)$	2.2	0.6	8.9	1.2	0.5	0.6	0.6	0.2	2.4	0.3	0.1	0.1
<hr/>												
	$\Sigma_{b2}^{-0,+}/\Xi_{b2}^{\prime-0}/\Omega_{b2}^-(1P, \frac{5}{2}^-)\gamma$					<hr/>						
	Σ_b^-	Σ_b^0	Σ_b^+	$\Xi_b'^-$	Ξ_b^0	Ω_b^-	<hr/>					
$\Sigma_{b2}^{-0,+}/\Xi_{b2}^{\prime-0}/\Omega_{b2}^-(1F, \frac{3}{2}^-)$	25.8	6.2	101.3	10.5	2.1	4.7	<hr/>					
$\Sigma_{b2}^{-0,+}/\Xi_{b2}^{\prime-0}/\Omega_{b2}^-(1F, \frac{5}{2}^-)$	38.8	9.0	149.9	20.1	4.3	10.5	<hr/>					
$\Sigma_{b3}^{-0,+}/\Xi_{b3}^{\prime-0}/\Omega_{b3}^-(1F, \frac{5}{2}^-)$	24.2	5.5	92.6	14.2	2.4	8.6	<hr/>					
$\Sigma_{b3}^{-0,+}/\Xi_{b3}^{\prime-0}/\Omega_{b3}^-(1F, \frac{7}{2}^-)$	102.1	23.3	390.8	63.0	11.0	39.1	<hr/>					
$\Sigma_{b4}^{-0,+}/\Xi_{b4}^{\prime-0}/\Omega_{b4}^-(1F, \frac{7}{2}^-)$	12.6	2.8	47.8	9.5	1.1	7.3	<hr/>					
$\Sigma_{b4}^{-0,+}/\Xi_{b4}^{\prime-0}/\Omega_{b4}^-(1F, \frac{9}{2}^-)$	120.9	26.9	456.4	93.3	9.8	73.2	<hr/>					

-Continue.-

-Continue.-

	$\Sigma_b^{-,0,+}/\Xi_b'^{-,0}/\Omega_b^-(2S, \frac{1}{2}^+)\gamma$						$\Sigma_b^{*,0,+}/\Xi_b'^{*,-,0}/\Omega_b^{*-}(2S, \frac{3}{2}^+)\gamma$					
	Σ_b^-	Σ_b^0	Σ_b^+	$\Xi_b'^-$	$\Xi_b'^0$	Ω_b^-	Σ_b^-	Σ_b^0	Σ_b^+	$\Xi_b'^-$	$\Xi_b'^0$	Ω_b^-
$\Sigma_{b2}^{-,0,+}/\Xi_{b2}'^{-,0}/\Omega_{b2}^-(1F, \frac{3}{2}^-)$	0.0	0.0	0.1	0.0	0.0	0.0	12.5	3.2	50.2	4.6	1.1	1.8
$\Sigma_{b2}^{-,0,+}/\Xi_{b2}'^{-,0}/\Omega_{b2}^-(1F, \frac{5}{2}^-)$	9.3	2.4	37.5	3.6	0.8	1.5	6.2	1.6	25.0	2.3	0.6	0.9
$\Sigma_{b3}^{-,0,+}/\Xi_{b3}'^{-,0}/\Omega_{b3}^-(1F, \frac{5}{2}^-)$	2.9	0.7	11.7	1.4	0.3	0.7	2.9	0.7	11.7	1.4	0.3	0.7
$\Sigma_{b3}^{-,0,+}/\Xi_{b3}'^{-,0}/\Omega_{b3}^-(1F, \frac{7}{2}^-)$	1.8	0.5	7.3	0.9	0.2	0.5	4.4	1.1	17.5	2.1	0.5	1.1
$\Sigma_{b4}^{-,0,+}/\Xi_{b4}'^{-,0}/\Omega_{b4}^-(1F, \frac{7}{2}^-)$	1.4	0.3	5.5	1.0	0.2	0.8	0.3	0.1	1.4	0.3	0.1	0.2
$\Sigma_{b4}^{-,0,+}/\Xi_{b4}'^{-,0}/\Omega_{b4}^-(1F, \frac{9}{2}^-)$	0.0	0.0	0.0	0.0	0.0	0.0	1.5	0.4	6.0	1.1	0.2	0.8
	$\Sigma_{b2}^{-,0,+}/\Xi_{b2}'^{-,0}/\Omega_{b2}^-(1D, \frac{1}{2}^+)\gamma$						$\Sigma_{b2}^{-,0,+}/\Xi_{b2}'^{-,0}/\Omega_{b2}^-(1D, \frac{3}{2}^+)\gamma$					
	Σ_b^-	Σ_b^0	Σ_b^+	$\Xi_b'^-$	$\Xi_b'^0$	Ω_b^-	Σ_b^-	Σ_b^0	Σ_b^+	$\Xi_b'^-$	$\Xi_b'^0$	Ω_b^-
$\Sigma_{b2}^{-,0,+}/\Xi_{b2}'^{-,0}/\Omega_{b2}^-(1F, \frac{3}{2}^-)$	170.5	67.0	866.3	120.7	55.5	84.7	32.3	12.8	164.5	22.5	10.5	15.4
$\Sigma_{b2}^{-,0,+}/\Xi_{b2}'^{-,0}/\Omega_{b2}^-(1F, \frac{5}{2}^-)$	0.4	0.1	1.8	0.2	0.1	0.1	202.9	79.0	1025.1	143.3	65.1	100.2
$\Sigma_{b3}^{-,0,+}/\Xi_{b3}'^{-,0}/\Omega_{b3}^-(1F, \frac{5}{2}^-)$	1.6	0.4	6.4	1.0	0.7	0.6	0.5	0.1	1.8	0.3	0.2	0.2
$\Sigma_{b3}^{-,0,+}/\Xi_{b3}'^{-,0}/\Omega_{b3}^-(1F, \frac{7}{2}^-)$	0.1	0.0	0.3	0.0	0.0	0.0	2.0	0.5	7.8	1.2	0.8	0.7
$\Sigma_{b4}^{-,0,+}/\Xi_{b4}'^{-,0}/\Omega_{b4}^-(1F, \frac{7}{2}^-)$	0.0	0.0	0.0	0.0	0.0	0.0	0.0	0.0	0.0	0.0	0.0	0.0
$\Sigma_{b4}^{-,0,+}/\Xi_{b4}'^{-,0}/\Omega_{b4}^-(1F, \frac{9}{2}^-)$	0.0	0.0	0.0	0.0	0.0	0.0	0.0	0.0	0.0	0.0	0.0	0.0
	$\Sigma_{b3}^{-,0,+}/\Xi_{b3}'^{-,0}/\Omega_{b3}^-(1D, \frac{3}{2}^+)\gamma$						$\Sigma_{b3}^{-,0,+}/\Xi_{b3}'^{-,0}/\Omega_{b3}^-(1D, \frac{5}{2}^+)\gamma$					
	Σ_b^-	Σ_b^0	Σ_b^+	$\Xi_b'^-$	$\Xi_b'^0$	Ω_b^-	Σ_b^-	Σ_b^0	Σ_b^+	$\Xi_b'^-$	$\Xi_b'^0$	Ω_b^-
$\Sigma_{b2}^{-,0,+}/\Xi_{b2}'^{-,0}/\Omega_{b2}^-(1F, \frac{3}{2}^-)$	71.3	25.5	343.3	42.8	21.3	24.9	8.8	3.0	41.6	4.9	2.4	2.7
$\Sigma_{b2}^{-,0,+}/\Xi_{b2}'^{-,0}/\Omega_{b2}^-(1F, \frac{5}{2}^-)$	6.8	2.3	31.7	3.8	1.8	2.2	73.9	26.3	355.8	44.1	21.9	25.6
$\Sigma_{b3}^{-,0,+}/\Xi_{b3}'^{-,0}/\Omega_{b3}^-(1F, \frac{5}{2}^-)$	133.2	54.9	694.9	101.5	44.2	76.8	9.0	3.8	47.4	6.8	3.0	5.0
$\Sigma_{b3}^{-,0,+}/\Xi_{b3}'^{-,0}/\Omega_{b3}^-(1F, \frac{7}{2}^-)$	0.1	0.0	0.5	0.1	0.0	0.0	141.4	57.7	733.4	107.4	46.3	81.2
$\Sigma_{b4}^{-,0,+}/\Xi_{b4}'^{-,0}/\Omega_{b4}^-(1F, \frac{7}{2}^-)$	0.8	0.2	3.2	0.6	0.4	0.4	0.1	0.0	0.3	0.1	0.0	0.0
$\Sigma_{b4}^{-,0,+}/\Xi_{b4}'^{-,0}/\Omega_{b4}^-(1F, \frac{9}{2}^-)$	0.0	0.0	0.0	0.0	0.0	0.0	0.8	0.2	3.2	0.6	0.4	0.4
	$\Sigma_{b4}^{-,0,+}/\Xi_{b4}'^{-,0}/\Omega_{b4}^-(1D, \frac{5}{2}^-)\gamma$						$\Sigma_{b4}^{-,0,+}/\Xi_{b4}'^{-,0}/\Omega_{b4}^-(1D, \frac{7}{2}^+)\gamma$					
	Σ_b^-	Σ_b^0	Σ_b^+	$\Xi_b'^-$	$\Xi_b'^0$	Ω_b^-	Σ_b^-	Σ_b^0	Σ_b^+	$\Xi_b'^-$	$\Xi_b'^0$	Ω_b^-
$\Sigma_{b2}^{-,0,+}/\Xi_{b2}'^{-,0}/\Omega_{b2}^-(1F, \frac{3}{2}^-)$	7.2	2.3	32.4	3.3	1.7	1.4	0.6	0.2	2.4	0.2	0.1	0.0
$\Sigma_{b2}^{-,0,+}/\Xi_{b2}'^{-,0}/\Omega_{b2}^-(1F, \frac{5}{2}^-)$	0.9	0.2	3.7	0.3	0.1	0.1	7.2	2.2	32.1	3.2	1.7	1.4
$\Sigma_{b3}^{-,0,+}/\Xi_{b3}'^{-,0}/\Omega_{b3}^-(1F, \frac{5}{2}^-)$	51.8	18.5	250.0	30.7	15.1	17.5	2.8	1.0	13.6	1.6	0.8	0.8
$\Sigma_{b3}^{-,0,+}/\Xi_{b3}'^{-,0}/\Omega_{b3}^-(1F, \frac{7}{2}^-)$	2.4	0.8	11.3	1.3	0.6	0.8	52.9	18.9	254.8	31.2	15.4	17.9
$\Sigma_{b4}^{-,0,+}/\Xi_{b4}'^{-,0}/\Omega_{b4}^-(1F, \frac{7}{2}^-)$	101.0	43.5	540.3	82.6	33.9	67.3	3.8	1.6	20.1	3.0	1.3	2.4
$\Sigma_{b4}^{-,0,+}/\Xi_{b4}'^{-,0}/\Omega_{b4}^-(1F, \frac{9}{2}^-)$	0.2	0.0	0.8	0.1	0.1	0.1	104.3	44.5	555.0	85.3	34.7	69.4

- [88] M. Karliner and J. L. Rosner, Very narrow excited Ω_c baryons, *Phys. Rev. D* **95**, 114012 (2017).
- [89] M. Padmanath and N. Mathur, Quantum numbers of recently discovered Ω_c^0 baryons from lattice QCD, *Phys. Rev. Lett.* **119**, 042001 (2017).
- [90] W. Wang and R. L. Zhu, Interpretation of the newly observed Ω_c^0 resonances, *Phys. Rev. D* **96**, 014024 (2017).
- [91] Z. G. Wang, Analysis of $\Omega_c(3000)$, $\Omega_c(3050)$, $\Omega_c(3066)$, $\Omega_c(3090)$ and $\Omega_c(3119)$ with QCD sum rules, *Eur. Phys. J. C* **77**, 325 (2017).
- [92] H. M. Yang and H. X. Chen, P -wave bottom baryons of the $SU(3)$ flavor **6_F**, *Phys. Rev. D* **101**, 114013 (2020), [Erratum: *Phys. Rev. D* 102, 079901 (2020)].
- [93] G. Yang, J. Ping, and J. Segovia, The S - and P -wave low-lying baryons in the chiral quark model, *Few Body Syst.* **59**, 113 (2018).
- [94] Z. Zhao, D. D. Ye, and A. Zhang, Hadronic decay properties of newly observed Ω_c baryons, *Phys. Rev. D* **95**, 114024 (2017).
- [95] R. Aaij *et al.* (LHCb Collaboration), Observation of new Ω_c^0 states decaying to the $\Xi_c^+ K^-$ final state, *Phys. Rev. Lett.* **131**, 131902 (2018).
- [96] J. Yelton *et al.* (Belle Collaboration), Observation of excited Ω_c charmed baryons in e^+e^- collisions, *Phys. Rev. D* **97**, 051102 (2018).
- [97] R. Aaij *et al.* (LHCb Collaboration), Observation of excited Ω_c^0 baryons in $\Omega_c^- \rightarrow \Xi_c^+ K^- \pi^-$ decays, *Phys. Rev. D* **104**, 109102 (2021).
- [98] G. L. Yu, Y. Meng, Z. Y. Li, Z. G. Wang, and L. Jie, Strong decay properties of single heavy baryons Λ_Q , Σ_Q and Ω_Q , *Int. J. Mod. Phys. A* **38**, 2350082 (2023).
- [99] Z. G. Wang, F. Lu, and Y. Liu, Analysis of the D -wave Σ -type charmed baryon states with the QCD sum rules, *Eur. Phys. J. C* **83**, 689 (2023).
- [100] M. Karliner and J. L. Rosner, Excited Ω_c baryons as $2S$ states, *Phys. Rev. D* **108**, 014006 (2023).
- [101] J. H. Pan and J. Pan, Investigation of the mass spectra of singly heavy baryons Σ_Q , Ξ'_Q , and Ω_Q ($Q = c, b$) in the Regge trajectory model, *Phys. Rev. D* **109**, 076010 (2024).
- [102] J. X. Lu, Y. Zhou, H. X. Chen, J. J. Xie, and L. S. Geng, Dynamically generated $J^P = 1/2^-(3/2^-)$ singly charmed and bottom heavy baryons, *Phys. Rev. D* **92**, 014036 (2015).
- [103] C. Garcia-Recio, C. Hidalgo-Duque, J. Nieves, L. L. Salcedo, and L. Tolos, Compositeness of the strange, charm, and beauty odd parity Λ states, *Phys. Rev. D* **92**, 034011 (2015).
- [104] N. A. Tornqvist and P. Zenczykowski, Ground state baryon mass splittings from unitarity, *Phys. Rev. D* **29**, 2139 (1984).
- [105] T. Barnes and E. S. Swanson, Hadron loops: General theorems and application to charmonium, *Phys. Rev. C* **77**, 055206 (2008).
- [106] M. R. Pennington and D. J. Wilson, Decay channels and charmonium mass-shifts, *Phys. Rev. D* **76**, 077502 (2007).
- [107] Z. Y. Zhou and Z. Xiao, Hadron loops effect on mass shifts of the charmed and charmed-strange spectra, *Phys. Rev. D* **84**, 034023 (2011).
- [108] N. Isgur, Spin orbit inversion of excited heavy quark mesons, *Phys. Rev. D* **57**, 4041–4053 (1998).
- [109] P. Geiger and N. Isgur, The quenched approximation in the quark model, *Phys. Rev. D* **41**, 1595 (1990).
- [110] E. van Beveren and G. Rupp, Observed $D_s(2317)$ and tentative $D(2100\text{--}2300)$ as the charmed cousins of the light scalar nonet, *Phys. Rev. Lett.* **91**, 012003 (2003).
- [111] D. S. Hwang and D. W. Kim, Mass of $D_{sJ}^*(2317)$ and coupled channel effect, *Phys. Lett. B* **601**, 137–143 (2004).
- [112] Y. A. Simonov and J. A. Tjon, The coupled-channel analysis of the D and D_s mesons, *Phys. Rev. D* **70**, 114013 (2004).
- [113] P. G. Ortega, J. Segovia, D. R. Entem, and F. Fernandez, Molecular components in P -wave charmed-strange mesons, *Phys. Rev. D* **94**, 074037 (2016).
- [114] H. Y. Cheng and F. S. Yu, Masses of scalar and axial-vector B mesons revisited, *Eur. Phys. J. C* **77**, 668 (2017).
- [115] Y. B. Dai, C. S. Huang, C. Liu, and S. L. Zhu, Understanding the $D_{sJ}^+(2317)$ and $D_{sJ}^+(2460)$ with sum rules in HQET, *Phys. Rev. D* **68**, 114011 (2003).
- [116] B. Q. Li, C. Meng, and K. T. Chao, Coupled-channel and screening effects in charmonium spectrum, *Phys. Rev. D* **80**, 014012 (2009).
- [117] Y. S. Kalashnikova, Coupled-channel model for charmonium levels and an option for $X(3872)$, *Phys. Rev. D* **72**, 034010 (2005).
- [118] I. V. Danilkin and Y. A. Simonov, Dynamical origin and the pole structure of $X(3872)$, *Phys. Rev. Lett.* **105**, 102002 (2010).
- [119] M. X. Duan, S. Q. Luo, X. Liu, and T. Matsuki, Possibility of charmoniumlike state $X(3915)$ as $\chi_{c0}(2P)$ state, *Phys. Rev. D* **101**, 054029 (2020).
- [120] B. Silvestre-Brac and C. Gignoux, Unitary effects in spin orbit splitting of P -wave baryons, *Phys. Rev. D* **43**, 3699–3708 (1991).
- [121] S. Q. Luo, B. Chen, Z. W. Liu, and X. Liu, Resolving the low mass puzzle of $\Lambda_c(2940)^+$, *Eur. Phys. J. C* **80**, 301 (2020).
- [122] Z. L. Zhang, Z. W. Liu, S. Q. Luo, F. L. Wang, B. Wang, and H. Xu, $\Lambda_c(2910)$ and $\Lambda_c(2940)$ as conventional baryons dressed with the D^*N channel, *Phys. Rev. D* **107**, 034036 (2023).
- [123] Y. Yamaguchi, S. Ohkoda, A. Hosaka, T. Hyodo, and S. Yasui, Heavy quark symmetry in multihadron systems, *Phys. Rev. D* **91**, 034034 (2015).
- [124] Q. Mao, H. X. Chen, A. Hosaka, X. Liu, and S. L. Zhu, D -wave heavy baryons of the $SU(3)$ flavor **6_F**, *Phys. Rev. D* **96**, 074021 (2017).
- [125] Z. Y. Li, G. L. Yu, Z. G. Wang, J. Z. Gu, J. Lu, and H. T. Shen, Systematic analysis of strange single heavy baryons Ξ_c and Ξ_b , *Chin. Phys. C* **47**, 073105 (2023).
- [126] Z. P. Li, The Kaon photoproduction of nucleons in the chiral quark model, *Phys. Rev. C* **52**, 1648–1661 (1995).
- [127] Z. Li, Compton scattering and polarizabilities of the nucleon in the quark model, *Phys. Rev. D* **48**, 3070–3080 (1993).
- [128] A. Le Yaouanc, L. Oliver, O. Pene, and J. C. Raynal, The spin orbit term in radiative transitions of hadrons, *Z. Phys. C* **40**, 77 (1988).
- [129] E. E. Salpeter and H. A. Bethe, A relativistic equation for bound state problems, *Phys. Rev.* **84**, 1232–1242 (1951).
- [130] E. E. Salpeter, Mass corrections to the fine structure of hydrogen-like atoms, *Phys. Rev.* **87**, 328–342 (1952).
- [131] X. Y. Du, S. Y. Pe, W. Li, M. Jia, Q. Li, T. Wang, and G. L. Wang, $\eta_{c2}(^1D_2)$ and its electromagnetic decays, *arXiv:2408.03011 [hep-ph]*.
- [132] H. W. Ke and X. Q. Li, What do the radiative decays of $X(3872)$ tell us, *Phys. Rev. D* **84**, 114026 (2011).